

**ACTIVITY OF AQUEOUS *Tetrapleura tetraptera* FRUIT  
EXTRACT ON LEAD ACETATE-INDUCED CEREBELLAR  
DYSFUNCTION IN WISTAR RATS**

**BY  
OSIWU SOLOMON CHIGOZIE  
PG/BMS2215617**

**UNIVERSITY OF BENIN  
BENIN CITY**

**JUNE, 2025.**

**ACTIVITY OF AQUEOUS *Tetrapleura tetraptera* FRUIT  
EXTRACT ON LEAD ACETATE-INDUCED CEREBELLAR  
DYSFUNCTION IN WISTAR RATS**

**BY  
OSIWU SOLOMON CHIGOZIE  
PG/BMS2215617  
B.Sc. (UNIZIK, 2019)**

**A THESIS WRITTEN IN THE DEPARTMENT OF ANATOMY,  
SCHOOL OF BASIC MEDICAL SCIENCES AND  
SUBMITTED TO THE SCHOOL OF POSTGRADUATE  
STUDIES, IN PARTIAL FULFILMENT OF THE  
REQUIREMENTS FOR THE AWARD OF MASTER'S  
DEGREE (M.Sc.) IN ANATOMY OF THE UNIVERSITY OF  
BENIN.**

**JUNE, 2025**

**CERTIFICATION**

This is to certify that this M.Sc. thesis was written by Osiwu Solomon Chigozie in the Department of Anatomy, School of Basic Medical Sciences, University of Benin, Benin City, Nigeria.

.....

**ADAZE B. ENOGIERU (PhD)** **DATE**

*Associate Professor*

**Supervisor**

.....

**ADAZE B. ENOGIERU (PhD)** **DATE**

*Head of Department*

**Head of Department**

.....

**EXTERNAL SUPERVISOR** **DATE**

## **DEDICATION**

To God almighty, for His never ending mercies and favour, my parents, Mr. and Mrs. T.O. Osiwu, and my wonderful siblings.

## ACKNOWLEDGEMENTS

My deepest gratitude to God Almighty, the beginning and end of everything, whose provision, love, and mercy are so immeasurable.

I would like to express my deepest appreciation to my project supervisor and Head of Department, Adaze B. Enogeiru (PhD), whose diligence and result-oriented approach have contributed immensely to the success of this work.

My sincere thanks also go to all lecturers in the Department of Anatomy, University of Benin, Benin City, for their good mentorship and moral support.

At last, my sincere thanks go to my beloved parents, Mr. and Mrs. Osiwu, my friends and well-wishers, Dr. Emmaneul Bienonwu, Mr Victor Uwagboe, Mr Ikponmwosa Aikpitanyi, who have all been there for me through their prayers, moral and financial support throughout the period of the programme.

God bless you all, and may he *meet all* your needs in life.

## TABLE OF CONTENTS

Commented [h1]: Remove all the dotted lines.

TITLE PAGE.....	i
CERTIFICATION.....	ii
DEDICATION.....	iii
ACKNOWLEDGEMENTS.....	iv
TABLE OF CONTENTS .....	v
LIST OF FIGURES .....	x
LIST OF PLATES .....	xi
LIST OF TABLES .....	xii
ABSTRACT .....	xiii
CHAPTER ONE .....	1
INTRODUCTION.....	1
1.1 BACKGROUND OF THE STUDY .....	1
1.2 STATEMENT OF RESEARCH PROBLEM .....	4
1.3 AIM OF THE STUDY .....	5
1.4 SPECIFIC OBJECTIVES .....	5
1.5 JUSTIFICATION OF THE STUDY .....	6
CHAPTER TWO .....	8
LITERATURE REVIEW .....	8
2.1 THE BRAIN.....	8
2.2 THE CEREBELLUM.....	9
2.2.1 Gross Anatomy of the Cerebellum.....	10
2.2.1.1 Anatomical Division.....	11
2.2.1.2 Functional Division.....	11
2.2.1.3 Phylogenetic Division.....	13
2.2.2 Histology of the Cerebellum.....	14
2.2.2.1 Cortical Layers of the Cerebellum.....	14

2.2.2.2 Deep Nuclei of the Cerebellum.....	15
2.2.3 Cerebellar Connectivity.....	17
2.2.4 Functional Anatomy.....	18
2.2.5 Cerebellar Dysfunction.....	19
2.2.5.1 Ataxia.....	20
2.2.5.2 Dysmetria.....	21
2.2.5.3 Dysdiadochokinesia.....	21
2.2.5.4 Nystagmus.....	22
2.2.6 Aetiology of Cerebellar Dysfunction.....	23
2.2.6.1 Structural abnormalities and Genetic Factors.....	23
2.2.6.2 Praneoplastic Syndromes and Infections.....	24
2.2.6.3 Toxic and Metabolic Factors.....	24
2.3 LEAD.....	25
2.3.1 Pb Prevalence Rate.....	25
2.3.2 Human Exposure and Metabolism.....	26
2.3.3 Toxicity.....	27
2.3.4 Mechanism of Pb-induced Neurotoxicity.....	29
2.3.4.1 Oxidative Stress.....	30
2.3.4.2 Ionic Mechanism.....	31
2.3.4.3 Apoptosis.....	32
2.3.5 Effects of Pb on the Cerebellum.....	33
2.3.6 Current Treatment Options for Pb-Induced Cerebellar Dysfunction.....	35
2.4 <i>Tetrapleura tetraptera</i> .....	37
2.4.1 Description.....	28
2.4.1.1 Family (Fabaceae).....	38
2.4.1.2 Specie ( <i>Tetrapleura tetraptera</i> ).....	39
2.4.2 Taxonomy (Scientific Classification) .....	40
2.4.3 Conventional uses of <i>T. tetraptera</i> .....	40
2.4.4 Phytochemical Composition of <i>T. tetraptera</i> .....	42

2.4.5 Pharmacological Activities of <i>T. tetraptera</i> .....	43
2.4.5.1 Antioxidative Functions.....	43
2.4.5.2 Anti-Microbial Functions.....	44
2.4.5.3 Anti-Inflammatory Functions.....	45
2.4.5.4 Anti-Proliferative Functions.....	46
2.4.5.5 Anti-Hyperglycemic Functions.....	47
CHAPTER THREE .....	48
MATERIALS AND METHOD .....	48
3.1 ETHICAL APPROVAL .....	48
3.2 REAGENTS / CHEMICALS .....	48
3.3 PLANT COLLECTION AND IDENTIFICATION.....	48
3.4 EXTRACT PREPARATION .....	48
3.5 ACUTE TOXICITY TEST.....	49
3.6 PHYTOCHEMICAL SCREENING (QUALITATIVE).....	49
3.6.1 Test for Flavonoids.....	49
3.6.2 Test for Alkaloids.....	49
3.6.3 Test for Tannins.....	49
3.6.4 Test for Saponins.....	50
3.6.5 Test for Steroids.....	50
3.6.6 Test for Phenol.....	50
3.7 EXPERIMENTAL ANIMALS AND HANDLING.....	50
3.8 ADMINISTRATION METHOD AND DOSAGE SELECTION.....	50
3.9 EXPERIMENTAL DESIGN.....	51
3.10 ASSESSMENTS OF NEUROBEHAVIOURAL ACTIVITY.....	52
3.10.1 Open FieldTest.....	52
3.10.2 String Test.....	53
3.10.3 Movement Initiation Test.....	54
3.10.4 Step Test.....	55

3.11 EVALUATION OF BODY AND BRAIN WEIGHT .....	55
3.12 CEREBELLAR OXIDATIVE STRESS PARAMETERS.....	55
3.12.1 Catalase (CAT) Activity Estimation.....	56
3.12.2 Estimation of Malondialdehyde (MDA) Concentration.....	57
3.12.3 Glutathione Peroxidase (GPx) Activity Estimation.....	58
3.12.4 Analysis of Superoxide Dismutase (SOD).....	59
3.12.5 Estimation of Glutathione (GSH) Concentration.....	61
3.13 ESTIMATION OF Pb ACETATE CONCENTRATION.....	61
3.14 CEREBELLAR HISTOLOGICAL PROCEDURE.....	62
3.14.1 Paraffin Tissue Processing.....	62
3.14.2 Method of Hematoxylin and Eosin Staining .....	63
3.15 PHOTOMICROGRAPHY.....	63
3.16 MOLECULAR DOCKING.....	64
3.16.1 High Performance Liquid Chromatography (HPLC) Analysis.....	64
3.16.1.1 Extraction.....	64
3.16.1.2. Analysis.....	64
3.16.2 Ligand-Protein Interacton.....	66
3.16.2.1 Preparation of Crystal Protein.....	66
3.16.2.2 Preparation of The Phyto-Compounds.....	67
3.16.2.3 Receptor Grid Generation.....	67
3.16.2.4 Glide Extra Precision Docking.....	67
3.16.2.5 ADME Profiles.....	68
3.17 STATISTICAL ANALYSIS.....	67
CHAPTER FOUR.....	69
RESULTS.....	69
4.1 PRELIMINARY PHYTOCHEMICAL SCREENING.....	69
4.2 ACUTE TOXICITY STUDY AND OBSERVATION.....	70
4.3 EFFECT OF TREATMENT ON BODY AND BRAIN WEIGHT.....	71
4.4 EFFECT OF TREATMENT ON NEUROBEHAVIOURAL ACTIVITY.....	76

4.5 EFFECT OF TREATMENT ON ANTIOXIDANT ENZYMES ACTIVITY.....	82
4.6 EFFECT OF TREATMENT ON LIPID PEROXIDATION.....	85
4.7 EFFECT OF TREATMENT ON CEREBELLAR Pb CONCENTRATION.....	86
4.8 EFFECT OF TREATMENT ON THE HISTOLOGY OF THE CEREBELLUM.....	87
4.9 <i>T. tetraptera</i> HPLC-IDENTIFIED PHENOLIC COMPOUNDS.....	92
4.10 <i>T. tetraptera</i> LIGAND–RECEPTOR INTERACTIONS.....	94
CHAPTER FIVE.....	101
DISCUSSION, CONCLUSION, RECOMMENDATIONS AND CONTRIBUTION TO KNOWLEDGE.....	101
5.1 <i>T. tetraptera</i> is a Rich Source of Phytochemicals.....	101
5.2 <i>T. tetraptera</i> Attenuates Weight Loss in Pb-Exposed Rats.....	102
5.3 <i>T. tetraptera</i> Inhibits Neurobehavioural Deficits in Pb-Exposed Rats.....	103
5.4 <i>T. tetraptera</i> Inhibits Oxidative Stress in Pb-Exposed Rats.....	105
5.5 <i>T. tetraptera</i> Mitigates Pb Accumulation and Histological Alterations in the cerebellum of Pb-Exposed Rats.....	107
5.6 <i>T. tetraptera</i> HPLC Analysis and Ligand- Receptor Interactions.....	108
5.7 CONCLUSION .....	111
5.8 RECOMMENDATIONS.....	112
5.9 CONTRIBUTION TO KNOWLEDGE.....	113
REFERENCES.....	114

## LIST OF FIGURES

**Commented [h2]:** Remove all the grid lines in your list of figures, list of plates and list of tables. They are not necessary.

Figure 2.1	Functional division of the cerebellum	13
Figure 2.2	Representation of the deep cerebellar nuclei	17
Figure 2.3	<i>Tetrapleura tetraptera</i> plant	37
Figure 2.4	Various applications of <i>T. tetraptera</i>	42
Figure 3.1	Open Field Test Apparatus	53
Figure 3.2	Step Test Apparatus	54
Figure 3.3	Movement Initiation Test	54
Figure 4.1	Initial body weight across experimental groups	72
Figure 4.2	Final body weight across experimental groups	72
Figure 4.3	Weight change across experimental groups	73
Figure 4.4	Brain weight across experimental groups	73
Figure 4.5	Relative Brain weight across experimental groups	74
Figure 4.6	Cerebellar weight across experimental groups	74
Figure 4.7	Relative Cerebellar weight across experimental groups	75
Figure 4.8	Cerebellum Brain weight ratio across experimental groups	75
Figure 4.9	Immobility OFT across experimental groups	78
Figure 4.10	Ambulation OFT across experimental groups	78
Figure 4.11	Central square entry OFT across experimental groups	79
Figure 4.12	Line crossing OFT across experimental groups	79
Figure 4.13	Movement initiation test across experimental groups	80
Figure 4.14	String test across experimental groups	80
Figure 4.15	Step test across experimental groups	81
Figure 4.16	Cerebellum SOD across experimental groups	83
Figure 4.17	Cerebellum CAT across experimental groups	83
Figure 4.18	Cerebellum GPx across experimental groups	84
Figure 4.19	Cerebellum GSH across experimental groups	84
Figure 4.20	Cerebellum MDA across experimental groups	85
Figure 4.21	Cerebellar Pb concentration across experimental groups	86
Figure 4.22	HPLC-identified <i>T. tetraptera</i> phenolic compounds	93
Figure 4.23	The binding pose of 4-hydroxybenzoic acid and Resorcinol within the binding pocket of caspase 3 showing the interacting amino acids	96
Figure 4.24	The binding pose of 4-hydroxybenzoic acid and Resorcinol within the binding pocket of NRF2 showing the interacting amino acids	97
Figure 4.25	The binding pose of 4-hydroxybenzoic acid and Resorcinol within the binding pocket of TNF- $\alpha$ , showing the interacting amino acids	98

Figure 4.26	The binding pose of 4-hydroxybenzoic acid and Resorcinol within the binding pocket of Nf-kB showing the interacting amino acids	99
Figure 4.27	The binding pose of 4-hydroxybenzoic acid and Resorcinol within the binding pocket of IL-6, showing the interacting amino acids	100

#### LIST OF PLATES

Plate 4.1	Representative histology of the cerebellar cortex in the Control Group	88
Plate 4.2	Representative histology of the cerebellar cortex in the Pb-Only treatment Group	88
Plate 4.3	Representative histology of the cerebellar cortex in Pb co-administered with <i>T. tetraptera</i> (500 mg/kg) Treatment Group	89
Plate 4.4	Representative histology of the cerebellar cortex in Pb + <i>T. tetraptera</i> (1000 mg/kg) Treatment Group	89
Plate 4.5	Representative histology of the cerebellar cortex in Pb + Vit E (200 mg/kg) Treatment Group	90
Plate 4.6	Representative histology of the cerebellar cortex in <i>T. tetraptera</i> -Only (500 mg/kg) Treatment Group	90
Plate 4.7	Representative histology of the cerebellar cortex in <i>T. tetraptera</i> -Only (1000 mg/kg) Treatment Group	91
Plate 4.8	Representative histology of the cerebellar cortex in Vit E-Only (200 mg/kg) Treatment Group H	91

### LIST OF TABLES

Table 2.1	<i>T. tetraptera</i> classification	40
Table 3.1	Summary of Experimental Design	51
Table 4.1	Preliminary Phytochemical findings (qualitative) of the aqueous fruit extract of <i>T. tetraptera</i>	69
Table 4.2	Acute toxicity study and observations in Wistar rats treated with aqueous fruit extract of <i>T. tetraptera</i> after 72 hours	70

## ABSTRACT

Cerebellar dysfunction (CD), via oxidative stress, is an established effect of lead (Pb), a known heavy metal, even at low exposure. *Tetrapleura tetraptera* (*T. tetraptera*) fruit exhibits various pharmacological properties, such as antioxidant and anti-inflammatory activities. This study investigated the activity of aqueous *T. tetraptera* fruit extract against lead acetate (PbA)-induced CD in Wistar rats. Sixty-eight Wistar rats were assigned to eight groups (n=8) and treated for twenty-eight days as follows: Groups A (control); B (100 mg/kg body weight (bw) of PbA); C (500 mg/kg bw of *T. tetraptera* and 100 mg/kg bw of PbA); D (1000 mg/kg bw of *T. tetraptera* and 100 mg/kg bw of PbA); E (200 mg/kg bw of Vitamin E and 100 mg/kg bw of PbA); F, G and H (500 mg/kg of *T. tetraptera*, 1000 mg/kg of *T. tetraptera*, and 200 mg/kg bw of Vitamin E), respectively. Subsequently, weights, neurobehavior, Pb concentration, antioxidant enzymes, lipid peroxidation, and cerebellar histology were assessed. High-performance liquid chromatography was used to identify phenolic compounds in *T. tetraptera*, and *in-silico* studies evaluated the binding interaction of some of the identified phenolic compounds (4-hydroxybenzoic acid and Resorcinol) to markers of apoptosis (caspase-3), inflammation (IL-6, TNF- $\alpha$ , and Nf- $\kappa$ B), and oxidative stress (NRF2). A significant decrease ( $p<0.05$ ) in weights and antioxidant enzymes, as well as a significant increase ( $p<0.05$ ) in neurobehavioral deficits, lipid peroxidation, Pb concentration, and alterations in cerebellar histoarchitecture were observed in the PbA-exposed rats when compared to control. However, co-treatment of PbA-exposed rats with *T. tetraptera* significantly attenuated ( $p<0.05$ ) these PbA-induced effects. Additionally, *in-silico* studies revealed a high binding affinity of 4-hydroxybenzoic acid and Resorcinol to caspase-3, IL-6, TNF- $\alpha$ , Nf- $\kappa$ B, and NRF2, thus suggesting possible anti-apoptotic, anti-inflammatory, and antioxidant effects of *T. tetraptera*. This study provides research evidence suggesting that *T. tetraptera* has the potential for further development as a therapeutic agent against CD.

## CHAPTER ONE

### INTRODUCTION

#### 1.1 BACKGROUND OF THE STUDY

Cerebellar dysfunction (CD) is characterised by a wide range of neurological disorders that alter the cerebellum's feedback loops with other regions of the nervous system, thereby affecting its regulation of motor control, balance, and motor learning (Goodlett & Mittleman, 2017). Regardless of the location or manner of cerebellar injury, motor-related symptoms are frequently the most common complications of CD (Knierim, 2020; Lara-Aparicio *et al.*, 2022). A changed and uneven walking gait, with a broad stance due to trouble balancing, as well as errors in the speed, force, amplitude, and direction of motions, are some of the symptoms (Patestas *et al.*, 2025; Tada *et al.*, 2015; Pedroso *et al.*, 2019). Additional symptoms include intention tremor (unconscious movement brought on by alternating spasms of opposing muscle groups), dysarthria (difficulty with speech expression), dysmetria (difficulty in determining ranges or distances of movement), dysphagia (difficulty in swallowing), dysdiadochokinesia (difficulty performing rapid alternating movements like walking), hypotonia (reduced muscle tone), and nystagmus (rapid, uncontrollable eye movements) (Schmahmann, 2019; Gudlavalleti *et al.*, 2022). These dysfunctions may arise as a result of acute or chronic underlying factors such as infections, autoimmune disorders, vascular problems, genetics, and heavy metal toxicants such as lead (Roostaei *et al.*, 2014; Pedroso *et al.*, 2019).

Lead (Pb) and its compounds, like lead acetate (PbA), are one of the most prevalent heavy metal toxicants (Assi *et al.*, 2016). The frequent utilisation of Pb in a variety of sectors, such as mining, industrial processing, burning of fossil fuels, and Pb-containing materials has made Pb ubiquitous

in the ecological systems, leading to its accumulation in soil, water, and air. After entering the body via food, air, or dermal routes (Aktepe *et al.*, 2022), Pb circulates via the bloodstream to soft tissues and is eventually deposited in bones, where it can be released gradually, causing long-lasting harmful effects (Boskabady *et al.*, 2022; Brodziak-Dopierala, 2020). Pb is known to interact with a variety of bodily functions, with the central nervous system (CNS) being particularly vulnerable (de Souza, 2018). Acute toxicity is associated with occupational exposure and is infrequent, with adverse symptoms arising immediately. Chronic toxicity, on the other hand, is significantly more prevalent and occurs when blood Pb concentrations are around 40-60 µg/dL, with symptoms seeming to get worse over the course of the weeks (Kim *et al.*, 2015; Stoodley, 2016). The primary mechanism responsible for Pb-induced cerebellar dysfunction relates to its ionic mechanism, which substitutes calcium ions with Pb, permitting it to cross the blood-brain barrier. As a result, Pb accumulates in cerebellar astrocytes, disrupting the formation of myelin sheaths, which, even at very low concentrations, alters neuronal excitation and hence neurotransmitter activity (Carocci *et al.*, 2016). Additionally, oxidative stress, a pathological state characterised by an excess of reactive oxygen species (ROS) and a corresponding reduction of endogenous antioxidant defences, is closely linked to Pb exposure. In this context, much of the neurodegenerative pathology brought on by Pb, such as apoptotic neuronal death, neuroinflammation, and mitochondrial dysfunction, is caused by oxidative damage to lipids, proteins, and DNA. These effects are implicated in neuropathological findings of CD, such as ataxia, dysmetria, dysarthria, nystagmus, tremor, and hypotonia, where the cerebellum often shows early and profound degenerative changes (Gudlavalleti *et al.*, 2022). Given the prevalence of Pb and its known toxicity, there is a need for more efficacious therapeutic solutions to mitigate Pb-induced neurological perturbation, such as CD. In this regard, human cultures have recognised the

preventive benefits of medicinal plants since ancient times, and this knowledge has been passed down through the centuries (Rahman *et al.*, 2023). Medicinal plants, also referred to as herbal remedies, are readily used in healthcare to combat chronic illnesses (Adusei *et al.*, 2019; Rahman *et al.*, 2023). These substances have a reputation for suppressing ROS, boosting the body's natural antioxidant enzyme activity, and controlling inflammatory processes (Enogieru & Momodu, 2022; Adusei *et al.*, 2019). *Ginseng*, *Chamomile*, *Gingko*, *Echinacea*, *Feverfew*, and *Garlic* are a few of the well-known medicinal plants and because they have therapeutic qualities, plants like *Tetrapleura tetraptera* can also be categorised as such (Adesina *et al.*, 2016).

*Tetrapleura tetraptera* (*T. tetraptera*), or Gum tree in English, is a flowering plant of the leguminosae family, mostly found in western Africa, where it is referred to as *Prekese* (Twi), *Aridan* (Yoruba), *Ighimiaka* (Edo), and *Oshosho* (Igbo) in the Ghanaian and Nigerian languages (Uyoh *et al.*, 2013). *T. tetraptera* has been shown to contain an array of nutrients, including carbohydrates, lipids, ash, vitamins, fibre, and proteins (Uyoh *et al.*, 2013; Adesina *et al.*, 2016), as well as a substantial level of phytochemicals, such as flavonoids, steroids, tannins, alkaloids, phylates, and triterpenoids (Adusei *et al.*, 2019). The plant's potent constituents have allowed it to be applied in a variety of sectors, including food and animal feeds, beverages, as well as traditional medicine. Amongst *T. tetraptera*'s most potent pharmacological characteristics is its antioxidant activity, which helps explain why it is used in herbal medicine. It functions as a reducing agent, limiting injury to cells by eliminating reactive oxygen species and preventing additional oxidation (Adusei *et al.*, 2019; Kuate *et al.*, 2015). Previous studies have also shown that *T. tetraptera* can be utilised to treat rheumatic pain, arthritis and diabetes due to its anti-inflammatory (Ayoola *et al.*, 2018; de Carvalho *et al.*, 2020), anti-proliferative (Ozaslan *et al.*, 2016; Aikins *et al.*, 2021), and Anti-hyperglycemic (Omonkhua *et al.*, 2014; Bacanli *et al.*, 2019) effects.

## 1.2 STATEMENT OF RESEARCH PROBLEM

The cerebellum, a brain region crucial for intricate motor activities such as motor coordination, equilibrium and motor learning, is notably sensitive to Pb-induced neurotoxicity. Pb's ability to dissolve in both glycerine and water makes it readily available in the bloodstream (Abd El-Monem, 2012), with the ingestion rate ranging from 20 to 70%, and children taking in a larger proportion than adults (Tarrago, 2012). By replacing endogenous cerebellar calcium ions, Pb accumulate in cerebellar tissues, where it impairs neurogenesis, disrupts synaptic signalling, and promotes pro-oxidative, as well as pro-inflammatory and pro-apoptotic factors. (Singh *et al.*, 2024; Gudlavalleti *et al.*, 2022). These pathological processes frequently result in motor function deficits, synaptic degeneration, cortical atrophy, and other signs of cerebellar neurodegeneration that ultimately lead to CD.

No amount of Pb seems to be essential to the body, and no "safe" level of Pb exposure has been identified. Pb toxicity remains a pressing global public health issue due to its non-biodegradable property, long-term survival, widespread environmental presence, as well as its well-established toxicity across multiple organ systems. Though Pb toxicity is a highly investigated and comprehensively documented topic, complete management and prevention of contact with Pb, particularly in the developing world, is still far from being attained (Carocci *et al.*, 2016). One direct result of Pb exposure is encephalopathy, a gradual degeneration of certain parts of the brain, which, at very high exposure, manifests as delirium, lack of coordination, seizures, paralysis, unconsciousness, and ataxia (Mason *et al.*, 2014; Kim *et al.*, 2015; Alisha *et al.*, 2018). Particularly in children, whose developing brains are especially susceptible to neurotoxins, even modest levels of Pb exposure have been linked to a variety of neurodevelopmental problems, including gait

ataxia, motor learning difficulties, developmental dyslexia, ADHD, and behavioural issues (Stoodley, 2016; Mandal *et al.*, 2022; Ortega *et al.*, 2021). The artisanal gold mining poisoning outbreak in Zamfara, Nigeria, serves as a prime example of the catastrophic effects of Pb-induced neurotoxicity in the real world. Documented evidence from the poisoning has shown that more than 400 children have died since 2010, and hundreds more have been chronically exposed and need immediate medical attention. This public health emergency emphasises how important long-term, efficient neuroprotective measures are needed, particularly in the underprivileged and vulnerable populations of the developing world (Tirima *et al.*, 2018; Akinwumi *et al.*, 2023).

### **1.3 AIM OF STUDY**

This study evaluated the activity of aqueous *Tetrapleura tetraptera* fruit extract on lead acetate-induced cerebellar dysfunction in Wistar rats.

### **1.4 SPECIFIC OBJECTIVES**

The specific objectives of the study were to:

- I. Investigate the activity of aqueous *Tetrapleura tetraptera* fruit extract on the brain and body weight changes in rats treated with or without lead acetate.
- II. Determine the activity of aqueous *Tetrapleura tetraptera* fruit extract on the neurobehavioral activities (Open Field, Movement Initiation, String, and Step Tests) in rats treated with or without lead acetate.
- III. Determine the activity of aqueous *Tetrapleura tetraptera* fruit extract on the antioxidant enzymes (SOD, GPx, GSH, and CAT) activity, Lipid peroxidation (MDA) and Pb (Pb) concentration in the cerebellum of rats treated with or without lead acetate.

- IV. Investigate the activity of aqueous *Tetrapleura tetraptera* fruit extract on the histology of the cerebellum of rats treated with or without lead acetate.
- V. Determine the ligand-protein interaction of some of the HPLC-identified *T. tetraptera* compounds to markers of apoptosis (caspase-3), inflammation (IL-6, TNF- $\alpha$ , and Nf- $\kappa$ B), and oxidative stress (NRF2).

### 1.5 JUSTIFICATION OF STUDY

Numerous studies highlight how important antioxidants are for scavenging reactive oxygen species and maintaining the integrity of neurons (Adusei *et al.*, 2019; Kuate *et al.*, 2015). Although the body produces antioxidants naturally, reinforcing it with exogenous sources can improve the body's overall antioxidant defence as well as support the activity of endogenous antioxidants. These substances have a reputation for suppressing ROS, boosting the body's natural antioxidant enzyme activity, and controlling inflammatory processes (Adusei *et al.*, 2019). Due to their strong capacity to scavenge free radicals, medicinal plants have become one of the most popular exogenous sources of antioxidants (Enogieru & Momodu, 2022; Adusei *et al.*, 2019). Traditionally regarded as innocuous, these plants are typically used to combat chronic illnesses and therefore serve as candidates for pharmaceutical research and drug development given their natural chemical makeup, cost, and minimal risk of side effects (Rahman *et al.*, 2023). Despite a profound knowledge of the ameliorative and medicinal value of *T. tetraptera* fruit in traditional medicine, there is a paucity of information on the protective effects of *T. tetraptera* against neurotoxic heavy metals such as Pb. Equally, there is little correlation between the therapeutic effects of *T. tetraptera* and its protective capacity on specific regions of the central nervous system, such as the cerebellum. By bridging these gaps in the literature, this study can provide a basis for evaluating

the protective effects of the aqueous *Tetrapleura tetraptera* fruit extract on Pb acetate-induced neurotoxicity in adult Wistar rats.

## CHAPTER TWO

### LITERATURE REVIEW

#### 2.1 THE BRAIN

The skull's bony structure, known as the neurocranium, safely houses and protects the brain, a crucial and intricate organ that is a key part of the central nervous system (Bhushan *et al.*, 2022). The brain is divided into three main and functionally separate regions: the cerebellum, which coordinates motor control, balance, and motor learning; the brainstem, which controls many of the body's automatic and life-sustaining processes; and the cerebrum, which is in charge of higher cognitive functions (Bhushan *et al.*, 2022). In relation to embryology, the formation and differentiation of the three main brain vesicles during early neural development are the source of these three main brain regions:

i. Prosencephalon (forebrain) gives rise to two secondary brain vesicles.

- The telencephalon, which develops into the paired cerebral hemispheres (cerebrum) and the neocortex, is involved with cognition, motor, and sensory activities.
- The diencephalon, the junctional part of the forebrain that forms the thalamus, hypothalamus, and metathalamus, serves as a relay, autonomic, and limbic centre (Carstens and Sarnat, 2023).

ii. Mesencephalon (the midbrain). According to Carstens and Sarnat (2023), it develops into the tectum, tegmentum, and cerebral peduncles, which serve as a relay centre for auditory and visual information.

iii. The rhombencephalon (hindbrain) gives rise to two secondary brain vesicles.

**Commented [h3]:** Remove all bullets from your work. You can use numbers, 1,2,3 etc instead.

- The metencephalon, which gives rise to the pons and cerebellum that serve as a relay, autonomic, and motor control centre.
- The myelencephalon forms the medulla oblongata, a major relay and autonomic centre.

## 2.2 CEREBELLUM

Resembling a distinct structure affixed to the base of the brain, nestled just beneath the cerebral hemispheres, the small brain, also known as the cerebellum, is one of the main components of the rhombencephalon of vertebrates (Carstens and Sarnat, 2023; Bhushan *et al.*, 2022; Lara-Aparicio *et al.*, 2022). Though it makes up only 10% of the brain's volume, the cerebellum is home to more than half of all the neurons (Lara-Aparicio *et al.*, 2022; Roostaei *et al.*, 2014). Despite its typically smaller relative size, this structure can be quite large in certain animals, surpassing the cerebrum in size sometimes, as seen in the mormyrid fishes (Sukhum *et al.*, 2018). Though the cerebellum's role in movement is well-established, in humans, it is also crucial for executive processes like language, attention, and emotional functions such as controlling pleasure and fear reactions (Schmahmann *et al.*, 2019; Goodlett & Mittleman, 2017). The human cerebellum fine-tunes motor function, typically by aggregating information from the spinal cord's ascending pathways and other areas of the brain (via the descending tracts). This integration helps with the coordination, accuracy, and timing of movement (Roostaei *et al.*, 2014; Manto *et al.*, 2012). Human motor learning, gait, balance, and fine motor skills are all affected by an injury or dysfunction to the cerebellum (Gudlavalleti *et al.*, 2022; Manto *et al.*, 2012). Located in the cerebellar fossa of the posterior cranial base, the cerebellum is related superiorly to the occipital lobe of the cerebrum, from which it is separated by a dural reflection known as the tentorium cerebelli. Anteriorly, it is related to the pons, medulla, and the 4<sup>th</sup> ventricle (Roostaei *et al.*, 2014; Wright *et al.*, 2016). The

pons is where all of its connections to other brain areas pass. The pons and the cerebellum make up the metencephalon, which forms the superior portion of the hindbrain or rhombencephalon of vertebrates (Carstens and Sarnat, 2023; Bhushan *et al.*, 2022).

### **2.2.1 Gross Anatomy of the Cerebellum**

The cerebellum is divided and compartmentalised into two hemispheres (right and left cerebellar hemispheres) by a dura mater membrane known as the falx cerebelli. These hemispheres are then joined together by a midline mass called the vermis (Lara-Aparicio *et al.*, 2022; Roostaei *et al.*, 2014). The cerebellar cortex, a highly folded layer of grey matter, makes up the majority of the cerebellum's volume, with each slope or gyrus in this layer referred to as a folium. A mature human cerebellar cortex, according to high clarity MRI, is 730 square cm in size (Lyu *et al.*, 2024; Lara-Aparicio *et al.*, 2022) and is contained in a volume that is 6 cm by 5 cm by 10 cm. The white matter of the cerebellum, which is primarily composed of myelinated nerve axons that travel to and from the cortical areas, is located beneath the cortex. A total of four deep cerebellar nuclei reside within the white matter, which is frequently referred to as the arbour vitae (tree of life) due to its branching, tree-like pattern in transverse section (Lara-Aparicio *et al.*, 2022; Wright *et al.*, 2016).

Unlike the vast uneven folding of the cerebral cortex, the cortical area of the cerebellum is dotted with precisely spaced symmetrical fissures. The cortex is essentially a thin, contiguous strip of tissue that is tightly wrapped in the manner of an accordion, an arrangement that is hidden by its parallel fissures. Three distinct criteria can be used to categorise the cerebellum: anatomical, functional, and phylogenetic (Knierim, 2020; Lara-Aparicio *et al.*, 2022; Wright *et al.*, 2016).

#### **2.2.1.1. Anatomical Division**

The cerebellar cortex is divided into three main lobes from rostral to caudal (top to bottom in humans) by two large fissures that run mediolaterally. The corpus cerebelli is divided into an anterior and a posterior lobe by the primary fissure, while the flocculonodular lobe is separated from the corpus cerebelli by the posterolateral fissure (Roostaei *et al.*, 2014). Traditionally, the entire structure is further divided into ten smaller "lobules" by a series of broad folds (Lara-Aparicio *et al.*, 2022; Wright *et al.*, 2016).

### **2.2.1.2 Functional division**

Functional criteria emphasise the connections of the cerebellum to other structures of the nervous system. Additionally, there are three sagittally separated zones in the cerebellum, extending from medial to lateral (Knierim, 2020; Roostaei *et al.*, 2014). The cerebellum's midsagittal plane corresponds to the vermis, the intermediate zone is situated next to the vermis, while the lateral hemispheres are situated lateral to the intermediate zone. From a gross specimen, it is impossible to discern distinct morphological boundaries between the last two (Lara-Aparicio *et al.*, 2022; Knierim, 2020). The vestibulocerebellum, which controls ocular movements and maintains equilibrium, corresponds to the flocculonodular lobe. It projects fibres to the medial and lateral vestibular nuclei after receiving vestibular input from those nuclei and the semicircular canals. Additionally, it integrates visual information from the visual cortex (employing the pontine nuclei, which form a corticopontocerebellar connection) and the superior colliculi. Gait and balance disorders are brought on by vestibulocerebellar lesions (Patestas *et al.*, 2025; Lara-Aparicio *et al.*, 2022). The spinocerebellum, which controls trunk and limb motions, corresponds to the vermis and intermediate zone. In addition to the acoustic and visual inputs, it receives proprioceptive signals from the trigeminal nerve and the spinocerebellar tract of the spinal cord (Knierim, 2020; Lara-Aparicio *et al.*, 2022). It equally provides modulation to the descending motor systems by

projecting fibres to the deep cerebellar nuclei, including the fastigial nucleus. The fastigial nucleus, in turn, projects fibres to the brainstem (utilising vestibular nuclei in the medulla and reticular formation in the pons) and the cerebral cortex (through the midbrain and thalamus). As it collects information on the location of different body regions in space, the spinocerebellum creates a sensory homunculus (Knierim, 2020; Lara-Aparicio *et al.*, 2022). Specifically, the vermis receives fibres from the upper sections of limbs and the trunk, while fibres from the lower sections of limbs are projected to the intermediate areas of the cerebellar hemispheres. Through a "feedforward" process, the spinocerebellum may clarify proprioceptive information to predict a body part's future positioning during locomotion (Knierim, 2020; Lara-Aparicio *et al.*, 2022; Roostaei *et al.*, 2014). The cerebrocerebellum corresponds to the lateral zone and mainly receives input from the cortical areas of the cerebrum, particularly the parietal lobe. It forms the corticopontocerebellar routes via the dentate deep nuclei of the cerebellum and the pontine nuclei in the pons, which in turn project fibres primarily to the red nucleus, inferior olivary nucleus and the ventrolateral thalamus (Knierim, 2020; Roostaei *et al.*, 2014). Subsequently, these fibres are then relayed back from the inferior olivary nucleus and ventrolateral thalamus to the cerebellar hemispheres, premotor area and the primary motor area (Lara-Aparicio *et al.*, 2022; Patesta *et al.*, 2025). The cerebrocerebellum has primarily cognitive functions and is engaged with preparing future movements by accessing sensory inputs before coordinating action (Buckner *et al.*, 2013; Lara-Aparicio *et al.*, 2022; Knierim, 2020).

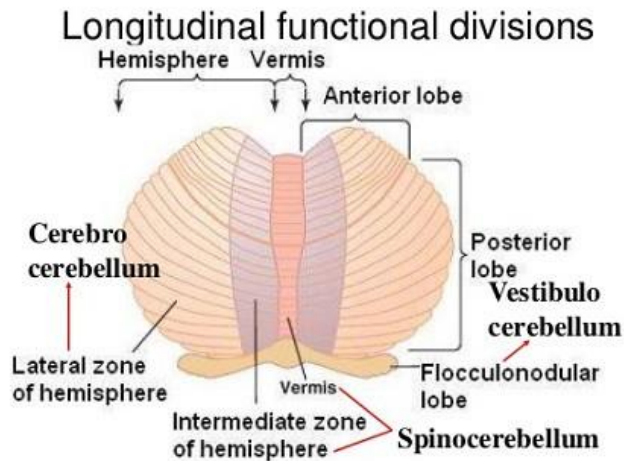


Figure 2.1 Functional division of the cerebellum (Knierim, 2020)

### 2.2.1.3 Phylogenetic Division

Phylogenetic criteria, which deal with the evolutionary age of each part of the cerebellum, can also be used to categorise the cerebellum into three sections: archicerebellum, paleocerebellum, and neocerebellum (Lara-Aparicio *et al.*, 2022; Knierim, 2020). The archicerebellum (vestibulocerebellum), the oldest component of the cerebellum that evolved in aquatic animals is mostly connected to the vestibular nuclei. It is made up of the lingula and flocculonodular lobes that aid in the balancing and toning of trunk muscles (Patestas *et al.*, 2025; Lara-Aparicio *et al.*, 2022). The paleocerebellum, which corresponds to the spinocerebellum, follows the emergence of limbs in terrestrial vertebrates and, except for the lingula, pyramid, and uvula, comprises most of the anterior lobe. It is consigned with the coordination of tone, posture, and rudimentary movements of the limbs (Knierim, 2020; Roostaei *et al.*, 2014). The neocerebellum, which corresponds to the cerebrocerebellum, is the newest component of the cerebellum that evolved in

primates, possibly due to the growth of the cerebral cortex in higher mammals (Buckner *et al.*, 2013; Lara-Aparicio *et al.*, 2022). Except for the pyramid and uvula, the neocerebellum contains the posterior lobe that is primarily involved with the seamless execution of dexterous voluntary motions via the corticopontocerebellar pathway (Buckner *et al.*, 2013; Lara-Aparicio *et al.*, 2022).

### **2.2.2 Histology of the Cerebellum**

Granule and Purkinje cells are the two main neuron types that dominate the cerebellar circuit. In addition, parallel fibres (which are the axons of granule cells) and climbing and mossy fibres (which penetrate the cerebellum from the outside) are the three most important axon types. Climbing fibres and mossy fibres form the starting points of the two primary pathways that pass through the cerebellar circuit before ultimately ending in the deep cerebellar nuclei (Goodlett & Mittleman, 2017; Roostaei *et al.*, 2014).

#### **2.2.2.1 Cortical Layers of the Cerebellum**

Three layers make up the cerebellar cortex, and from deep to superficial comprise of the granular, Purkinje and molecular layers. The thick layer of granule cells and interneurons, primarily Golgi, Lugaro, and unipolar brush cells, forms the deep layer. The Purkinje cell layer, a slender region in the centre, is home to the cell bodies of Bergmann glial and Purkinje cells (Knierim, 2020; Roostaei *et al.*, 2014). The flattened Purkinje cell dendritic trees with their connected array of parallel fibres are found in the molecular layer, which is located at the top. Stellate cells and basket cells, which form GABAergic synapses with Purkinje cell dendrites, are two other forms of inhibitory interneurons found in this outermost layer (Goodlett & Mittleman, 2017; Lara-Aparicio *et al.*, 2022). The Purkinje cells, identified by Jan Evangelista Purkyně, a Czech anatomist, in 1837, are

one of the first and most recognisable neurons in the brain. Their dendritic tree branch repeatedly and are characterised by their flat terminals, which are directed in the opposite direction of the cerebellar folds. Parallel fibres travel to and provide synaptic information through the thick planar net formed by a Purkinje cell's dendrites at exactly 90 degrees. In the brain, Purkinje cells generate more synaptic signals than any other cell type, with each Purkinje cell receiving up to 200,000 parallel fibre spines (Knierim, 2020; Llinas *et al.*, 2004). Following the release of collaterals that impact adjacent regions of the cortex, Purkinje cell axons proceed through the deep cerebellar nuclei, where they establish approximately 1,000 interactions with various nuclear cell types within a limited area. Targets are inhibited by Purkinje cells because they use GABA as their neurotransmitter (Paul & Limaïem, 2019; Lara-Aparicio *et al.*, 2022). Granule cells, unlike Purkinje cells, are among the brain's smallest and most abundant neurons, with an estimated 50 billion of them thought to exist in humans, emphasising that around three-quarters of all neurons in the brain are cerebellar granule cells (v, 2020; Llinas *et al.*, 2004). At the base of the cerebellar cortex, their cell bodies are densely packed together, with about four to five dendrites projecting as a dendritic claw, which is a terminal expansion. Mossy fibres provide excitatory input to these enlargements, while Golgi cells provide inhibitory input (Lara-Aparicio *et al.*, 2022; Knierim, 2020).

#### **2.2.2.2 Deep Nuclei of the Cerebellum**

It is essential to comprehend the inputs, outputs, and physical connections between the several deep cerebellar nuclei and other subdomains of the cerebellum. This is because, given that all cerebellar output originates from the deep nuclei, damage is equivalent to a lesion to the entire cerebellum (Knierim, 2020; Roostaei *et al.*, 2014). The fastigial nucleus, located most medially,

receives its inputs from the vermis and cerebellar afferents (that convey vestibular, visual, proximal somatosensory, and acoustic data) and sends out outputs to the reticular formation and vestibular nuclei (Patestas *et al.*, 2025; Knierim, 2020). The interposed nucleus, comprising of globose and emboliform nuclei, is lateral to the fastigial nucleus. It receives its inputs from the intermediate zone and cerebellar afferents (that convey visual, spinal, acoustic, and proximal somatosensory data) and sends out output to the contralateral red nucleus, from where the rubrospinal tract originates (Patestas *et al.*, 2025; Knierim, 2020). The dentate nucleus, situated laterally to the interposed nuclei, is the largest of the cerebellar nuclei. It receives input from both the lateral hemisphere and cerebellar afferents (which convey data from the cerebral cortex utilising the pontine nuclei) and sends out outputs to the ventrolateral (VL) thalamic nucleus and contralateral red nucleus (Knierim, 2020; Ristanovic *et al.*, 2010; Lara-Aparicio *et al.*, 2022). The vestibular nuclei, which are located in the medulla, have functionally similar connection patterns to those of the cerebellar nuclei, even though they are not exclusively cerebellar nuclei. It receives input from both the vestibular labyrinth of the inner ear and the flocculonodular lobe, while efferents form the vestibulospinal tracts that project to different motor nuclei (Knierim, 2020; Lara-Aparicio *et al.*, 2022). Besides these inputs, the inferior olive complex of the medulla provides unique inputs to all regions of the cerebellum, including the cerebellar nuclei. The regions of the cerebellar cortex from which the cerebellar nuclei receive input correspond to their physical placements. As a result, the medially placed vermis provides input to the medially placed fastigial nucleus, the relatively lateral intermediate zone provides input to the relatively lateral interposed nuclei, and the lateral hemispheres provide input to the most laterally placed dentate nucleus (Knierim, 2020; Ristanovic *et al.*, 2010).

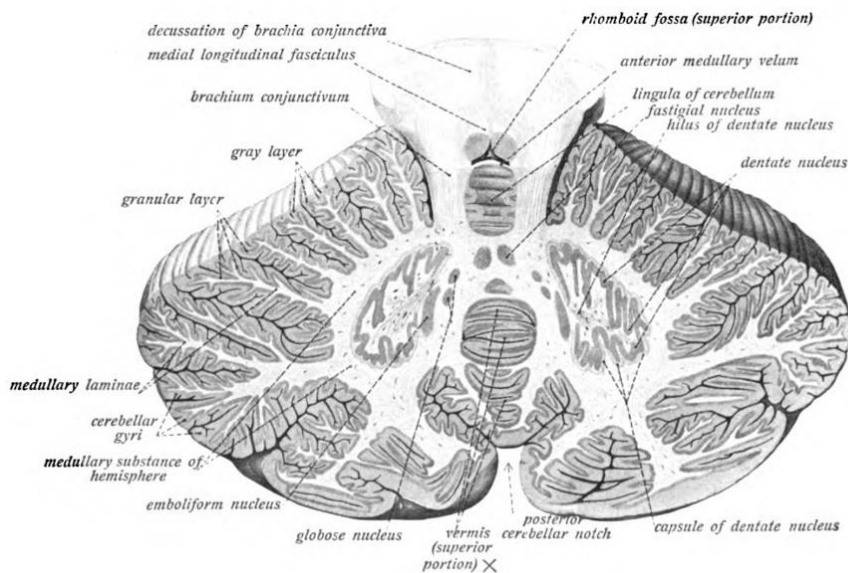


Figure 2.2: Representation of the deep cerebellar nuclei (Patestas *et al.*, 2025)

### 2.2.3 Cerebellar Connectivity

It has been projected that there are millions of mossy fibres in the human cerebellum that penetrate the granular layer from their origins, which include the pontine nuclei (main source), vestibular nuclei, and spinal cord, among others (Goodlett & Mittleman, 2017; Patestas *et al.*, 2025). These fibres connect to the cells of the deep cerebellar nuclei and cortical granule cells to produce excitatory synapses. A mossy fibre produces several expansions known as rosettes inside the granular layer where it forms structures known as glomeruli by synapsing with granule cell dendrites. A mossy fibre rosette sits in the middle of each glomerulus, and as many as twenty granule cell dendrites, which receive inhibitory synapses from Golgi cell endings, connect to it. Parallel fibres axons are sent upward into the Purkinje cell layer by the granule cells, where each

axon splits into two, releasing a collateral in opposing directions that form excitatory synapses with Purkinje cells. Due to the considerable amount of divergence of the synapses between mossy fibres and granule cells, each parallel fibre contacts hundreds of Purkinje cells, therefore, thousands of mossy fibres can dissynaptically impact each Purkinje cell's activity (Knierim, 2020; Goodlett & Mittleman, 2017). Climbing fibres carry information to Purkinje cells and collaterals to the deep cerebellar nuclei from the inferior olivary nucleus, which is located in the medulla oblongata (Knierim, 2020; Goodlett & Mittleman, 2017). Once inside the cortex, it divides into roughly ten terminal branches, each of which supplies input to a single Purkinje cell's dendrites, by twisting across them and creating up to 300 synapses in the process (Goodlett & Mittleman, 2017; Patesta *et al.*, 2025; Llinas *et al.*, 2004). Complex spike in the Purkinje cells can be produced by a single action potential from a climbing fibre given that their net input is usually the strongest. Purkinje cells serve as the cerebellar only output source, notably, by making contact with the cerebellar deep nuclei in an inhibitory manner. The deep cerebellar nuclei, in turn, act as the only output source for the entire cerebellum (Knierim, 2020; Patesta *et al.*, 2025; Llinas *et al.*, 2004).

#### **2.2.4 Functional Anatomy**

The cerebellum performs various functions, including the preservation of posture, maintaining of balance through postural modifications, as well as the learning of new motor skills. It adjusts signals to motor neurons based on input from proprioceptors and vestibular receptors to account for changes in muscle load or body position (Knierim, 2020; Paul & Limaiem, 2019; Pisotta *et al.*, 2014). In an attempt to compensate for their balance issues, patients with cerebellar impairment frequently adopt stereotypical postural techniques such as a wide-based stance. Coordinating the

time and strength of many distinct muscle groups working together in a time-coordinated manner to create seamless limb or body motions is one of the cerebellum's primary functions (Patestas *et al.*, 2025; Lara-Aparicio *et al.*, 2022; Apps *et al.*, 2005). Motor learning, a key component of motor training in the cerebellum, occurs via an approach of trial and error, such as the learning of how to strike a baseball (Roostaei *et al.*, 2014; Hoxha *et al.*, 2016). The cerebellum plays a role in some cognitive processes, including language, but its roles in motor regulation, which is crucial in adjusting and perfecting motor programs to produce precise motions, are best understood. As a result, similar to the basal ganglia, the cerebellum has long been seen as a component of the motor system, but its roles go further than motor control through mechanisms that are currently unclear (Goodlett & Mittleman, 2017; Knierim, 2020).

### **2.2.5 Cerebellar Dysfunction**

The cerebellum, is characterised by a wide range of neurological disorders that alter the cerebellum's feedback loops with other regions of the nervous system, thereby affecting its regulation of motor control, balance, and motor learning (Goodlett & Mittleman, 2017). Cerebellar dysfunction is a disorder marked by imbalance, coordination issues, and abnormalities of gait, which arises due to disruption to cerebellar integrity and connectivity (Roostaei *et al.*, 2014). A neurological evaluation consisting of finger-pointing tests, postural assessment, and gait examination (a broad-based gait is suggestive of ataxia) is used to detect cerebellar issues (Wright *et al.*, 2016). A magnetic resonance imaging test can be utilised to get a comprehensive image of any potential structural changes if cerebellar dysfunction is suspected (Heidelberg *et al.*, 2018; Gudlavalleti *et al.*, 2022; Goodlett & Mittleman, 2017).

### 2.2.5.1 Ataxia

There are many different causes of ataxia, which is a typical observation in neurological tests. These include acute cerebellar injuries brought on by oedema, haemorrhage, and infarction, as well as chronic, gradually progressing cerebellar damage. In previously healthy individuals, acute ataxia is a phenomenon that manifests in less than 72 hours. Hospitalisation and a thorough laboratory investigation are typically the outcomes of acute ataxia. Choosing the scope and frequency of the initial assessment is a common dilemma for clinicians, especially when trying to identify treatment options (Pedroso *et al.*, 2019; Kuo *et al.*, 2021).

Depending on which area of the cerebellum is affected and how it is injured, motor-related symptoms are frequently the most common complications of cerebellar damage. A changed, uneven walking gait, with a broad stance due to trouble balancing, is one of the symptoms of damage to the flocculonodular lobe (Patestas *et al.*, 2025; Knierim, 2020). Errors in the speed, force, amplitude, and direction of motions can result from damage to the lateral zone, which usually affects skilled, conscious, and planned movements. Injury concentrated further laterally is more likely to impair skilled motions of the hands or limbs, and damage to the midline section may impair movements throughout the entire body. Injury to the lower portion of the cerebellum could result in uncoordinated or poorly directed movements of the arms and hands, in addition to difficulty with speed of movement. Injury to the top section of the cerebellum tends to induce gait problems and other leg coordination issues (Tada *et al.*, 2015; Lara-Aparicio *et al.*, 2022).

### **2.2.5.2 Dysmetria**

Dysmetria, meaning difficulty in determining ranges or distances of movement, is one of the main symptoms of both cerebellar cognitive affective syndrome (dysmetria of cognition) and cerebellar motor dysfunction. In 1899, Babinski published the first report on dysmetria with hypermetria, a movement that overshoots the target, as its most prevalent type. In the finger-to-nose test, for instance, the index finger first moves in the desired direction before hitting the cheek after going over the targeted nose (Cabaraux *et al.*, 2020). Until the finger eventually reaches the nose, that movement finishes in a few oscillations. Hypometria, an undershoot or abrupt arrest before the goal, is another symptom that cerebellar patients may exhibit. Both types of dysmetria can coexist in certain patients. Others experience an abnormal recovery following an acute cerebellar lesion, which could be as a result of cerebellar stroke, with hypometria following hypermetria. These notable characteristics were described by Garcin as disruptions in the amplitude of motions (Cabaraux *et al.*, 2020; Schmahmann, 2019). When tasks are executed as quickly as feasible, motor deviation increases more substantially, and patients struggle to use a compensating approach. In contrast to healthy controls, cerebellar victims had a circuitous spatial path with Subjects rectifying their movements toward the objective using visual direction. The clinical observation implies that the abnormal motions seen in dysmetria are caused by a defect in the central processing and peripheral feedback loop (Schmahmann, 2019; Cabaraux *et al.*, 2020).

### **2.2.5.3 Dysdiadochokinesia**

The incapacity to execute quick, alternating muscular movements is known as dysdiadochokinesia. Rapid tapping of fingers, supination/pronation, tapping with the foot, and fist opening and closing are examples of actions that can occur quickly and synchronously. In patients who may

have cerebellar dysfunction, it is crucial to assess this component. Many lifetime assessments of disability that result in a loss of speech and limb coordination are well correlated with these activities (Cabrero & De Jesus, 2023). Using the alternative motion rate (AMR), it can be measured for instance, that vocal commands, including noting the amount of syllable recurrence in a given amount of time (usually less than one minute), can be used to measure speech AMR. The reason for this deficit could be that corticocerebellar connections increases later in life, while myelination declines at younger age (Cabrero & De Jesus, 2023; Schmahmann, 2019).

#### **2.2.5.4 Nystagmus**

It is an oscillatory, repetitive, and uncontrolled eye movement, that could be rapid, sluggish, or a mix of the two. It may have positional gaze or head posture inducements, be persistent, or be intermittent. It can be differentiated from fast acting, mimicking aberrant spontaneous eye movements, such as oscillations and saccades (Eggers, 2019; Gudlavalleti *et al.*, 2022). These motions can impair coordination, equilibrium, depth perception, and vision. Nystagmus is frequently a temporary condition that could be a sign of an underlying illness and can be classified as latent, apparent, or both. For clinical and scientific objectives, the Bárány Society Classification Committee created various categories of nystagmus, with a focus on a universal language for vestibular disorders. Diseases that impact the cerebellum, ventral visual pathways, cerebral cortex, peripheral vestibular apparatus, and brainstem can cause pathological nystagmus (Eggers, 2019; Schmahmann, 2019).

Additional symptoms of cerebellar dysfunction include intention tremor (unconscious movement brought on by alternating spasms of opposing muscle groups), dysarthria (difficulty with speech

expression), dysphagia (difficulty in swallowing), and hypotonia (reduced muscle tone) (Schmahmann, 2019; Gudlavalleti *et al.*, 2022).

### **2.2.6 Aetiology of Cerebellar Dysfunction**

These are caused by underlying factors with numerous clinical presentations secondary to non-degenerative conditions, such as heavy metal poisoning, cancer, stroke, haemorrhage, cerebral oedema, gunshot wounds, as well as chronic degenerative conditions like olivopontocerebellar atrophy (Kuo *et al.*, 2021; Pedroso *et al.*, 2019; Roostaei *et al.*, 2014).

#### **2.2.6.1 Structural Abnormalities and Genetic Factors**

Clinical examination may imply a variety of hereditary diseases with other symptoms of spinocerebellar ataxias such as peripheral neuropathy, ophthalmoplegia of autosomal dominant inheritance, and signals related to the higher motor neurons and extrapyramidal system usually present. Friedreich ataxia as observed through fundoscopy is an autosomal recessive disorder that is associated with hearing loss, cardiac hypertrophy, diabetes mellitus, peripheral nerve damage, spasms, and visual atrophy (Kuo *et al.*, 2021; Gudlavalleti *et al.*, 2022). Patients with Friedreich ataxia often need wheelchairs, with the condition usually manifesting between the ages of 8 and 15. Although dystonia, chorea, skin and eye telangiectasia are clinical indicators, telangiectasia ataxia is additionally a disorder that is autosomal recessive. Predominant cerebellar characteristics can be seen in von Hippel-Lindau syndrome, bilateral or unilateral pontocerebellar degeneration, hypoplasia, multiple system atrophy, and cerebellar haemangioblastomas that is linked to cancer of kidney cells (Schmahmann, 2019; Kuo *et al.*, 2021).

### **2.2.6.2 Paraneoplastic Syndromes and Infections**

Clubbing, lymph node swelling, tar staining, hepatocellular inflammation, palpable lumps, and other clinical characteristics linked to small cell respiratory tumours, hepatic cell cancer, chronic liver disorders, uterine, testicular, and breast cancers, as well as Hodgkin lymphoma, may be seen. Toxoplasmosis, borreliosis, AIDS, syphilis, and viral infections are examples of infectious etiologies. Chronic degenerative conditions like olivopontocerebellar atrophy can also cause cerebellar injury (Pedroso *et al.*, 2019; Roostaei *et al.*, 2014; Schmahmann, 2019). Cerebellar injury can also be caused by diseases such as Creutzfeldt-Jakob disease, Bickerstaff encephalitis and Whipple disease (Kuo *et al.*, 2021).

### **2.2.6.3 Toxic and Metabolic Factors**

Cerebellar integrity can be subtly compromised by toxins (such as Pb), pharmacologic etiologies (such as carbamazepine, phenytoin, and barbiturates), and metabolic imbalances (such as a lack of vitamin E, B12, or copper) (Kuo *et al.*, 2021; Gudlavalleti *et al.*, 2022). Wernicke-Korsakoff syndrome, a thiamine deficiency disorder brought on by chronic alcohol abuse, causes significant cerebellar atrophy and ataxia. Excitotoxic cascades that specifically damage cerebellar Purkinje cells are also triggered by hypoglycemia, hepatic encephalopathy, severe electrolyte abnormalities (such as hyponatremia), hypothyroidism, mood disorders, bowel and sleep habit dysfunction, or in relation to other autoimmune diseases. With the supposition that toxicity and density are connected, Tchounwou *et al* (2012) described heavy metals as metallic elements or compounds with a comparatively high density to water. Because they are frequently utilised, certain elemental or mixed compounds of these metals are highly poisonous. Lead (Pb), chromium, arsenic, mercury, and cadmium are commonly found in the environment and thus have

the highest toxic impact on the body (Baird & Cann, 2012). Pb and mercury produce a deficit in the nervous system, cadmium produces a degenerative bone condition, and arsenic and chromium normally cause cancer (Lawal *et al.*, 2021). In cerebellar neurons, heavy metals such as Pb build up, causing oxidative stress and neurotransmission loss (Saleh & Meligy, 2018; Roostaei *et al.*, 2014).

### **2.3 Lead**

Lead (Pb) is a compact, bluish-grey heavy metal that is renowned for its ductility, malleability, and capacity to create both inorganic salts and organo-Pb compounds. It melts at 621.43°F, has a density of 11.34 g/cm<sup>3</sup> and an atomic weight of 207.2 u. Pb is a persistent environmental pollutant because it is chemically stable and nondegradable. Pb and its compounds, like lead acetate (PbA), are one of the most prevalent heavy metal toxicants (Assi *et al.*, 2016). It is the main active component in progressive hair dyes where Pb is utilised as a fixative for certain dye types and as a reagent to create other Pb compounds.

#### **2.3.1 Pb prevalence rate:**

The Solar System has 0.121 parts per billion (ppb) of Pb per particle (Boldyrev, 2018). The majority of heavier metals, each of which is unstable, eventually decay to Pb (Lochner *et al.*, 2005), thereby raising the universe's Pb content level (Roederer *et al.*, 2009). Its earth prevalence rate is 4 mg/kg in plants, 0.1 µg/m<sup>3</sup> in the air, 5 µg/L in salt and freshwater, and 100 mg/kg in the soil, which are the approximate environmental values of Pb (Rieuwerts, 2015). Pb hardly exists in its natural, metallic state (Davidson *et al.*, 2014), rather, per the Goldschmidt classification, Pb is a chalcophile, implying that it is typically found in combination with sulfur (Langmuir & Broecker, 2012). Galena (PbS), the primary Pb-bearing mineral, is primarily found alongside zinc ores

(Davidson *et al.*, 2014). Due to their relative lightness, many Pb minerals have stayed in the crust throughout Earth's history rather than moving deeper into the planet's interior. This clarifies why Pb, the 36th most prevalent element in the crust, has a comparatively high crustal prevalence of 14 ppm (Emsley, 2011).

### **2.3.2 Human Exposure and Metabolism**

As one of the first metals identified by humans, Pb is ubiquitous, with its non-biodegradable property being the primary cause of its long-term survival in the environment. Pb's special qualities, such as its pliable nature, flexibility, toughness, and corrosion resistance, have led to its extensive use in a variety of sectors, including paint, polymers, ceramics, and automotive. As a result, free Pb has become far more common in our environment. Given that Pb extraction, processing, battery production, waste disposal, and reuse are widespread in many nations, Pb contact has become a key global concern. Pb normally enters the body through skin, food, or airways (Aktepe *et al.*, 2022; United States Food and Drug Administration, 2015). The body absorbs almost all of the Pb that is inhaled, with the ingestion rate ranging from 20 to 70%, and children taking a larger proportion than adults (Tarrago, 2012). Ingestion of Pb-contaminated food or drink is primarily the cause of Pb poisoning. Pb can be present in fruits and vegetables that have been grown in Pb-tainted soil; Pb containing water pipes that have been degraded by soft acidic water; as well as seawater products that have been impacted by adjacent runoff industrial waste (Dongre, 2020). Though Pb toxicity is a highly investigated and comprehensively documented topic, complete management and prevention of contact with Pb is still far from being attained. The duodenum is a particularly active site of absorption for ingested Pb via both DMT1-mediated and DMT1-independent pathways (Aktepe *et al.*, 2022). Particle solubility, age,

nutritional status, and the presence of competing dietary minerals (like calcium and iron) are some of the factors that affect gastrointestinal uptake. Under one per cent of the ingested Pb in the blood stays dissolved in plasma, with the remaining 99% attaching itself to red blood cells that travels to tissues and organs such as bone, liver, kidneys, and the brain. Pb storage in the human body is primarily in the bones (Boskabady *et al.*, 2022; Brodziak-Dopierała, 2020). Bones have two Pb storage compartments, which include the exchangeable pool at the bone's surface, from where Pb can quickly enter plasma, and the non-exchangeable pool deep in the bone's cortical region, from where Pb can transfer to the surface during active bone reabsorption (Boskabady *et al.*, 2022). Stable Pb isotope methods have confirmed that between 40 and 70% of the Pb released into the bloodstream of adults comes from bones (Brodziak-Dopierała, 2020). Given that adults keep 85–95% of Pb in their bones compared to 70% in children, it is believed that children have greater levels of Pb in their soft tissues when compared to adults (Reuben, 2018). Several variables, including age, pregnancy, gestation, race, and the amount of Pb exposure, affect how Pb is stored and mobilised in bones. Pb is gradually removed from the body, mostly through urine (about 70–80% of total output), with the rest being lost through sweat, faeces, nails, and hair (Collin *et al.*, 2022). Due to the slow detoxification process and the fact that most Pb hides in bone, even low exposure to Pb can have a lasting adverse effect on a patient's health.

### **2.3.3 Toxicity**

No amount of Pb seems to be essential to the body, and no "safe" level of Pb exposure has been identified, Pb toxicity is a notably severe hazard that can cause lasting health issues. It is known to interact with a variety of bodily functions, particularly affecting the nervous, renal, hepatic, and haematological systems, resulting in significant illnesses (de Souza, 2018). Acute toxicity is associated with occupational exposure and is infrequent. Chronic toxicity, on the other hand, is

significantly more prevalent and occurs when blood Pb concentrations are around 40-60 µg/Dl (Acharya, 2024).

In contrast to other organ systems, the nervous system seems to be the most vulnerable and primary target for Pb-induced toxicity (Singh *et al.*, 2018). Pb exposure causes effects on both the central and peripheral nervous systems, with the peripheral nervous system being more pronounced in adults and the central nervous system being more prominent in children (Kim *et al.*, 2015). One direct result of Pb exposure is encephalopathy, which is a gradual degeneration of certain parts of the brain and manifests as dullness, irritability, headaches, tremors, cognitive impairment, peripheral neuropathy, and hallucinations (Ortega *et al.*, 2021; Alisha *et al.*, 2018). At very high exposures, more severe manifestations include delirium, lack of coordination, seizures, paralysis, unconsciousness, and ataxia (da Silva *et al.*, 2020; Mason *et al.*, 2014). By getting through the blood-brain barrier via the imitation of calcium, Pb can weaken neurons' myelin sheaths, diminish their quantity, slow down the formation of new neurons, and obstruct neurotransmission pathways (Singh *et al.*, 2024; Mandal *et al.*, 2022).

Pb inhibits several important enzymes involved in the heme production pathway, which limits the manufacture of haemoglobin and has a direct impact on the haematological system. This makes cell membranes more brittle, thereby shortening the lifespan of circulating erythrocytes. Anaemia results from the combined effects of these two mechanisms (Ghasemi *et al.*, 2017; Mani *et al.*, 2019).

Renal impairment typically happens at elevated concentrations of exposure to Pb (>60 µg/dL), with an altered tubular transport system being the functional hallmark of acute nephropathy (Kuraeiad & Kotepui 2021). Conversely, chronic nephropathy is distinguished by glomerular and

tubulointerstitial alterations that lead to hypertension, hyperuricemia, and renal failure (Kuraeiad & Kotepui, 2021).

Pb poisoning, whether acute or chronic, damages the heart and arteries, which can result in potentially fatal outcomes such as hypertension, peripheral vascular disease, cerebrovascular accidents, and ischemic coronary cardiac disease (Singh *et al.*, 2018).

Both male and female reproductive functions are negatively impacted by Pb in several ways. Common impact on men include chromosomal damage, infertility, aberrant prostatic function, altered serum testosterone levels, decreased sexual desire, and defective spermatogenesis (lower motility and quantity). According to Flora *et al.* (2011), women are more likely to experience fertility problems, miscarriage, premature rupture of the membrane, pre-eclampsia, pregnancy arterial hypertension, and early birth (León & Pacheco, 2020).

#### **2.3.4 Mechanism of Pb-induced neurotoxicity**

Pb's neurotoxicity results from its propensity to disrupt the normal activity of enzymes, accumulate in neurons and glia, disrupt synapse development and plasticity, and cross the blood–brain barrier (via calcium transporters). It accomplishes this by either imitating and dislodging other metals that function as cofactors in numerous enzyme-mediated processes or by attaching itself to the sulfhydryl groups present on various enzymes (Carocci *et al.*, 2016). Insufficient amounts of iron and calcium enhance vulnerability to Pb toxicity, whereas elevated concentrations appear to offer some protection (Talpur *et al.*, 2018). The most researched heavy metal is most likely Pb, with numerous cellular, intracellular, and molecular pathways having been shown to underlie the toxicological mechanism of Pb in the brain, according to studies conducted in this area (Flora *et al.*, 2012).

#### 2.3.4.1 Oxidative stress

Oxidative stress is characterised by an imbalance between the production of free radicals and the body's ability to detoxify or repair the damage caused by reactive intermediates (Carocci *et al.*, 2016). Pb exposure has been identified as a key mechanism for this type of toxicity, with two distinct processes working together to induce oxidative stress. At the beginning, ROS such as hydrogen peroxide ( $H_2O_2$ ), singlet oxygen, and hydroperoxides ( $HO_2$ ) are produced, and subsequently, the oxidative enzyme reserves get depleted (Carocci *et al.*, 2016). In cells, the body's antioxidant defences are triggered to neutralise ROS, with the tripeptide glutathione (GSH) playing the largest role out of the cell's antioxidant arsenal. GSH, containing sulfhydryl groups, is present in mammalian tissues at millimolar levels, serving as a critical antioxidant to silence free radicals (Averill-Bates, 2023). Glutathione redox cycle is critical in the maintenance of cellular homeostasis and signal transduction. The ratio of glutathione to glutathione disulfide (GSH/GSSG) serves as a sensitive indicator of the cell's overall redox state, which must be tightly controlled to limit oxidative damage to cellular components. Oxidative stress causes the ratio of GSSG to GSH to increase and triggers stress response pathways within the cell. Under normal conditions, the concentration of reduced glutathione, GSH, is much higher than that of oxidised glutathione, GSSG. Covalent bonds are formed as a result of Pb's propensity to share electrons and these bonds are made between the Pb molecule and the sulfhydryl groups found in antioxidant enzymes, which are Pb's most vulnerable targets, inducing their deactivation. By attaching itself to glutathione's sulfhydryl groups, Pb renders it inactive. According to Averill-Bates, 2023, Pb also depresses glutathione levels by inactivating enzymes such as glutathione reductase (GR), glutathione peroxidase (GPX), glutathione-S-transferase, and  $\delta$ -aminolevulinic acid dehydratase (ALAD). In addition to targeting the sulfhydryl chains, Pb may additionally substitute the zinc ions that are

crucial substrates for these antioxidant enzymes, rendering them inactive. Two other noteworthy antioxidant enzymes that are made inactive by Pb are catalase (CAT) and superoxide dismutase (SOD), where a decrease in CAT concentration hinders the scavenging of superoxide radicals ( $O_2\bullet^-$ ) and a decrease in SOD concentration diminishes the elimination of superoxide radicals (Carocci *et al.*, 2016).

As established in Carocci *et al.*, (2016) research, oxidative stress has impacts that may be detected using a variety of indicators, including lipid peroxidation, which is one of the most well-researched ROS effects on lipid membranes. Cell membranes are made up of lipids, and free radicals produced by ROS steal electrons from them, inducing damage. In addition to lipid peroxidation, Pb inhibits ALAD, with the resulting haemoglobin oxidation leading to red blood cell hemolysis. Subsequently, an increase in the substrate ALA levels in both the blood and urine can be used as an indicator. These elevated ALA levels generate superoxide and hydrogen peroxide radicals that react with oxyhemoglobin, causing the formation of hydroxyl radicals. As these processes develop, the cell becomes more vulnerable to oxidative stress, which could result in cell death.

#### **2.3.4.2 Ionic mechanism**

Pb's primary mechanism of action is due to its capacity to displace monovalent cations such as  $Na^+$  and other bivalent cations such as  $Ca^{2+}$ ,  $Mg^{2+}$ , and  $Fe^{2+}$ , though bivalent cations are more readily substituted. Numerous basic physiological functions, including intracellular and intercellular communication, cell adhesion, protein structure and development, apoptosis, ionic transport, enzyme control, and neurotransmitter release, are significantly affected (Carocci *et al.*, 2016). The ionic mechanism primarily contributes to neurological disorders, as Pb, after replacing calcium ions, can effectively cross the blood-brain barrier (BBB) at a higher rate and accumulate in astroglial cells that contain Pb-binding proteins. Pb readily harms developing astroglial cells and

obstructs the formation of the myelin sheath, both essential to the formation of the blood-brain barrier (BBB). Key mediators like protein kinase C, which controls long-term brain excitation and memory storage, can be impacted by Pb's ability to replace calcium, even at picomolar concentrations. It also has an impact on sodium ion concentration, which is in charge of many essential biological processes, such as the production of action potentials in excitatory tissues for communication between cells, the uptake of chemical messengers (choline, dopamine, and GABA), and the control of synaptosomes' uptake and retention of calcium (Talpur *et al.*, 2018). The regular operation of the previously indicated sodium dependent activities is significantly hampered by this association involving Pb and sodium (Carocci *et al.*, 2016).

#### **2.3.4.3 Apoptosis**

According to Han *et al.* (2021), Pb mostly causes programmed cell death by interfering with mitochondrial integrity and starting the intrinsic apoptotic cascade. Cytochrome c can escape into the cytosol when Pb builds up inside cells because it encourages the opening of the mitochondrial permeability transition pore (mPTP), which collapses the inner membrane potential. When cytochrome c enters the cytoplasm, it attaches itself to apoptotic protease activating factor-1 (Apaf-1) and draws procaspase-9 to create the apoptosome, which cleaves and activates caspases that are executors, including caspase-3. The distinctive morphological and biochemical characteristics of apoptosis are then caused by activated caspase-3 cleaving a variety of downstream substrates, such as structural proteins, DNA repair enzymes, and cell cycle regulators (Asadi *et al.*, 2022). Another important factor that triggers Pb-mediated apoptosis is a persistent increase in intracellular  $\text{Ca}^{2+}$  concentration. Pb overloads the cell's buffering capacity by causing both extracellular  $\text{Ca}^{2+}$  inflow and mitochondrial  $\text{Ca}^{2+}$  release, which upsets calcium homeostasis (Panda *et al.*, 2021). This calcium spike intensifies the formation of reactive oxygen species (ROS)

and encourages mPTP opening, resulting in a vicious cycle of mitochondrial damage and oxidative damage. Calcium driven apoptotic signalling in neuronal cells is accelerated by an excitotoxic component added by excessive glutamate release, which is made worse by mitochondrial malfunction (Panda *et al.*, 2021). The balance shifts toward mitochondrial outer membrane permeabilisation and cell death in rodent models when Pb exposure increases pro-apoptotic BAX and decreases anti-apoptotic BCL-2. Pb accumulated in mitochondria and other organelles continues to alter ionic gradients and redox status even after external exposure has ended, occasionally inducing death in vulnerable cell types such as neurons, haematological precursors, and renal tubular cells (Panda *et al.*, 2021).

### **2.3.5 Effects of Pb on the Cerebellum**

The susceptibility of the cerebellum to Pb neurotoxicity has been the subject of several studies, all of which have consistently shown significant histopathological changes in a variety of animal models. Saleh & Meligy (2018) demonstrated that rats treated with 30 mg/kg Pb acetate for two months had significantly fewer Purkinje cells that were smaller, deformed, and had irregular nuclei. observed under an electron microscope, Purkinje cells exhibited a poorly defined nucleus, vacuolated or rarified cytoplasm, as well as small electron-dense mitochondria. Granular cells displayed mitochondria with damaged cristae and vacuolated cytoplasm. Similarly, Enogieru & Iyoha (2024) found that exposing rats to 100 mg/kg of Pb for 28 days not only increased the levels of cerebellar Pb, lipid peroxidation, neurobehavioral deficits, and antioxidant enzymes impairment but also induced structural changes in the cerebellum of Pb-exposed rats, which they attributed to oxidative stress. A study by Zhang *et al.*, (2024) demonstrated the neurotoxic effects of Pb exposure on the cerebellum via its mechanism of interference with neurotransmission, oxidative stress, structural damage, and aberrant apoptosis in a bird animal model utilising Japanese quail

(*Coturnix japonica*). For five weeks, male chicks that were one week old were fed a diet that contained 50, 200, and 500 mg/kg of Pb. The findings demonstrated that Pb produced structural alterations to the cerebellum, which was characterised by Purkinje, granule, and neuroglia cell deformity along with Nissl body abnormalities. Additionally, Pb disrupted cerebellar neurotransmission by raising acetylcholine (ACh) and lowering dopamine (DA),  $\gamma$ -Aminobutyric Acid (GABA), acetylcholinesterase (AChE), and Na<sup>+</sup>/K<sup>+</sup> ATPase. Malondialdehyde (MDA) and reactive oxygen species (ROS) were raised, whereas glutathione (GSH), catalase (CAT), glutathione peroxidase (GPX), and superoxide dismutase (SOD) were reduced. Furthermore, RNA-Seq investigation demonstrated that Pb exposure interfered with cellular signalling networks in the cerebellum. Abdulmajeed *et al.* (2016) reported that giving 0.2% of Pb in drinking water to male Wistar rats for 28 days can cause damage to neural networks, leading to the impairment of neurotransmission, reduced antioxidants, locomotory and exploratory activities, as well as an increase in anxiety and lipid peroxidation. Enogieru and Egbon (2022) observed a considerable drop in brain weights, ambulation, rearing, and discrimination index, and a corresponding increase in grooming and immobility, as well as histological analysis revealing a reduction in cerebellar Purkinje cells following a 28-day, 100 mg/kg Pb exposure. Nam *et al.*, (2019) documented that Pregnant rats which were given Pb in drinking water (0.3% of Pb), had their offspring sacrificed at postnatal day 21, which is when the cerebellar cortex of developing pups resembles the adult brain in form. Result showed that Pb exposure in the cerebellum markedly decreased Purkinje cells, the expression of the synaptic marker (synaptophysin), the  $\gamma$ -aminobutyric acid (GABA) synthesizing enzyme (glutamic acid decarboxylase 67), as well as axonal myelin structural protein. In addition, it also increased the expression of NMDAR1, PSD95, and SODs, whereas glutamatergic N-

methyl-d-aspartate receptor subtype 1 (NMDAR1), anchoring postsynaptic density protein 95 (PSD95), and antioxidant superoxide dismutases (SODs) showed negative changes.

### **2.3.6 Current Treatment Options for Pb-Induced Cerebellar Dysfunction**

To restore excitatory-inhibitory balance, halt the progression of disease, and maintain motor function, treatment options for cerebellar disorders include pharmacological, surgical, transcranial magnetic stimulation (TMS), transcranial direct current stimulation (tDCS), as well as emerging regenerative techniques (Mitoma *et al.*, 2019; Kuo *et al.*, 2021). In individuals who have type 2 episodic ataxia, 4-aminopyridine 15 mg/d likely lowers the frequency of ataxia attacks during a three-month period. Following a period of eight weeks, riluzole most likely improves ataxia symptoms in people with mixed aetiology ataxia, believed to be by modulating the SK channel activities that correct the firing burst of Purkinje cells to tonic firing (Kuo *et al.*, 2021). For individuals with Friedreich ataxia or spinocerebellar ataxia (SCA), deferiprone may exacerbate ataxia symptoms during a 6-month period, but riluzole likely improves ataxia symptoms after 12 months, possibly by normalising the firing pattern of Purkinje cells (Kuo *et al.*, 2021). Lithium most likely has little effect on ataxia symptoms at 48 weeks, whereas valproic acid 1,200 mg/d may help ataxia in people with SCA type 3 after 12 weeks of treatment (Zesiewicz *et al.*, 2018). Thyrotropin-releasing hormone may alleviate some ataxia symptoms in those with spinocerebellar degeneration over a period of 10 to 14 days. Regarding nonpharmacologic alternatives, transcranial magnetic stimulation may enhance cerebellar motor activity at 21 days, where a 4-week inpatient neuromuscular rehabilitation likely improves ataxia and performance for individuals with degenerative ataxias (Kuo *et al.*, 2021). For people with multiple sclerosis-associated ataxia, pressure splints, when used alone, may not offer more support than neuromuscular therapy. Also, the application of stochastic whole-body vibration therapy cannot

be supported or refuted based on available data (Zesiewicz *et al.*, 2018). According to previous studies, administering different antioxidants may help prevent or lessen Pb's harmful effects, including the production of oxidative stress that causes lipid peroxidation, cell membrane rupture, protein oxidation, as well as the oxidation of the genetic materials such as DNA and RNA (Zhang *et al.*, 2024; Carocci *et al.*, 2016). An antioxidant is a material that can stop the oxidation of an oxidizable substrate when it is present in small amounts relative to the substrate's concentration. This is accomplished by transforming lipid radicals and ROS that are present in the biological system into stable molecules by transferring free electrons to them, thereby preventing lipid peroxidation, which harms cell membranes. Flavonoids, tocopherol, minerals, and ascorbic acid are examples of common antioxidants (Parcheta *et al.*, 2021; Mehta & Gowder, 2015; Atta *et al.*, 2017). The goals of treating Pb poisoning are to reduce oxidative damage, expedite excretion, and remove exposure (Collin *et al.*, 2022). By promoting the synthesis of GSH, vitamin B6 also functions as a mild chelator and antioxidant (Hsu *et al.*, 2015). As a potent antioxidant, Vitamin E is present in cell membranes where it protects against lipid peroxidation by blocking the chain reaction of free radicals. When combined with other antioxidants, vitamin E has been shown to exert a more profound impact than when taken alone (Onitsha & Okutu, 2021). Alpha-lipoic acid (ALA) is sometimes called the “global antioxidant” since it is both lipophilic and hydrophilic (Udaipurwala *et al.*, 2025). According to Shanaida *et al.* (2025), its antioxidant activity seems to work by stopping the formation of lipid peroxides and recycling other antioxidants, including vitamin C and vitamin E. Lipoic acid has been shown to be efficient at eliminating Pb from the nervous system (Pande and Flora, 2002). Given their low cost and few side effects, herbal antioxidants can function as effective clinical medicines. Garlic, in addition to being used as a food additive, is said to possess exceptional pharmacological and medicinal qualities, with Allicin, its

active ingredient, giving it both its distinctive smell and therapeutic qualities (Tesfaye, 2021). Garlic eliminates free radicals and neutralises Pb ions to safeguard against oxidative damage, with its preventive effect in lowering Pb load in soft tissues being well documented (Manoj *et al.*, 2017). Curcumin, the active ingredient in turmeric is a polyphenol molecule that is extracted from the plant *Curcuma longa*. It provides chelation capabilities, as well as antioxidant and free radical scavenging activities (Mary *et al.*, 2018). In a 2018 study by Abu-Taweel, curcumin was shown to shield against Pb-induced neurotoxicity in rats. Given the prevalence of Pb and its known toxicity, there is a need for more efficacious medicinal solutions to mitigate Pb-induced neurological perturbation, such as cerebellar dysfunction.

#### **2.4 *Tetrapleura tetraptera***



Figure 2.3: *Tetrapleura tetraptera* plant (Adesina *et al.*, 2016)

Human cultures have recognised the preventive benefits of medicinal plants since ancient times, and this knowledge has been passed down through the centuries (Rahman *et al.*, 2023). Medicinal plants, also referred to as herbal remedies, are readily used in healthcare, especially in the developing world, to combat chronic illnesses (Adusei *et al.*, 2019; Rahman *et al.*, 2023). These substances have a reputation for suppressing ROS, boosting the body's natural antioxidant enzyme activity, and controlling inflammatory processes (Enogieru & Momodu, 2022; Adusei *et al.*, 2019). *Ginseng*, *Chamomile*, *Gingko*, *Echinacea*, *Feverfew*, and *Garlic* are a few well-known medicinal plants. Because they have therapeutic qualities, plants like *Tetrapleura tetraptera* can also be categorised as such (Adesina *et al.*, 2016).

#### **2.4.1 Description**

*Tetrapleura tetraptera* (*T. tetraptera*), or Gum tree in English, is a flowering deciduous plant of the Fabaceae (Leguminosae) family, mostly found in western Africa, where it is referred to as *Prekese* (Twi), *Aridan* (Yoruba), *Ighimiaka* (Edo) and *Oshosho* (Igbo) in the Ghanaian and Nigerian languages (Uyoh *et al.*, 2013). The diverse chemical makeup of *T. tetraptera* contributes to its nutritional benefits. *T. tetraptera* contains a considerable array of nutrients, including carbohydrates, lipids, ash, vitamins, fibre, and proteins (Uyoh *et al.*, 2013). varied portions of the plant's fruit may have varied chemical constituents. For instance, there are notable differences in the mineral and carbohydrate contents of *T. tetraptera* fruit's woody coatings, pulp, and seeds (Adadi *et al.*, 2020).

##### **2.4.1.1 Family (Fabaceae):**

The bean, pea, or legume family, also known as Fabaceae or Leguminosae, and consisting of trees, shrubs, and herbaceous plants (both annual and perennial), are easily identifiable by their compound, stipulate leaves and fruit (legume). The Fabaceae is an extensive and significant family of flowering plants in the tropics (McNeill *et al.*, 2012), that are the most prevalent family in the Americas and Africa's dry forests and tropical rainforests (Siddiqui, 2025). Boasting over 765 genera and close to 20,000 species, the family is broadly dispersed as well as being the third biggest land plant family in terms of species, only surpassed by the Orchidaceae and Asteraceae (Christenhusz *et al.*, 2016). For thousands of years, a variety of Leguminosae, along with grains, some fruits, and tropical roots, have been a staple meal, with their use strongly correlated to the evolution of humans (Smykal *et al.*, 2015).

#### **2.4.1.2 Specie (*Tetrapleura tetraptera*):**

With natural heights of 20 to 25 m and diameters of 1.2 to 3 m, *T. tetraptera* flourishes naturally in the rainforests (Adesina *et al.*, 2016). The plant has a common stem that is 15 to 30 cm long with mild siphoning on top, and leaves that are confined and lightly stubbly. The spike-like panicles, which are 5 to 20 cm long and usually occur in sets on the upper leaf axils, are adorned with pinkish cream flowers. Ten short stamens, anthers with a gland at their ends, and a thin stalk are all present in each flower. On sturdy, 25cm long stalks, are fruit that constantly hang at the tips of the branches, which are dark purple-brown, glabrous, and usually somewhat curled (Adesina *et al.*, 2016). These fruits are generally 15 to 25 cm long and 5 cm wide and features four vertical, wing like folds that are almost 3 cm wide. The small, black, hard, and rattle-adhering flat seeds that are around 8 mm long clutter and firmly embed within the pod's body (Adesina *et al.*, 2016).

#### 2.4.2 Taxonomy (Scientific classification)

Table 2.1: *T. tetraptera* classification according to Schumach and Thonn (1891).

Domain	Eukaryota
Kingdom	Plantae
Phylum	Streptophyta
Class	Equisetopsida
Subclass	Magnoliidae
Order	Fabales
Family	Fabaceae (or Leguminosae)
Subfamily	Mimosoideae
Genus	<i>Tetrapleura</i>
Species	<i>Tetrapleura tetraptera</i>

#### 2.4.3 Conventional Uses of *Tetrapleura tetraptera*

Due to its flavour, *T. tetraptera* is typically utilised in local cuisines. It is used to make "palm nut" soup, a traditional West African delicacy, that is mixed with vegetables like palm fruits, pepper, and garlic (Abugri, 2013). Given that *T. tetraptera* has strong antibacterial qualities, it can be used to preserve foods like chicken and pork. In its use as a natural preservative in the meat industry, *T. tetraptera* root extracts (1% v/v) were applied to pork loaded with  $1 \times 10^4$  CFU/mL of

Staphylococcus aureus and Escherichia coli, for 6 days, which resulted in the reduction of microbial load by about 99.99% (Lin *et al.*, 2019). After being treated with varying doses of aqueous *T. tetraptera* extract (0.25 mg/mL to 1 mg/mL), it was observed that the duration of stored perishables like pepper and tomatoes was extended. The antibacterial, phytochemical, and antioxidant qualities of *T. tetraptera's* aqueous extract are responsible for these actions (Ogunwande *et al.*, 2014)

*T. tetraptera* is included in the boiled wort during the brewing procedure of sorghum beer, also known locally as "Pito," that is widely accessible in northern Ghana as well as other West African countries. It enhances the nutritional value as well as the taste of the brewed "Pito" by aiding in the separation of accessible bioactive components and fragrance (Adadi *et al.*, 2020). According to previous studies, *T. tetraptera* extracts may improve yeast nutrition within the wort, ensuring a smooth and quick fermentation. Gypsum, Calcium chloride, and other minerals are employed in the brewing operations to improve the nutrition of yeast. As 100 mg/mL of *T. tetraptera* extracts were added to a freshly made watermelon beverage, the bacterial and fungal load decreased over seven days as compared to the unpreserved juice (Anumudu *et al.*, 2020). The market for wholesome food that is microbially safe and devoid of chemical preservation agents is growing, given that juices that are freshly prepared in this way are often taken without being chemically or thermally processed, preserving the majority of the nutrients that the user needs.

In addition to its wide range of uses in healthcare and food, *T. tetraptera* can also be added to pet and farm animal feeds for several purposes (Raphaël, 2017). *T. tetraptera* can be used as an alternative to antibiotics in feed additive due to the difficulties associated with the later use in animal feeds. In comparison to chickens on a meal comprising 0.4% *T. tetraptera* and a diet

without supplements, *T. tetraptera* fruit powder showed an increase in body weight (Raphaël, 2017). The aforementioned study found that the feed conversion ratio (FCR) for rosters given a diet supplemented with antibiotics (FCR = 2.02) and 0.2% *T. tetraptera* (FCR = 2.03) was comparable. *T. tetraptera* powder might be used as a potential antibiotic growth enhancer to produce chicken meat without antibiotic residues, as well as halt the development of antibiotic resistance because of its cheaper production costs and better growth performance.



Figure 2.4: Various applications of *T. tetraptera* (Mensah *et al.*, 2024)

#### 2.4.4 Phytochemical Composition of *Tetrapleura tetraptera*

Given its medicinal qualities due to the presence of numerous active phytochemical components, including phenols, flavonoids, steroids, alkaloids, tannins, and saponins, numerous health advantages are believed to be provided by *T. tetraptera* (Kemigisha *et al.*, 2018). An isolate of *T. tetraptera* pulp contains approximately  $0.87 \pm 0.03$  mg QE/g flavonoids,  $3.51 \pm 0.03$  mg GAE/g phenols,  $5.03 \pm 0.15$  %w/w alkaloids, and  $4.27 \pm 0.03$  mg DE/g saponins (Adusei *et al.*, 2019). *T.*

*tetraptera* peels also include  $20.48 \pm 1.18$  mg/100 g flavonoids,  $23.87 \pm 0.44$  mg/100 g tannin,  $1.43 \pm 0.43$  % alkaloids, and  $2.76 \pm 0.15$  % saponins (Erukainure *et al.*, 2017). Although nothing is known about their bioactivity, Additional bioactive substances found in *T. tetraptera* include glycidol, piperazine, 2-hydroxy-gamma-butyrolactone, octodrine, n-decanoic acid, and 6-octadecenoic acids (Erukainure *et al.*, 2017).

#### **2.4.5 Pharmacological Activities of *Tetrapleura tetraptera***

The phytochemicals and other bioactive substances found in *T. tetraptera* offer the plant's extracts vital biological characteristics that are important in traditional medicine. Antioxidant, antimicrobial (e.g., antibacterial, and antifungal), anti-inflammatory, anti-diabetic, antiproliferative (anticancer) are among the biological characteristics of *T. tetraptera* extracts that have been indicated (Anyamele *et al.*, 2023).

##### **2.4.5.1 Antioxidative functions:**

Among *T. tetraptera*'s most potent biological characteristics is its antioxidant activity, which helps explain why it's used in herbal medicine. It functions as a reducing agent, limiting injury to cells by eliminating reactive oxygen species and preventing further oxidation (Adusei *et al.*, 2019). The plant's leaf, fruit, and stem bark all interact to perform this purpose, with the stem bark believed to have a higher capacity to scavenge free radicals than its leaves according to Famobuwa *et al.* (2016) and Koma *et al.*, (2016). This supports the claim that *T. tetraptera*'s fruit and stem bark's possible antioxidant activity may be responsible for the plant effectiveness in traditional medicine (Famobuwa *et al.* 2016). Despite this, Adusei *et al.* (2019) found that *T. tetraptera* pulp has greater antioxidant capacity than both the entire fruit as well as the seeds. One of the main causes of the

antioxidant qualities displayed by plant different parts is the presence of phenolic compounds. Dzah (2022) identified twenty-four (24) phenolic compounds by using an HPLC/LC-MS study and ultrasound assisted on *T. tetraptera* dried fruit extract. Orientin, Epigallocatechin (310.22 µg/g), caffeic acid (344.91 µg/g), ferulic acid 4-O-glucuronide (493.02 µg/g), and ferulic acid 4-O-glucoside (370.58 µg/g) are the numerous components based on concentrations. Compared to gallic acid in HepG2 cells, the extract demonstrated a strong physiological antioxidant effect in a dose-dependent way. The *T. tetraptera* extract and pure gallic acid had the lowest inhibitory concentrations of 171.79 and 242.70 µg/mL, respectively (Dzah, 2022). This effect was anticipated because the *T. tetraptera* extract contains more phenolic chemicals.

#### 2.4.5.2 Anti-microbial functions

Due to the rising cost and resistance of pharmaceutical antibiotics (Ebana *et al.*, 2016), the use of herbal remedies like *T. tetraptera* for the alleviation of a variety of human ailments, including respiratory illnesses, rheumatism, and convulsions, has gained healthcare attention in recent years, particularly in Africa (Koma *et al.*, 2016). **Certain** plant parts such as the leaf, stem bark, and fruits have important roles in antimicrobial action (Ebana *et al.*, 2016). It has been established that *T. tetraptera* leaf extract exhibits antibacterial action against *Candida albicans*, *Pseudomonas aeruginosa*, *Escherichia coli*, and *Staphylococcus aureus* (Larbie, 2020). However, it has also been found that the stem bark extract of *T. tetraptera* exhibits greater antibacterial effect against *Streptococcus pneumoniae*, *S. aureus*, and *Candida spp.* than its leaves (Koma *et al.* 2016). Because of its antibacterial properties, the plant's components may be used sporadically to treat a variety of bacterial and fungal illnesses (Koma *et al.* 2016). Depending on the kind of bacteria being treated and the solvent used to extract the plant's active ingredients, this effect could change.

Commented [h4]: Upper case letter C

In contrast to ethanolic extract, investigations by Enabulele *et al.*, (2019) showed that aqueous extracts of *T. tetraptera* fruit and seed may suppress the growth of *S. aureus* and *Klebsiella pneumoniae*. *T. tetraptera* extracts have antifungal properties against a variety of pathogenic fungi, which are comparable to their antibacterial properties. The components of the plant and the extraction solvent may also have an impact on this. Aqueous fruit extract of *T. tetraptera* can suppress *Mucor* and *Aspergillus*, however, it has been proven inefficient against *Rhizopus*, according to Anyamele *et al.* (2022). Nevertheless, *Rhizopus* growth can be reduced by ethanol, petroleum, and ether extracts (Ebana *et al.*, 2016).

#### **2.4.5.3 Anti-inflammatory functions**

Given that *T. tetraptera* can also be used to treat rheumatic pain, inflammation, and arthritis, its anti-inflammatory properties are another significant biological characteristic (Ayoola *et al.*, 2018). The leaf's anti-inflammatory properties vary depending on the solvent content (Ayoola *et al.*, 2018). Furthermore, *T. tetraptera* fruit's anti-inflammatory properties are responsible for its anti-arthritic properties (Onda *et al.*, 2017). The plant extract's anti-inflammatory properties could be mostly due to *T. tetraptera*'s carvacrol content (Anyamele *et al.* 2022). The vital oil of certain plants contains the monoterpene carvacrol, with its medicinal function rendering it useful in indigenous medicine (de Carvalho *Et al.*, 2020). When measured against some specific pro-inflammatory cytokines, like IL-1 $\beta$  and IL-8, carvacrol has a beneficial lowering impact in a dose-dependent way (de Carvalho *et al.*, 2020). Additionally, research has demonstrated that carvacrol suppresses nitric oxide synthase, cyclooxygenase-2 production as well as inflammatory cytokine levels (Cicalău *et al.*, 2021). Other substances found in *T. tetraptera*, including methyl eugenol, menthol, octadecanoic acid and  $\alpha$ -copaene, are known to offer anti-inflammatory effects

(Anyamele *et al.* 2022). The anti-inflammatory properties of *T. tetraptera* fruit extract were investigated by Ojewole *et al.*, (2004) in a rat model of hind foot oedema induced by egg albumin, with findings showing a dose-dependent decrease in the generated inflammation of 50 to 800 mg/kg (Mensah *et al.*, 2024).

#### **2.4.5.4 Anti-proliferative functions**

Since modern cancer treatments have adverse side effects like toxic exposure, chemo-resistance, and thinning of hair (Ozaslan *et al.*, 2016), chemotherapeutic compounds that have been used in the management and cure of cancer have been produced from medicinal plants (Ozaslan *et al.*, 2016). Less harmful and more efficient methods of cancer management have been demanded due to the impacts of cancer medications (Aikins *et al.*, 2021). *T. tetraptera* is a medicinal plant that has been shown to lower tumour burden as well as proven to be cytotoxic to cancer cells (Ozaslan *et al.*, 2016). Furthermore, it has been revealed that the plant's fruit methanolic extract possesses anti-proliferative properties against human breast cancer and leukaemia (Aikins *et al.*, 2021). The cytotoxicity of different *T. tetraptera* extract concentrations on the human hepatic malignant cell line HepG2 was investigated by Dzah (2022). In comparison to the same quantities of gallic acid, *T. tetraptera* extract exhibited a high cytotoxic profile at all doses (50 µg/mL to 350 µg/mL) (Dzah, 2022). Through a variety of ways, polyphenols have been correlated to triggering cellular death, here, polyphenols may turn into prooxidants under oxidative pressure and generate high levels of reactive oxygen species, which might cause cancer cells to undergo cell death (Dzah, 2022). *T. tetraptera* aqueous extract exhibits prooxidant effects by altering the membrane potential of mitochondria in several tumour cells (Mbaveng *Et al.*, 2021). Additionally, plant polyphenols can

mimic calorie restriction mimetics in cells, which can trigger the molecular processes that control mitophagy and biosynthesis of mitochondria (Davinelli *et al.*, 2020).

#### **2.4.5.5 Anti-hyperglycemic functions**

The World Health Organisation (WHO) estimates that 180 million people globally suffer from diabetes mellitus (DM), which arises as a result of Insulin insufficiency (Omonkhua *et al.*, 2014). Due to the rising number of ailments, diabetes treatment has received an extensive amount of attention in recent years. The majority of allopathic medications have been used to treat diabetes mellitus, however, new research has shown that *T. tetraptera* can also be utilised to treat hyperglycemic episodes (Omonkhua *et al.*, 2014). Many studies have connected diabetes mellitus to the production of reactive oxygen species and a decline in antioxidant competence with antioxidant markers believed to decline in diabetic individuals. Because phytochemicals can scavenge reactive oxygen species and have antioxidant potential, research has proposed using them to treat diabetes (Bacanli *et al.*, 2019). Flavonoids and other phytochemicals have been shown to combat the complications of diabetes (Bacanli *et al.*, 2019), and given that *T. tetraptera* contains a high concentration of flavonoids, this helps to explain its potential for diabetes management (Dzah, 2022). It has been determined that the antioxidant and antihyperglycemic cyclic monoterpene limonene is present in the leaf and stem preparation of *T. tetraptera*, which can help alleviate the complications of diabetes (Anyamele *et al.* 2022). Additionally, a research investigation by Adesina *et al.*, (2016) demonstrated that fruit extract of *T. tetraptera* has superior glucose-lowering efficacy in comparison to glibenclamide, the conventional medication for diabetes mellitus.

Other ailments, treated with *T. tetraptera* in traditional West African medicine include malaria, rheumatism, rash, convulsions, fevers, smallpox, gastric ulcers, diarrhoea, hypertension, coughs, leprosy, jaundice, and haemorrhoids, are (Mensah *et al.*, 2024).

## **CHAPTER THREE**

### **MATERIALS AND METHODS**

#### **3.1 ETHICAL APPROVAL**

The Research Ethics Committee, College of Medical Sciences, University of Benin, Benin City, Nigeria, granted ethical approval for this study before its commencement, with REC Approval Number: CMS/REC/2025/796.

#### **3.2 REAGENT / CHEMICALS**

For the study, Pb acetate (LOBA Chemie, UN NO. 1616) was purchased and utilised. Cerebellar dysfunction was induced at a dose of 100 mg/kg body weight according to earlier studies by Ayuba *et al.*, (2017); Enogieru and Momodu (2022); Enogieru and Iyoha (2023).

#### **3.3 PLANT COLLECTION AND IDENTIFICATION**

*T. tetraptera* fruit was purchased from a Benin market and identified by a plant taxonomist from the Department of Plant Biology and Biotechnology, University of Benin, with the herbarium number (UBH-T472)

#### **3.4 EXTRACT PREPARATION**

*T. tetraptera* fruit was rinsed with tap water, then shade-dried and milled into a powder. The powder was soaked in distilled water for a full day in a separating funnel and was shaken occasionally. The solution was then filtered. After the filtrate had settled, it was decanted. The

filtrate was then freeze-dried using a freeze-drying apparatus and subsequently kept in a refrigerator at -4°C till use.

### **3.5 ACUTE TOXICITY TEST**

An acute toxicity study for aqueous *T. tetraptera* fruit extract was conducted according to Lorke's method (Lorke, 1983).

### **3.6 PHYTOCHEMICAL SCREENING (QUALITATIVE)**

To determine if a class of chemicals is present or not, qualitative screening is utilised (Adusei *et al.*, 2019). A qualitative screening of *T. tetraptera* fruit was conducted at the University of Benin's Pharmacognosy Department. The plant material was checked for flavonoids, tannins, phenols, saponins, steroids, and alkaloids.

#### ***3.6.1 Test for Flavonoids***

1g of extract from *T. tetraptera* fruit was added to 5ml of ethyl acetate and heated over a steam bath for 3 minutes. The mixture was filtered, and 4ml of the filtrate was mixed with 1ml of diluted ammonia solution. Formations of yellow colour that disappear on standing indicate the presence of flavonoids (Edeoga *et al.*, 2005).

#### ***3.6.2 Test for Alkaloids***

Alkaloid determination in the extract was done according to the method of Harborne (1973) as described by Edeoga *et al.* (2005). The prepared 3ml aqueous extract was mixed with an equal volume of 1% hydrochloric acid in a test tube on a steam bath. Mayers and Wagner's reagent was

added to the mixture separately. The turbidity of the resulting precipitate was taken as evidence for the presence of alkaloids.

### **3.6.3 Test for Tannins**

To 1 ml of aqueous extract, 1 ml of newly made 10% KOH was added. The presence of tannins was indicated by dirty white precipitates.

### **3.6.4 Test for Saponins**

2g of extract was boiled in 20ml of distilled water in a water bath and filtered. 5ml from the filtrate were mixed with 2.5ml of distilled water and shaken vigorously for a stable, persistent froth. The frothing was then mixed with three drops of olive oil and shaken vigorously, after which it was observed for the formation of an emulsion, which indicates the presence of saponins (Brunner, 1984).

### **3.6.5 Test for Steroids**

2ml of acetic anhydride was added to 0.5g of extract with 2ml of sulphuric acid. The colour change from violet to green showed the presence of steroids (Edeoga *et al.*, 2005).

### **3.6.6 Test for Phenol**

2ml of distilled water was mixed with a 2ml of plant extract, subsequently 10 % FeCl<sub>3</sub> solution was added. The presence of phenol was indicated by a bluish black colour (Harborne, 1973).

## **3.7 EXPERIMENTAL ANIMALS AND HANDLING**

Sixty four (64) adult Wistar rats were purchased for this study from the Animal House, Department of Anatomy, University of Benin, Benin City, Edo State, Nigeria. The rats were given two weeks to acclimatise before the study began. During this time, the animals were housed in gauze cages equipped with drinkers and faecal collecting bases under standard laboratory conditions for temperature, humidity, and light throughout the experiment. They had unfettered access to normal

**Commented [h5]:** See correction.

**Commented [h6]:** Capital letter T

animal feed (Topfeeds grower mash) and water ad libitum. To determine the total weight required for the experiment, the animals were weighed once every seven days during the trial. The National Research Council's (2011) guidelines for the use and care of laboratory animals were followed by the methods employed in this investigation.

**3.8 ADMINISTRATION METHOD AND DOSAGE SELECTION**

An oral gavage was used to administer the extract to guarantee accurate solution distribution. According to previous studies, the following dosages were administered after determining the acute toxicity of the substances, specifically focusing on estimating the LD50 (Lethal Dose 50%) using Lörke's method (1983). 500mg/kg and 1000mg/kg of aqueous *T. tetraptera* fruit extract, respectively (Bonsou *et al.*, 2022), 100mg/kg of Pb acetate (Ayuba *et al.*, 2017), and 200mg/kg of vitamin E (Molavi *et al.*, 2024). Treatment groups were co-treated with *T. tetraptera* extract before the administration of Pb acetate.

**3.9 EXPERIMENTAL DESIGN**

After acclimatisation, the sixty-four (64) adult Wistar rats weighing 160-180 grams were randomly divided into eight (8) groups (A-H) of eight (8) rats each. The administration period lasted for twenty-eight (28) days.

**Table 3.1: Summary of Experimental Design**

GROUP	REGIMEN
GROUP A	Administered 1ml of distilled water.
GROUP B	100mg/kg body weight (bw) of Pb (Pb)
GROUP C	500mg/kg bw of <i>T. tetraptera</i> + 100mg/kg bw of Pb

GROUP D	1000mg/kg bw of <i>T. tetraptera</i> + 100mg/kg bw of Pb
GROUP E	200mg/kg bw of Vitamin E + 100mg/kg bw of Pb
GROUP F	500mg/kg bw of <i>T. tetraptera</i> only
GROUP G	1000mg/kg bw of <i>T. tetraptera</i> only
GROUP H	200mg/kg bw of Vitamin E

### 3.10 ASSESSMENT OF NEUROBEHAVIORAL ACTIVITY

A digital camera was used to capture all neurobehavioural tests in real time, 24 hours before sacrifice, and at least two separate, qualified observers manually graded the results. The following behavioural tests related to motor skills were carried out:

#### 3.10.1 Open Field Test:

The Open Field Test assess the locomotor activity and exploratory motor function. Every rat was positioned in the middle of a 72 cm x 72 cm by 20 cm hardwood arena, which was divided into 18 cm by 18 cm squares by lines on the floor. Experimental rats were allowed to roam around the open field arena for five minutes for this test. Activities like ambulation (assesses motor function, exploration and anxiety) central square entry (count how many times a rat enters the centre of a square arena and the time spent with all four paws), line crossing (The rat's movement across grid lines within the arena is counted), immobility (the amount of time the rat was fully stationary),

were recorded using a video camera that was positioned on top of the open field apparatus (Perals *et al.*, 2017).

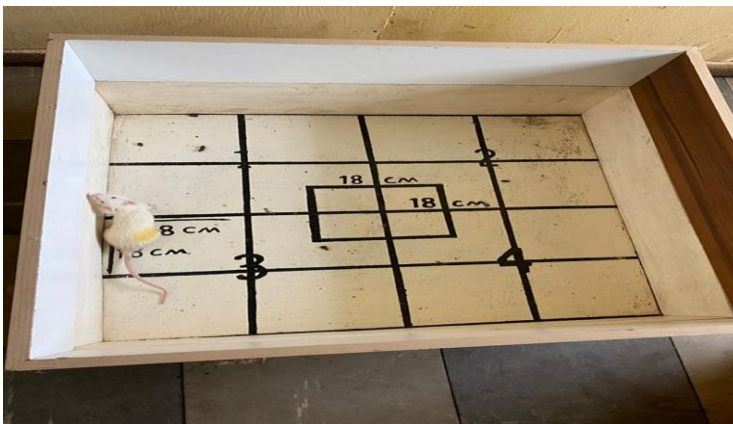


**Figure 3.1: Open Field Test Apparatus**

### 3.10.2 String Test

Measures the duration that it took a rat to gain hindlimb traction after forelimb hanging. Defects in latency time indicate deficient coordination (Fujiwara *et al.*, 2017). This was utilised to gauge limb disability and grip strength. A steel wire that is 60 cm long and 2 mm in diameter is put 50 cm above a cushion support for the rat to grasp with its forepaws. A threshold time of 180 seconds was used to record how long the rat could hold the wire before it fell. An indirect indicator of grip strength is thought to be the latency to grip loss. Rats were given three points for clutching the

wire with both hind paws, two points for gripping it with one hind paw, and one point for not gripping it with either hind paw to measure limb impairment. The overall score was used to represent the results.



**Figure 3.2: String Test Apparatus**

### **3.10.3 Movement Initiation Test**

Measures voluntary movements control (Ijonome *et al.*, 2014). With its hindlimbs and one forelimb raised above the tabletop, the rat will be grasped by its trunk, allowing one forelimb to bear the whole weight of its body. For each forelimb, the time it takes to start one step is noted.



**Figure 3.3: Movement Initiation Test**

#### **3.10.4 Step Test**

Postural stability is assessed using the step test. Animals are held in this test in the same way as in the movement initiation test, which involves bearing the animal's weight on one forelimb. Next, over five seconds, the animal is moved sideways across a 90-cm distance on a tabletop. Each forelimb's number of adjustment steps is noted when the animal is moved over the table. Each forelimb's average number of steps across three trials is utilised for analysis. measures coordination and balance as well as asymmetric motor movement (Ijomone et al., 2014).

**Commented [h7]:** Please recast this sentence.

#### **3.11 EVALUATION OF BODY AND BRAIN WEIGHT**

After the neurobehavioral assessments were completed, the rats were weighed and euthanised with low-level anaesthesia, followed by cervical dislocation after the 28-day treatment period. To reveal the brain, a transverse cut was made through the rats' skulls, with the brain excised, and blotted clean of blood. The following formula will be used to determine the relative brain weight.

Relative brain weight = [absolute brain weight (g) / body weight (g)] x 100

Cerebellar-brain weight ratio = cerebellar weight/ absolute brain weight

#### **3.12 CEREBELLAR OXIDATIVE STRESS PARAMETERS**

Following its harvest, the brain was cleaned and weighed on an automated weighing balance that was calibrated in milligrams to the nearest two decimal places. The collected and weighed cerebellar tissues were rinsed twice in cold phosphate-buffered saline (PBS) before being mixed with acid-washed sand and PBS in a porcelain mortar and pestle. The homogenate underwent a 10,000 g centrifugation for 15 minutes at 4 °C. The supernatant was collected to estimate the various oxidative tests.

### 3.12.1 Catalase (CAT) Activity Estimation

The Cohen *et al.* (1993) approach was used to determine this.

#### The Principle

Almost every cell of an animal, plant, or bacterial organism contains catalase. It works to stop harmful H<sub>2</sub>O<sub>2</sub> from building up and being transformed into O<sub>2</sub> and H<sub>2</sub>O.

#### Reagent Preparation

- 0.158g of KMnO<sub>4</sub> was dissolved in 100ml of distilled water to create 0.01M KMnO<sub>4</sub>.
- Phosphate buffer (pH 7.4); 100 millilitres of distilled water were used to dissolve 0.426 g of NaHPO<sub>4</sub> and NaH<sub>2</sub>PO<sub>4</sub>.
- 6M H<sub>2</sub>SO<sub>4</sub>: 66.7ml of distilled water was mixed with 32.3ml of concentrated H<sub>2</sub>SO<sub>4</sub>.
- The 30 millilitre H<sub>2</sub>O<sub>2</sub> solution was made by measuring 0.34 millilitres of 30% H<sub>2</sub>O<sub>2</sub> in 1001 millilitres of phosphate buffer.

**Commented [h8]:** Please number the items under this section.

Procedure: 5.0 ml of H<sub>2</sub>O<sub>2</sub> was combined with a known volume of tissue sample (0.5 ml). After inverting this, it was allowed to stand for half an hour. The addition of 6 M H<sub>2</sub>SO<sub>4</sub> halted the process. The absorbance against distilled water was measured at 480 nm in 30–60 seconds.

### **Calculation**

Activity=

OD=Absorbance

L = light path = 1 cm

V<sub>t</sub> = reaction sample total volume

M is the H<sub>2</sub>O<sub>2</sub> molar extinction coefficient (40/M/cm).

### **3.12.2 Malondialdehyde (MDA) Concentration Estimation**

The thiobarbituric acid assay was used to measure malondialdehyde (Buege and Aust, 1978).

#### **The Principle**

Lipid peroxidation produces malondialdehyde, which combines with thiobarbituric acid to produce a red species.

#### **Reagent Preparation**

Stock 15 g of trichloroacetic acid, 0.375 g of thiobarbituric acid, and 0.25 N hydrochloric acid were combined to create TCA-TCB-HCL. To facilitate the decomposition of thiobarbituric acid, this solution was gradually heated.

## **Methodology**

One milliliter of tissue sample and two millilitres of TCA-TBA-HCL were well combined. The solution was heated to a boil for fifteen minutes in a water bath. After cooling, the flocculent precipitate was removed by centrifugation at 1000 g for 10 minutes. At 535 nm, the absorbance was measured in relation to a blank.

This formula was used to calculate the concentration of MDA.

MDA (unit/mg protein) =  $A \times \frac{1000}{V_t} \times \frac{1}{Y} \times \frac{1}{M} \times \frac{1}{l}$

$V_t$  = reaction's total volume = 3 ml

$V$  = volume of tissue extract used = 1ml

$Y$  = mg tissue in the volume of the sample used

$M$  = molar extinction co-efficient of product =  $1.56 \times 10^5 \text{m}^{-1}\text{cm}^{-1}$

$l$  = light path = 1cm

### **3.12.3 Glutathione Peroxidase (Gpx) Activity Estimation**

This was ascertained using Ellman's (1959) approach.

#### **The Pinciple**

This is based on the fact that peroxidase activity converts pyrogallol to purpurogallin, giving the substance a deep brown colour that can be measured at 430 nm.

### **Reagent Preparation**

Pyrogallol (20mM):

100 mL of distilled water was used to dissolve 0.2552g of pyrogallol.

### **Methodology**

A 0.2 ml of tissue homogenate was mixed with 2.5 ml of phosphate buffer, 2.5 ml of H<sub>2</sub>O<sub>2</sub>, 1.5 ml of distilled water, and 2.5 ml of pyrogallol. The reaction was left to stand for 30 minutes at room temperature. At 420 nm, a deep brown colour was the end product.

### **calculation**

Activity= OD/Min × VtDf

E×Vs×Y

OD = Test Absorbance

Vt is the reaction mixture's total volume.

Df =Dilution factor= 1

E = (12/M/cm) Molar extinction coefficient

Vs = sample volume

Y = protein milligrams utilised

### **3.12.4 Analysis of Superoxide Dismutase (SOD)**

This was ascertained using Misra and Fridovich's (1972) methodology.

### **The Principle**

By catalysing the breakdown of the superoxide anion, superoxide dismutase prevents sample autooxidation. At 420 nm, the SOD activity is measured with a spectrophotometer, and the degree of inhibition reflects this. Reagent preparation: 0.2014 g of Na<sub>2</sub>CO<sub>3</sub> was dissolved to create a 0.05 M, pH 10.2 carbonate buffer. 100 millilitres of pure water, 0.0372 grams of EDTA, and 0.2604 grams of NaHCO<sub>3</sub>. Hydrochloric acid (0.005 M) was created by mixing 0.044 concentrated hydrochloric acid with 99.96 millilitres of clean water.

To make a brain sample solution (0.3M), 0.01098 g of the brain sample was dissolved in 100 mL of a 0.005 M HCl solution.

### **Methodology**

While 0.2 ml of tissue homogenate was mixed with 2.5 ml of carbonate buffer and 0.3 ml of sample solution, 0.2 ml of distilled water, 2.5 ml of carbonate buffer, and 0.3 ml of sample were used as a comparison sample. These were combined, and the absorbance at 420 nm was calculated.

### **Calculation**

$(O.D \text{ test} - O.D \text{ ref}) \times 100 / O.D \text{ test} = \% \text{ inhibition}$

Thus, the formula for calculating enzyme activity is

SOD activity (unit/mg protein) = % inhibition 50 x Y,

where Y is the amount of protein in the sample container.

### **3.12.5 Estimation of Glutathione (GSH) Concentration**

This was determined using the method described by Ellman (1959).

#### **Reagents**

5, 51-dithiobis-2-nitrobenzoic acid (DTNB), sodium citrate, and trichloroacetic acid (TCA)

#### **Procedure**

To 1.0 mL of the tissue homogenate, 2.5 mL of 10 % TCA was added and centrifuged at 3000 g for 10 min. Then, 1.0 mL of the supernatant was treated with 0.5 mL of Ellman's reagent (0.0189 % DTNB and 1 % sodium citrate) and 3.0 mL of 0.3 M phosphate buffer (pH 8.0). The yellow colour developed was read immediately at 412 nm and expressed as  $\mu\text{M}$  GSH/g plasma.

#### **Calculation**

Concentration of GSH =  $[\text{A}_{\text{test}} \times \text{Conc. of Standard}] / \text{A}_{\text{stand}} \times \text{Glutathione Reduced} = [(A_0 - A_1) \times 100] / A_0$

Where,  $A_0$  = Absorbance of reference sample

$A_1$  = Absorbance of sample

### 3.13 ESTIMATION OF PB ACETATE CONCENTRATION

Pb concentration was assayed using AAS according to methods described by Omotuyi *et al.* (2018). Fresh tissue samples were thoroughly digested in a 3.0 mL solution containing 15 mL nitric acid (HNO<sub>3</sub>, 69%) and 25 mL of perchloric acid (HClO<sub>4</sub>, 58%) at 100°C for 48 hours. The digestate was filtered and diluted to 100 mL using distilled/deionised water. The metal concentrations were determined by an atomic absorption spectrophotometer (AAS BUCK Scientific Model 211 VGP) at 283.2 nm wavelength.

### 3.14 CEREBELLAR HISTOLOGICAL PROCEDURE

#### 3.14.1 Paraffin Tissue Processing

Following their fixation in 10% formal saline, the extracted tissue was processed using the subsequent procedures:

1. Using ethanol as the preferred alcohol, the tissue was dehydrated using a series of alcohol gradients ranging from 70% to 90% and absolute alcohol.
2. The alcohol was entirely removed using xylene as a clearing agent; two xylene changes were utilised to ensure total clearance.

**Commented [h9]:** Number the procedures.

- Next, three stages of molten paraffin wax infiltration were performed on the tissue at a temperature between 65 and 70°C. Every phase lasted fifteen minutes, with the concluding phase lasting thirty minutes.
- To make longitudinal slices, the tissues were positioned longitudinally in an embedding mould, which was filled with melted paraffin wax. Tissue blocks were formed by allowing the melted paraffin wax to cool and solidify.
- The tissue blocks were trimmed by dividing them into thin, ribbon-like pieces that were 5 microns thick using a rotary microtome.

#### **3.14.2 Method of Hematoxylin and Eosin Staining**

A water bath at 30°C was used to float the sliced paraffin sections after tissue sections of suitable quality that looked like ribbons were chosen and submerged in 20% alcohol to disperse them. Subsequently, the tissues were placed on slides and allowed to air dry. After removing extra paraffin wax from the tissue slices by soaking them in xylene for 15 minutes, they were hydrated by alternating between progressively in lower alcohol concentrations (100%, 90%, and 70%) and water for 5 minutes each. The staining sections were as follows (Bancroft & Layton, 2018):

- Hematoxylin staining was applied to tissues for ten minutes.
- Bluing, or washing the tissue in running tap water, was then carried out.
- 1% eosin was used to counterstain the sections for five to ten minutes.
- Following a water rinse, the tissues were quickly dehydrated for five minutes using a range of alcohol concentrations, from 70% to 100% alcohol.
- The slides were mounted with a glass cover slip using an appropriate mounting medium, Distrene plasticiser, and Xylene (DPX) following a 5-minute xylene clearing of the tissues.

### **3.15 PHOTOMICROGRAPHY**

A Leica DM750 research microscope with a digital camera (LeicaCC50) attached was used to gather and examine the cerebellar slices. Digital photos of tissue sections were taken at objective magnifications of 100x and 400x.

### **3.16 MOLECULAR DOCKING**

#### **3.16.1 High Performance Liquid Chromatography (HPLC) Analysis**

High-performance liquid chromatography (HPLC) is a method used to separate mixtures of complex samples. HPLC is an active process in which materials are pumped at high pressure through a separation column, which contains a stationary phase, usually chemically functional beads that separate the compound mixtures. Samples are introduced through the injector and carried via the mobile phase across the stationary phase to effect the separations. After separation through the column, the samples are exposed to a detector system that identifies and quantifies the individual compounds. Reversed-phase HPLC (RP-HPLC), which is the most widely used HPLC technique due to its versatility, was employed.

##### **3.16.1.1 Extraction**

10g of sample was measured into the amber bottle, to which was added 20ml of acetonitrile, and both were shaken vigorously for 30 minutes. After that, it was stabilised by an organic solvent (ethyl acetate), collected into a 25 ml standard flask, made up to the mark, and ready for analysis.

##### **3.16.1.2 Analysis**

Standard form of analyte samples was first injected into the HPLC, and this generated a chromatogram, with a given peak area and peak profile. These were used to create a window in the HPLC for the preparation of the test sample analysis. Then, the extracted test sample was injected into the HPLC to obtain a corresponding peak area and peak profile in a chromatogram. Then the peak area of the sample is compared with that of the standard, relative to the concentration of the standard, to obtain the concentration of the sample.

### **Calculation**

Concentration of sample = peak area of sample × standard concentration

Peak area of the standard

General standard conc: 10.29mg/g

General standard peak area: 9998.8566

Individual standard conc: 0.85mg/g

Individual standard peak area: 833.2381

General conc = 14818.9575 × 10.29

9998.8566

= 15.25mg/g

### **HPLC Programming**

Make = Schimadzu (Nexera mix)

Column = uBONDApak C18

Length: 100mm

ID: 4.6mm

Thickness: 7mm

Mobile phase = Acetonitrile/ water (methanol/water)

Flow rate = 1ml/min

Sample injection = 10ul

Detector = UV e 254nm (Diode Array Detector, DAD)

Pump pressure = 15mpa

### **3.16.2 Ligand-Protein Interaction**

The binding relationships between specific HPLC-identified *T. tetraptera* compounds to protein marker targets linked to oxidative stress, inflammation, and apoptosis were assessed using molecular docking experiments. This method provides information about the possible therapeutic mechanisms of ligands by predicting their molecular interactions and binding affinities with important biological targets.

#### **3.16.2.1 Preparation of Crystal Protein**

The crystal structures of TNF- $\alpha$  (PDB ID-2AZ5), NRF2 (PDB ID-7OFE), Caspase 3 (PDB ID-3KJF), NF $\kappa$ B (PDB ID-1IKN) and Interleukin 6 (PDB ID-4YW7) were downloaded via the protein preparation wizard of Maestro v11.8. The protocol described in our previous studies was used to prepare the crystal structure of the protein (Elekofehinti *et al.* 2020a, b). The protein was preprocessed by creating zero bonds to metals, deleting waters from 5.0 Å of het groups, adjusting bond orders and setting the het states at pH 7.0  $\pm$  2.0 (Schrödinger Suite 2012). The protein was refined by optimising the H-bond network using PROPKA and removing water molecules with less than 3 H-bonds to non-waters. The restrained minimisation was carried out using the OPLS3 force field to avoid steric clashes that may exist in the structure. The minimisation was terminated while the RMSD of non-hydrogen atoms reached 0.30 Å.

#### **3.16.2.2 Preparation of The Phyto-Compounds**

The compounds were retrieved from the National Centre for Biotechnology Information (PubChem). The compounds were prepared using Ligprep. The Ligprep panel enables the conversion of structures, generates variations of structures and elimination unwanted structures. After stereoisomer computation was left to generate at most 32 per ligand, and the output format was left as maestro, the OPLS3 force field was left at pH 7.0  $\pm$  2.0 using epic.

#### **3.16.2.3 Receptor Grid Generation**

The receptor grid file was generated using a receptor grid generation panel, which represents the active sites of the receptor for Glide ligand docking jobs. The ligand-binding site was defined by picking the co-crystallised ligand of the protein structure on the workspace. The van der Waals radii of the receptor atoms with partial atomic charge were set scaling factor of 1.0 and a partial cutoff of 0.25 to soften the potential for non-polar parts of the receptor.

#### **3.16.2.4 Glide Extra Precision Docking**

The compounds were prepared by ligprep and docked into the active site of the protein crystal using extra precision with the ligand sampling set generated as flexible. The choice of the best-docked structure for each ligand was made using the model energy score (emodel) that combines glide score, the non-bonded interaction energy and the excess internal energy of the generated ligand conformation.

#### **3.16.2.5 ADME Profiles**

The absorption, distribution, metabolism, excretion and molecular properties of the compounds were predicted using the Qikprop panel (Release, 2018).

### **3.17 STATISTICAL ANALYSIS**

All statistical analyses were conducted using the GraphPad Prism software version 9, and data were presented as mean with standard error of mean (SEM). To determine statistical significance ( $p < 0.05$ ), a one-way analysis of variance (ANOVA) was conducted, followed by a post-hoc Tukey's multiple comparisons test. The statistical data obtained were transformed into graphical representations in the form of bar charts.

## **CHAPTER FOUR**

### **RESULTS**

#### **4.1 PRELIMINARY PHYTOCHEMICAL FINDINGS**

Table 4.1 shows the results of the qualitative analysis of the phytochemical constituents of the aqueous fruit extract of *Tetrapleura tetraptera* (*T. tetraptera*). Phytochemical analysis of *T. tetraptera* showed the absence of tannins, while alkaloids, phenols, saponins, flavonoids, and sterols were detected.

Table 4.1: Preliminary Phytochemical findings (qualitative) of the aqueous fruit extract of *Tetrapleura tetraptera*.

<b>PHYTOCHEMICALS</b>	
<b>Alkaloids</b>	+
<b>Tannins</b>	-
<b>Phenols</b>	+
<b>Saponins</b>	+
<b>Flavonoids</b>	+
<b>Steroids</b>	+

**+: Present**

**-: Absent**

#### **4.2 ACUTE TOXICITY STUDY AND OBSERVATION**

Table 4.2 shows the acute toxicity in adult Wistar rats treated with varying dosages of aqueous fruit extract of *Tetrapleura tetraptera* (10mg/kg, 100mg/kg, 1000mg/kg, 1600mg/kg, 2900mg/kg, and 5000mg/kg, respectively). There was no mortality recorded in all the rats administered with *T. tetraptera* (n=3/group) after 72 hours of observation. Also, no morbidity and diarrhoea were noticed after 72 hours of observation.

Table 4.2: Acute toxicity study and observations in Wistar rats treated with aqueous fruit extract of *Tetrapleura tetraptera* after 72 hours

**Commented [h10]:** Use 3 horizontal lines only. Remove all grid lines.

Observation	Group A (10 mg/kg)	Group B (100 mg/kg)	Group C (1000 mg/kg)	Group D (1600 mg/kg)	Group E (2900 mg/kg)	Group F (5000 mg/kg)
Morbidity	None	None	None	None	None	None
Mortality	None	None	None	None	None	None
Diarrhoea	None	None	None	None	None	None

n=3/group

### 4.3 EFFECT OF TREATMENT ON BODY AND BRAIN WEIGHT

Figures 4.1- 4.8 show the weight findings across experimental groups. Results showed that the weight change of the rats was significantly lower ( $p < 0.05$ ) in the Pb-only (100mg/kg) group when compared to the control group. However, a significant increase in weight change ( $p < 0.05$ ) was observed in the Pb co-administered with *T. tetraptera* (500mg/kg) group, Pb + *T. tetraptera* (1000mg/kg) group, and Pb + Vit E (200mg/kg) group when compared to the Pb-only group. Also,

no significant difference ( $p > 0.05$ ) was observed in the *T. tetraptera* and Vit E only treated group when compared to control. For the whole brain weight, Pb-only group showed a significant decrease ( $p < 0.05$ ) when compared to the control group. However, a significant increase ( $p < 0.05$ ) was observed in the Pb co-administered with *T. tetraptera* (1000mg/kg) group, and Pb + Vit E (200mg/kg) group when compared to Pb-only group. There was also no significant difference ( $p > 0.05$ ) observed in the *T. tetraptera* and Vit E only treated groups when compared to control. Findings also showed no significant differences ( $p > 0.05$ ) were observed in the relative brain weight, cerebellar weight, relative cerebellar weight, and cerebellum/brain weight ratio across experimental groups.

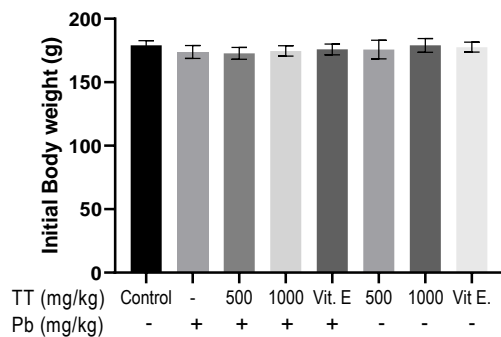


Figure 4.1: Initial body weight across experimental groups.

# and \* represent  $p < 0.05$  following comparison to the control and Pb-only group B, respectively.

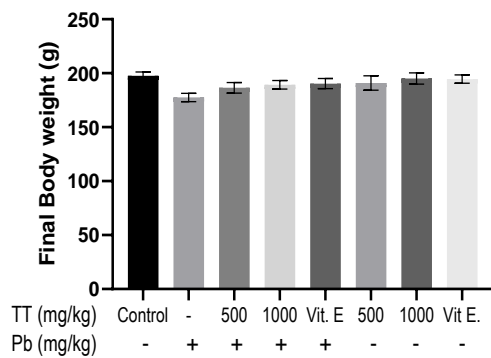


Figure 4.2: Final body weight across experimental groups.

# and \* represent  $p < 0.05$  following comparison to the control and Pb-only group B, respectively.

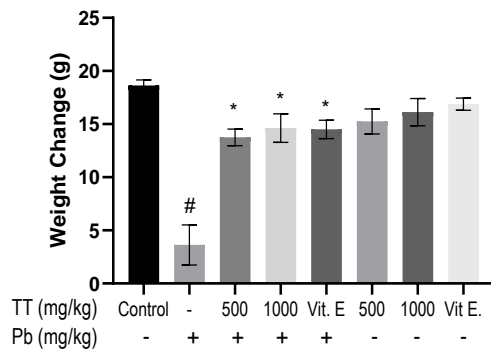


Figure 4.3: Weight change across experimental groups.

# and \* represent  $p < 0.05$  following comparison to the control and Pb-only group B, respectively.

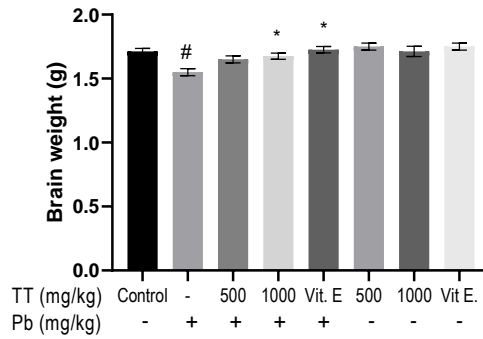


Figure 4.4: Brain weight across experimental groups.

# and \* represent  $p < 0.05$  following comparison to the control and Pb-only group B, respectively.

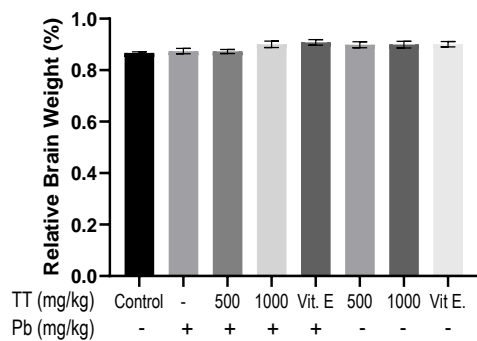


Figure 4.5: Relative Brain weight across experimental groups.

# and \* represent  $p < 0.05$  following comparison to the control and Pb-only group B, respectively.

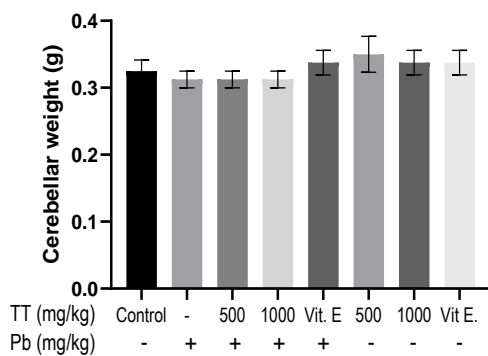


Figure 4.6: Cerebellar weight across experimental groups.

# and \* represent  $p < 0.05$  following comparison to the control and Pb-only group B, respectively.

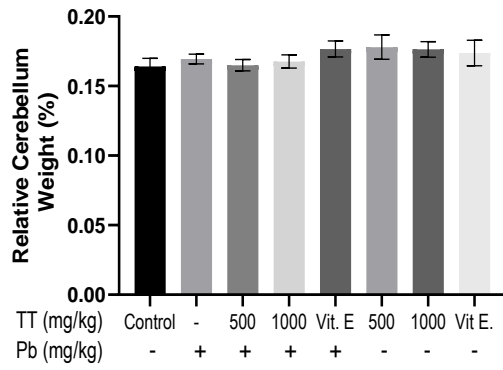


Figure 4.7: Relative Cerebellar weight across experimental groups.

# and \* represent  $p < 0.05$  following comparison to the control and Pb-only group B, respectively.

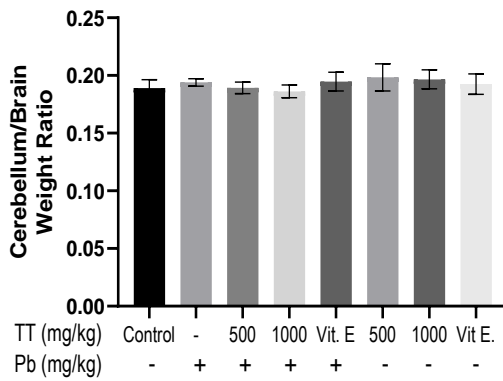


Figure 4.8: Cerebellum Brain weight ratio across experimental groups.

# and \* represent  $p < 0.05$  following comparison to the control and Pb-only group B, respectively.

#### **4.4 EFFECT OF TREATMENT ON NEUROBEHAVIOURAL ACTIVITY: OFT (IMMOBILITY, AMBULATION, CENTRAL SQUARE ENTRY, LINE CROSSING), MOVEMENT INITIATION, STRING, AND STEP TESTS**

Figure 4.9 shows the immobility open field test (OFT) across experimental groups. For the immobility test, there was a significant increase ( $p < 0.05$ ) in the Pb-only (100mg/kg) group when compared to the control group. However, a significant decrease ( $p < 0.05$ ) was observed in the Pb co-administered with *T. tetraptera* (500mg/kg) group, Pb + *T. tetraptera* (1000mg/kg) group, and Pb + Vit E (200mg/kg) group when compared to the Pb-only group. Also, no significant difference ( $p > 0.05$ ) was observed in the *T. tetraptera* and Vit E only treated group when compared to the control.

Figures 4.10-4.12 show the ambulation, central square crossing, and line crossing open field test (OFT) across experimental groups. There was a significant decrease ( $p < 0.05$ ) in the Pb-only (100mg/kg) group when compared to the control group. However, a significant increase ( $p < 0.05$ ) was observed in the Pb co-administered with *T. tetraptera* (500mg/kg) group, Pb + *T. tetraptera* (1000mg/kg) group, and Pb + Vit E (200mg/kg) group when compared to the Pb-only group. Also, no significant difference ( $p > 0.05$ ) was observed in the *T. tetraptera* and Vit E only treated group when compared to the control.

Figure 4.13 shows the movement initiation test across experimental groups. For the movement initiation test, there was a significant increase ( $p < 0.05$ ) in the Pb-only (100mg/kg) group when compared to the control group. However, a significant decrease ( $p < 0.05$ ) was observed in the Pb co-administered with *T. tetraptera* (500mg/kg) group, Pb + *T. tetraptera* (1000mg/kg) group, and Pb + Vit E (200mg/kg) group when compared to the Pb-only group. Also, no significant difference

( $p > 0.05$ ) was observed in the *T. tetraptera* and Vit E only treated group when compared to the control.

Figures 4.14-4.15 show the string and step tests across experimental groups. There was a significant decrease ( $p < 0.05$ ) in the Pb-only (100mg/kg) group when compared to the control group. However, a significant increase ( $p < 0.05$ ) was observed in the Pb co-administered with *T. tetraptera* (500mg/kg) group, Pb + *T. tetraptera* (1000mg/kg) group, and Pb + Vit E (200mg/kg) group when compared to the Pb-only group. Also, no significant difference ( $p > 0.05$ ) was observed in the *T. tetraptera* and Vit E only treated group when compared to the control.

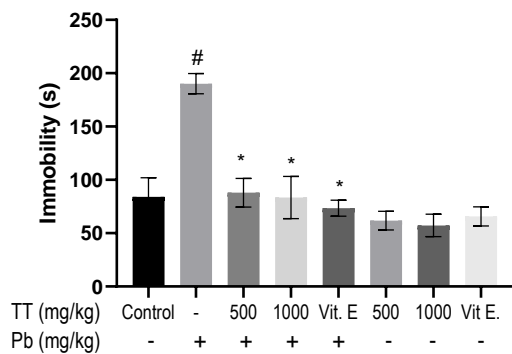


Figure 4.9: Immobility OFT across experimental groups.

# and \* represent  $p < 0.05$  following comparison to the control and Pb-only group B, respectively.

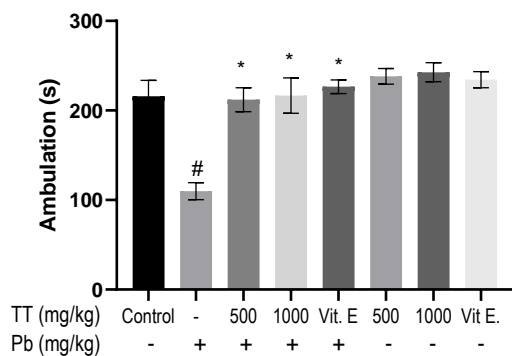


Figure 4.10: Ambulation OFT across experimental groups.

# and \* represent  $p < 0.05$  following comparison to the control and Pb-only group B, respectively.

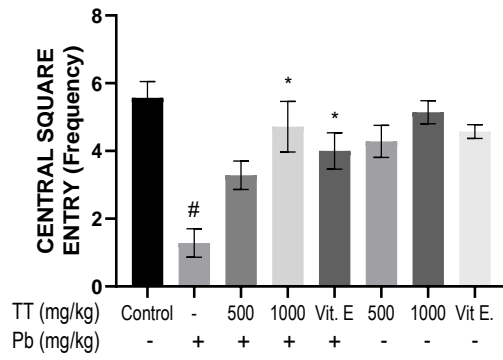


Figure 4.11: Central square entry OFT across experimental groups.

# and \* represent  $p < 0.05$  following comparison to the control and Pb-only group B, respectively.

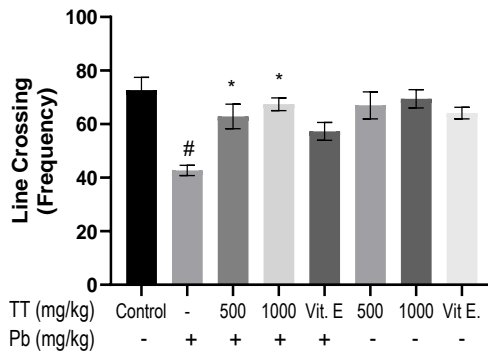


Figure 4.12: Line crossing OFT across experimental groups.

# and \* represent  $p < 0.05$  following comparison to the control and Pb-only group B, respectively.

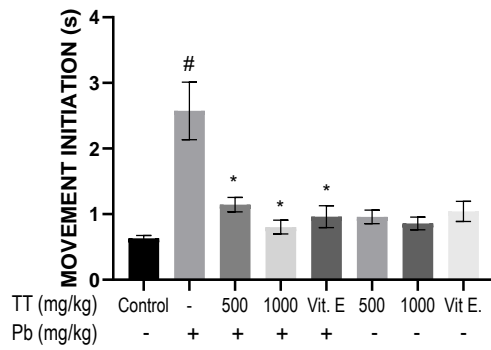


Figure 4.13: Movement initiation test across experimental groups.

<sup>#</sup> and <sup>\*</sup> represent  $p < 0.05$  following comparison to the control and Pb-only group B, respectively.

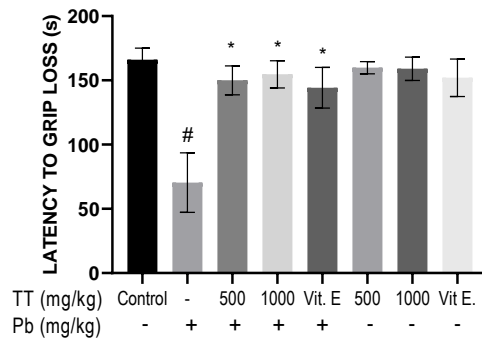


Figure 4.14: String test across experimental groups.

<sup>#</sup> and <sup>\*</sup> represent  $p < 0.05$  following comparison to the control and Pb-only group B, respectively.

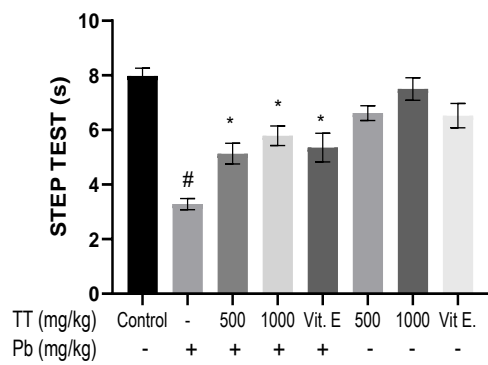


Figure 4.15: Step test across experimental groups.

# and \* represent  $p < 0.05$  following comparison to the control and Pb-only group B, respectively.

#### **4.5 EFFECT OF TREATMENT ON ANTIOXIDANT ENZYMES ACTIVITY (SOD, CAT, GPx, and GSH)**

Figures 4.16 to 4.19 show cerebellar superoxide dismutase (SOD), catalase (CAT), glutathione peroxidase (GPx), and glutathione (GSH) antioxidant activities across experimental groups. There was a significant reduction ( $p < 0.05$ ) in the Pb-only (100mg/kg) group (SOD, CAT, GPx and GSH) when compared to the control group. However, a significant increase ( $p < 0.05$ ) was observed in the Pb co-administered with *T. tetraptera* (500mg/kg) group (SOD and GPX), Pb + *T. tetraptera* (1000mg/kg) group (SOD, CAT, GPx and GSH), and Pb + Vit E (200mg/kg) group (SOD, CAT and GPx) when compared to the Pb-only group. Also, no significant difference ( $p > 0.05$ ) was observed in the *T. tetraptera* and Vit E only treated groups (SOD, CAT, GPx and GSH) when compared to the control.

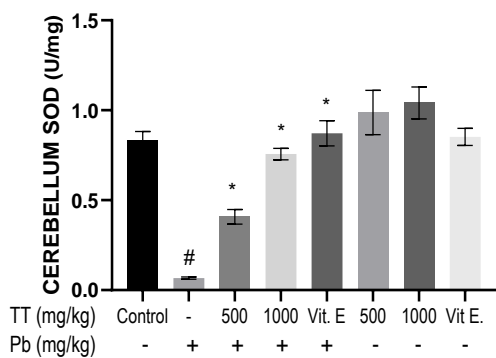


Figure 4.16: Cerebellum SOD across experimental groups.

# and \* represent  $p < 0.05$  following comparison to the control and Pb-only group B, respectively.

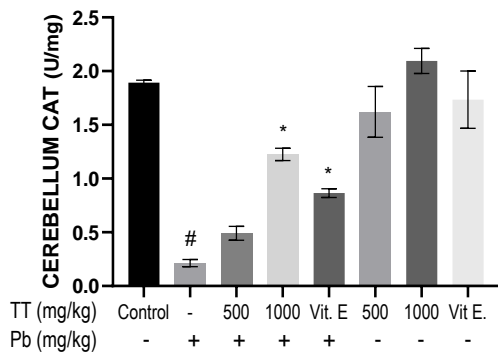


Figure 4.17: Cerebellum CAT across experimental groups.

# and \* represent  $p < 0.05$  following comparison to the control and Pb-only group B, respectively.

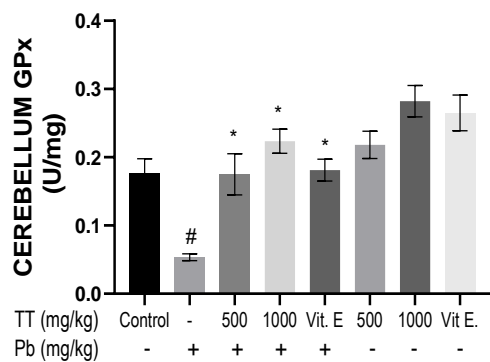


Figure 4.18: Cerebellum GPx across experimental groups.

# and \* represent  $p < 0.05$  following comparison to the control and Pb-only group B, respectively.

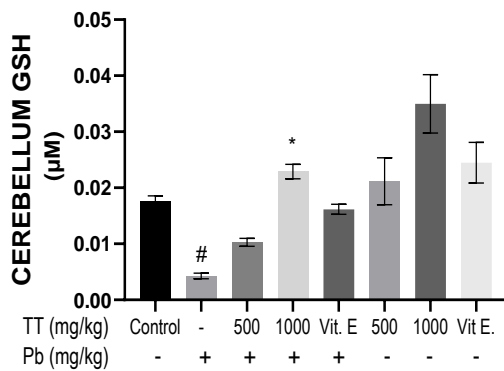


Figure 4.19: Cerebellum GSH across experimental groups.

# and \* represent  $p < 0.05$  following comparison to the control and Pb-only group B, respectively.

#### 4.6 EFFECT OF TREATMENT ON LIPID PEROXIDATION

Figure 4.20 shows Malondialdehyde (MDA) concentration in the cerebellum across experimental groups. There was a significant increase ( $p < 0.05$ ) in the Pb-only (100mg/kg) group when compared to the control group. However, a significant reduction ( $p < 0.05$ ) was observed in the Pb co-administered with *T. tetraptera* (500mg/kg) group, Pb + *T. tetraptera* (1000mg/kg) group, and Pb + Vit E (200mg/kg) group when compared to the Pb-only group. Also, no significant difference ( $p > 0.05$ ) was observed in the *T. tetraptera* and Vit E only treated group when compared to the control.

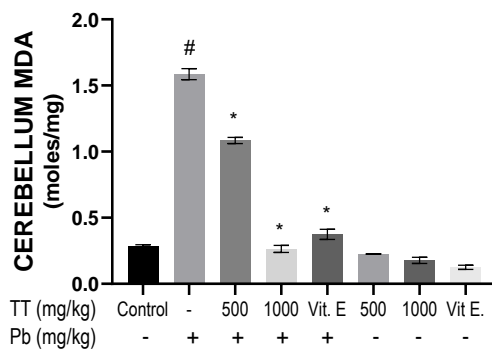


Figure 4.20: Cerebellum MDA across experimental groups.

# and \* represent  $p < 0.05$  following comparison to the control and Pb-only group B, respectively.

#### 4.7 EFFECT OF TREATMENT ON PB (Pb) ACCUMULATION

Figure 4.21 shows the cerebellar Pb concentration in the cerebellum across experimental groups. The cerebellar Pb concentration of the rats was significantly higher ( $p < 0.05$ ) in the Pb-only (100mg/kg) group when compared to the control group. However, a significant decrease in cerebellar Pb concentration ( $p < 0.05$ ) was observed in the Pb co-administered with *T. tetraptera* (500mg/kg) group, Pb + *T. tetraptera* (1000mg/kg) group, and Pb + Vit E (200mg/kg) group when compared to the Pb-only group. Also, no significant difference ( $p > 0.05$ ) was observed in the *T. tetraptera* and Vit E only treated group when compared to the control.

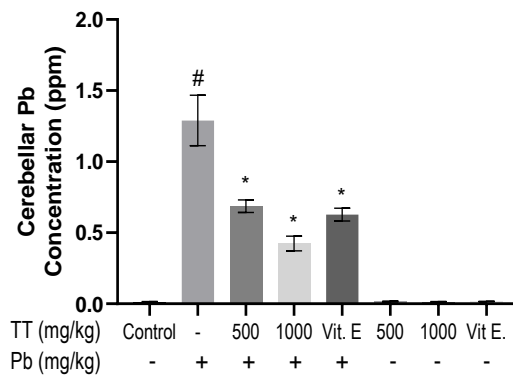


Figure 4.21: Cerebellar Pb concentration across experimental groups.

# and \* represent  $p < 0.05$  following comparison to the control and Pb-only group B, respectively.

#### **4.8 EFFECT OF TREATMENT ON THE HISTOLOGY OF THE CEREBELLUM**

Plate 4.1-4.8 shows the histoarchitecture of the cerebellum of rats across experimental groups.

Plate 4.1 shows the photomicrograph of the histoarchitecture of the cerebellum of the control group. The result shows normal molecular, Purkinje cell, and granular cell layers. Plate 4.2 shows the photomicrograph of the histoarchitecture of the cerebellum of the Pb-only group. For the Pb-only group, there was a significant alteration in the histological structure of the cerebellum, showing degenerating Purkinje cells, with irregular, darkly stained pyknotic nuclei as well as the presence of a vacuolated molecular layer. Plate 4.3-4.5 shows the photomicrograph of the histoarchitecture of the cerebellum of the Pb co-administered with *T. tetraptera* (500mg/kg) group, Pb + *T. tetraptera* (1000mg/kg) group, and Pb + Vit E (200mg/kg) group. Results show normal molecular, Purkinje cell, and granular cell layers. Plate 4.6-4.8 shows the photomicrograph of the histoarchitecture of the cerebellum of rats treated with *T. tetraptera* (500mg/kg and 1000mg/kg), and Vit E (200mg/kg) only. Results show normal histological structure of the molecular, Purkinje cell, and granular cell layers.

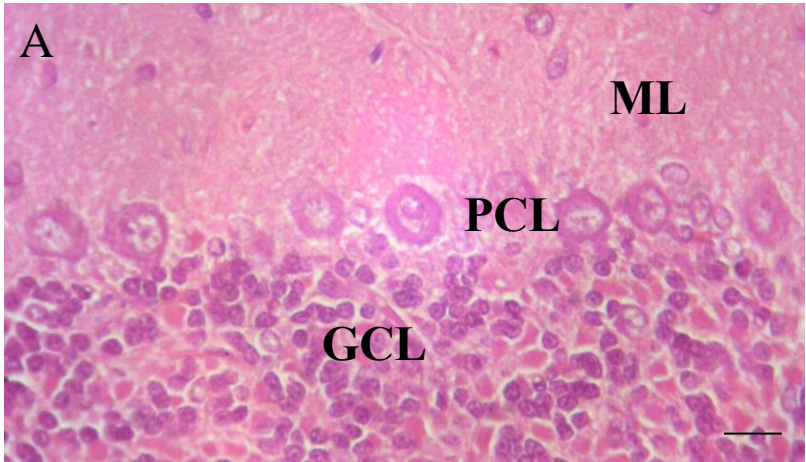


Plate 4.1: Representative histology of the cerebellar cortex in control Group showing normal molecular, pukinje cell, and granular (G) cells layer. (H&E; 400x - Scale bar: 25µm)

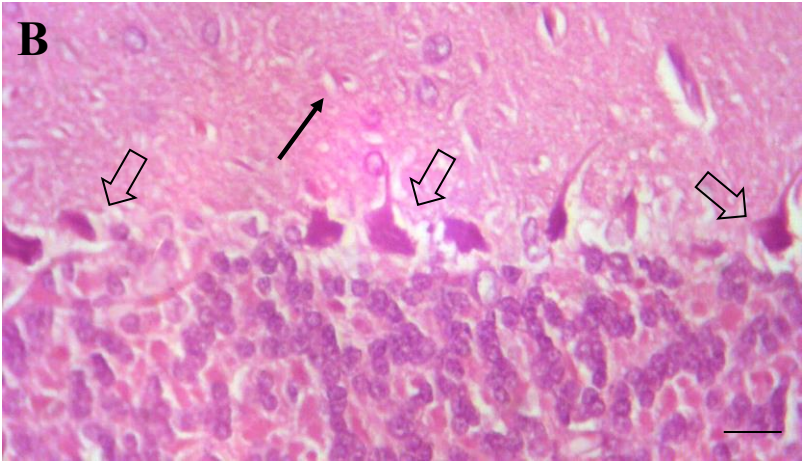


Plate 4.2: Representative histology of the cerebellar cortex in Pb-Only (100mg/kg) Treatment Group. Vacuolisation (arrows) and darkly stained pyknotic pukinje nuclei observed. Granular cells also seen (G). (H&E; 400x - Scale bar: 25µm)

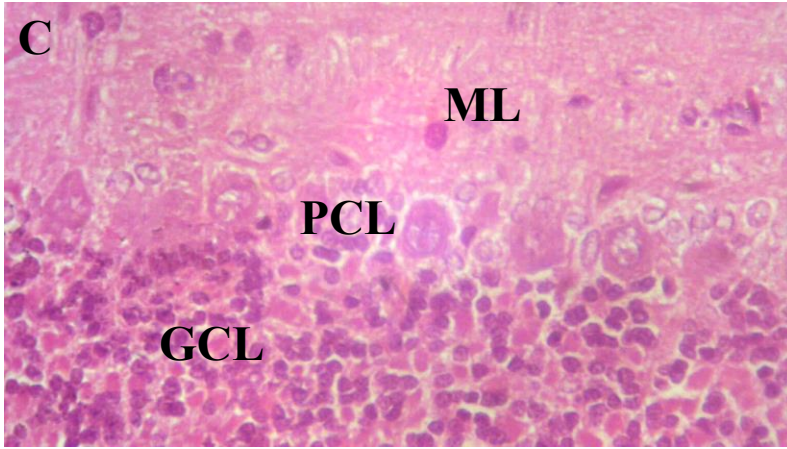


Plate 4.3: Representative histology of the cerebellar cortex in Pb co-administered with *T. tetraptera* (500mg/kg) Treatment group showing normal molecular, pukinje cell, and granular (G) cells layer. (H&E; 400x - Scale bar: 25µm)

Commented [h11]: Add legends explaining GCL etc

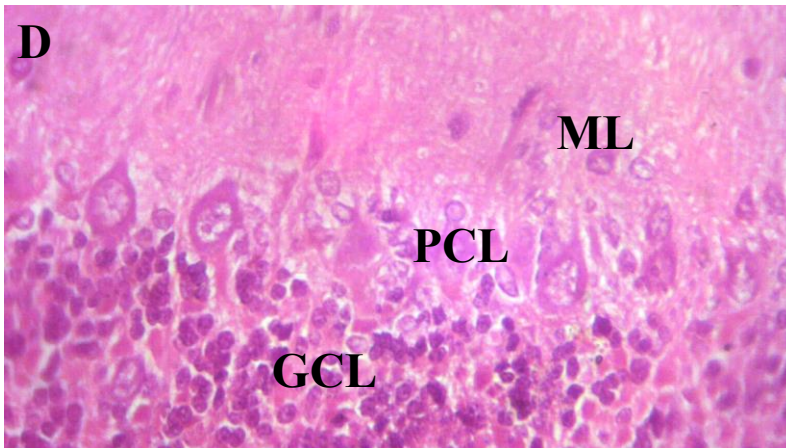


Plate 4.4: Representative histology of the cerebellar cortex in Pb + *T. tetraptera* (1000mg/kg)

Treatment Group showing normal molecular, pukinje cell, and granular (G) cells layer. (H&E;

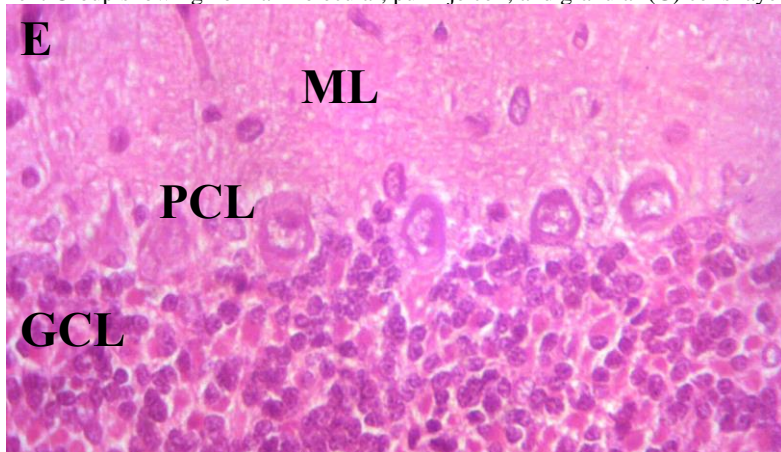


Plate 4.5: Representative histology of the cerebellar cortex in Pb + Vit E (200mg/kg) Treatment

Group showing normal molecular, pukinje cell, and granular (G) cells layer. (H&E; 400x - Scale

bar: 25µm)

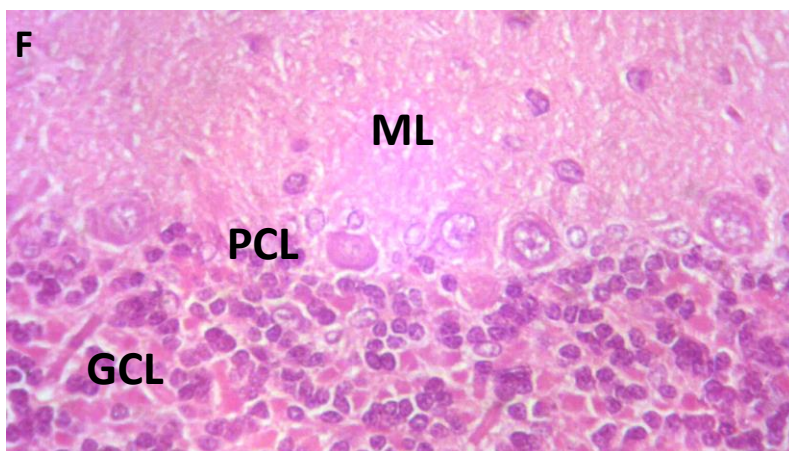


Plate 4.6: Representative histology of the cerebellar cortex in *T. tetraptera*-Only (500mg/kg)

Treatment Group showing normal molecular, pukinje cell, and granular (G) cells layer. (H&E;

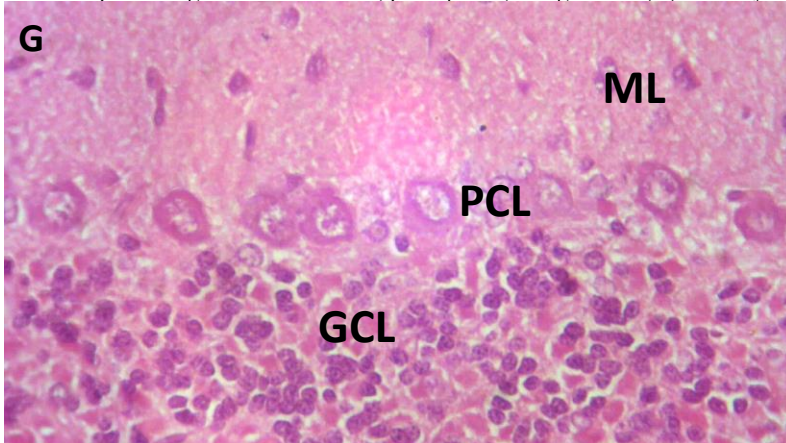


Plate 4.7: Representative histology of the cerebellar cortex in *T. tetraptera*-Only (1000mg/kg)

Treatment Group showing normal molecular, pukinje cell, and granular (G) cells layer. (H&E;

400x - Scale bar: 25µm)

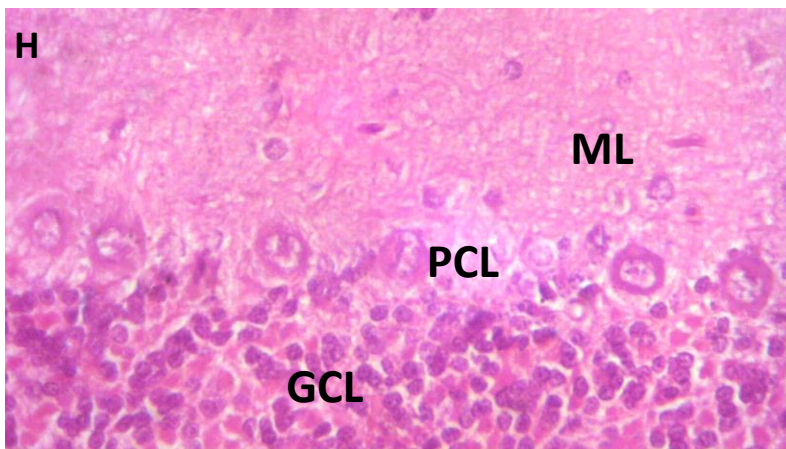


Plate 4.8: Representative histology of the cerebellar cortex in Vit E-Only (200mg/kg) Treatment Group showing normal molecular, pukiye cell, and granular (G) cells layer. (H&E; 400x - Scale bar: 25µm)

Add footnotes to all you micrographs

Commented [h12]: See this.

#### 4.9 *T. tetraptera* HPLC-IDENTIFIED PHENOLIC COMPOUNDS

Figure 4.22 shows the result of HPLC-identified *T. tetraptera* phenolic compounds. For compounds identified, the result shows the presence of 4-Hydroxybenzoic Acid (with a retention of 1.116; area of 208.2220; height of 20.840; and external of 20.8222), Eugenol (with a retention of 4.250; area of 101.6580; height of 6.918; and external of 10.1658), Salicylic Acid (with a retention of 8.800; area of 101.1305; height of 2.648; and external of 0.0000), and Resorcinol (with a retention of 10.366; area of 60.5825; height of 3.835; and external of 0.0000) respectively, all units are expressed in parts per million (ppm).

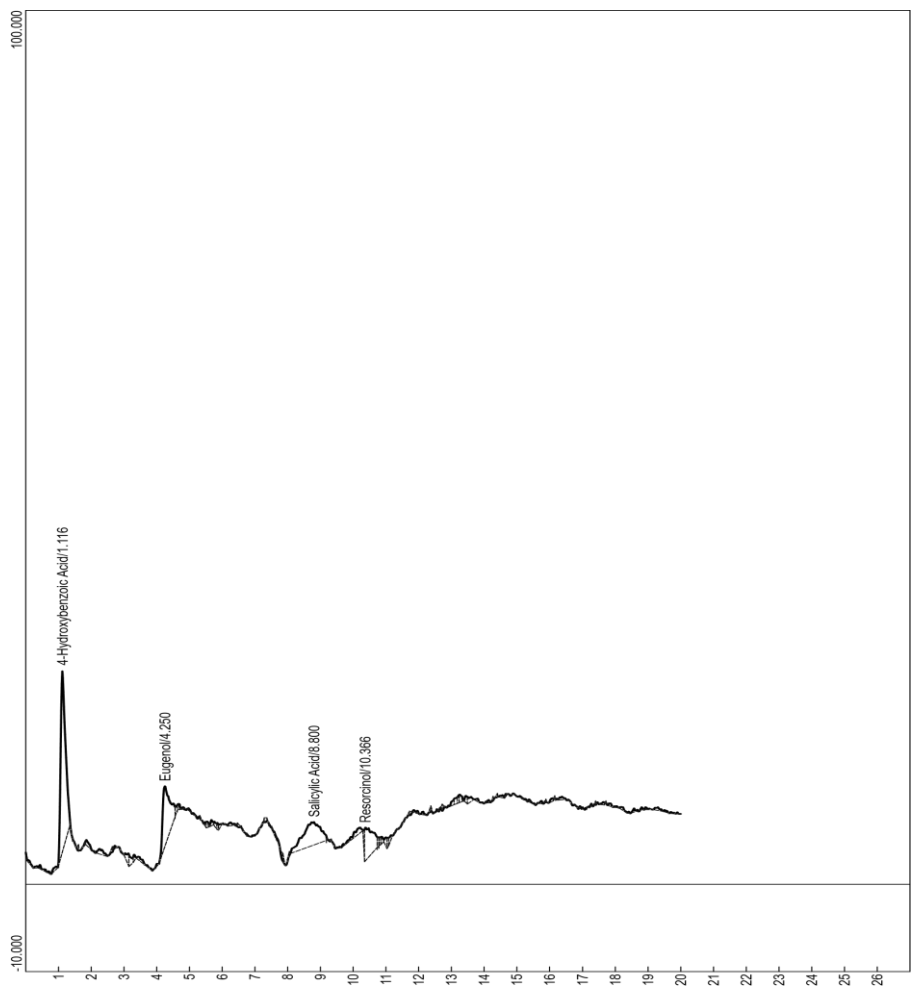


Figure 4.22: HPLC-identified *T. tetraptera* phenolic compounds

#### **4.10 TETRAPLEURA TETRAPTERA LIGAND-RECEPTOR INTERACTIONS**

Figure 4.23 – 4.27 show the 2D interaction of 4-hydroxybenzoic acid and Resorcinol with Caspase-3, NRF2, IL-6, TNF-alpha, and NF-κB, interacting amino acid residues within the binding pocket.

Figure 4.23 shows the binding pose of 4-hydroxybenzoic acid (docking score of -3.698) and Resorcinol (docking score of -3.983) with Caspase-3, a major apoptotic mediating protein. 4-hydroxybenzoic acid docks with tryptophan 214 and serine 251 of Caspase-3, while Resorcinol binds with tryptophan 214 and phenylalanine 250 of Caspase-3.

Figure 4.24 shows the binding pose of 4-hydroxybenzoic acid (docking score of -5.168) and Resorcinol (docking score of -3.196) with NRF2, an oxidative stress-mediating protein. 4-hydroxybenzoic acid binds with glutamine 530, serine 555, tyrosine 525, arginine 415, serine 508, and arginine 483 of NRF2, while Resorcinol docks with glutamine 530, serine 550, serine 508, and arginine 415 of NRF2.

Figure 4.25 shows the binding pose of 4-hydroxybenzoic acid (docking score of -3.044) and Resorcinol (docking score of -3.475) with TNF-α, a major inflammatory mediating protein. 4-hydroxybenzoic acid docks with tyrosine 151 of TNF-α, while Resorcinol docks with glutamine 61 and leucine 120 of TNF-α.

Figure 4.26 shows the binding pose of 4-hydroxybenzoic acid (docking score of -3.12) and Resorcinol (docking score of -3.622) with Nf-κB, an inflammatory mediating protein. 4-hydroxybenzoic acid binds with arginine 30 and alanine 188 of Nf-κB, while Resorcinol binds with aspartate 153, phenylalanine 184, and proline 189 of Nf-κB.

Figure 4.27 shows the binding pose of 4-hydroxybenzoic acid (docking score of -3.595) and Resorcinol (-4.424) with IL-6, a major inflammatory mediating protein. 4-hydroxybenzoic acid docks with asparagine 63, tyrosine 97, and asparagine 144 of IL-6, while Resorcinol docks with asparagine 63, tyrosine 97, and asparagine 144 of IL-6.

PUBCHEM ID	COMPOUND NAME	docking score (kcal/mol)
5054	Resorcinol	-3.983
5070	Riluzole (Standard)	-3.967
135	4-Hydroxybenzoic Acid	-3.698
2130	Amantadine (Standard)	0.18

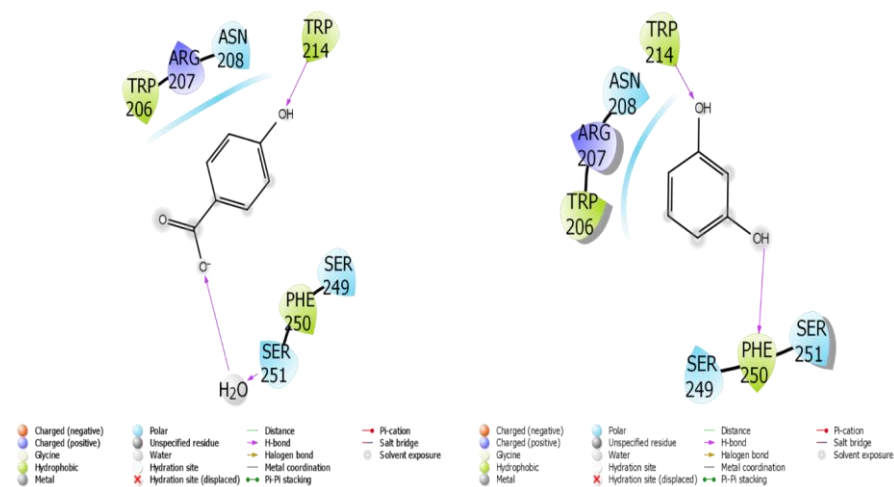


Figure 4.23: The binding pose of 4-hydroxybenzoic acid and Resorcinol within the binding pocket of caspase 3 showing the interacting amino acids

NRF2

PUBCHEM ID	COMPOUND NAME	docking score (kcal/mol)
135	4-Hydroxybenzoic Acid	-5.168
5054	Resorcinol	-3.196
5070	Riluzole (Standard)	-3.161
2130	Amantadine (Standard)	0.235

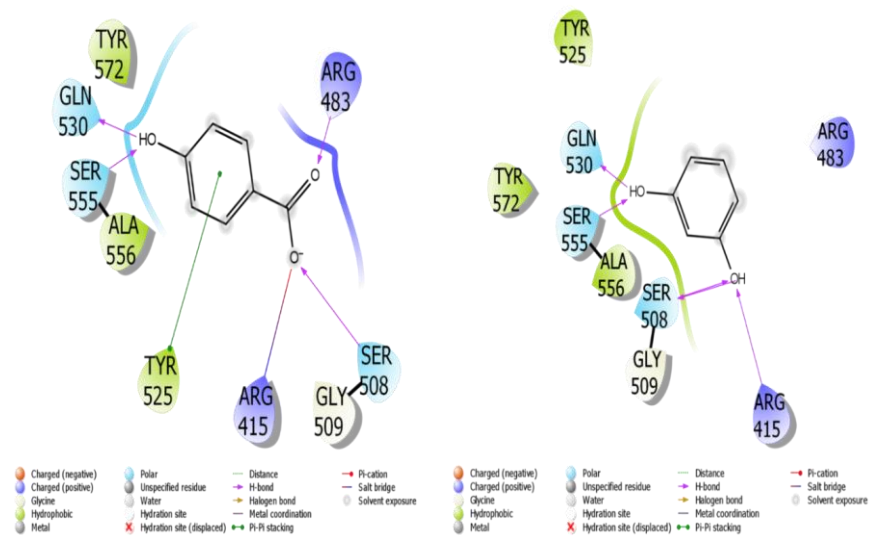


Figure 4.24: The binding pose of 4-hydroxybenzoic acid and Resorcinol within the binding pocket of NRF2 showing the interacting amino acids

TNF- $\alpha$

PUBCHEM ID	COMPOUND NAME	docking score (kcal/mol)
5054	Resorcinol	-3.475
135	4-Hydroxybenzoic Acid	-3.044
5070	Riluzole (Standard)	-2.906

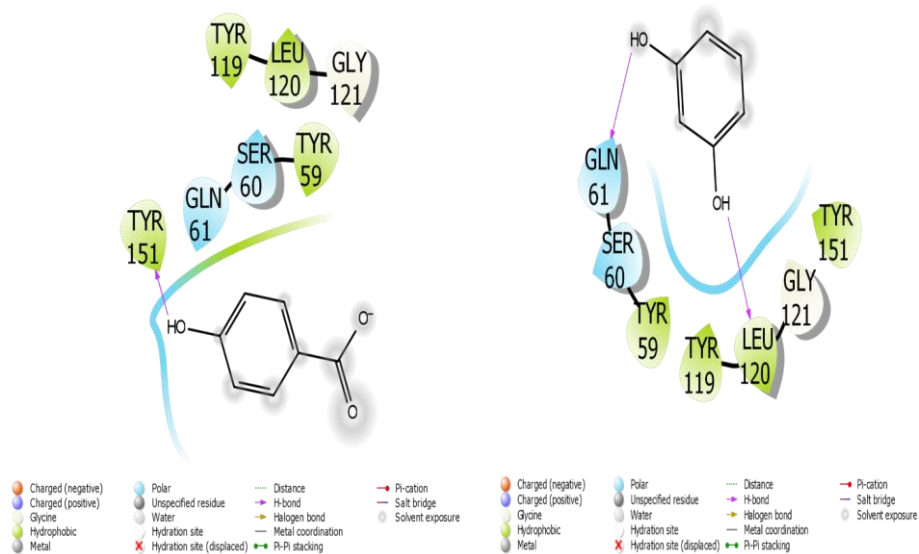


Figure 4.25: The binding pose of 4-hydroxybenzoic acid and Resorcinol within the binding pocket of TNF- $\alpha$ , showing the interacting amino acids

NF-κB

PUBCHEM ID	COMPOUND NAME	docking score (kcal/mol)
5054	Resorcinol	-3.622
135	4-Hydroxybenzoic Acid	-3.12
5070	Riluzole (Standard)	-2.689
2130	Amantadine (Standard)	-0.416

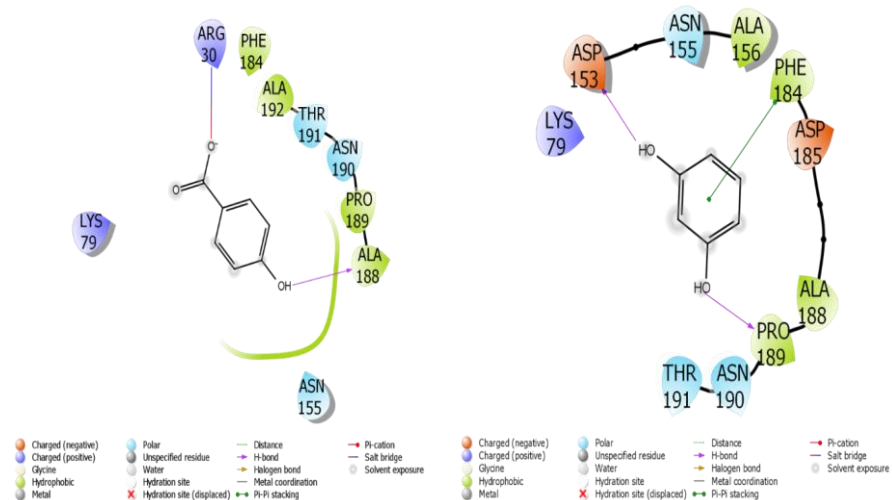


Figure 4.26: The binding pose of 4-hydroxybenzoic acid and Resorcinol within the binding pocket of Nf-κB showing the interacting amino acids

IL-6

PUBCHEM ID	COMPOUND NAME	docking score (kcal/mol)
5054	Resorcinol	-4.424
135	4-Hydroxybenzoic Acid	-3.595
5070	Riluzole (Standard)	-2.797
2130	Amantadine (Standard)	-1.615

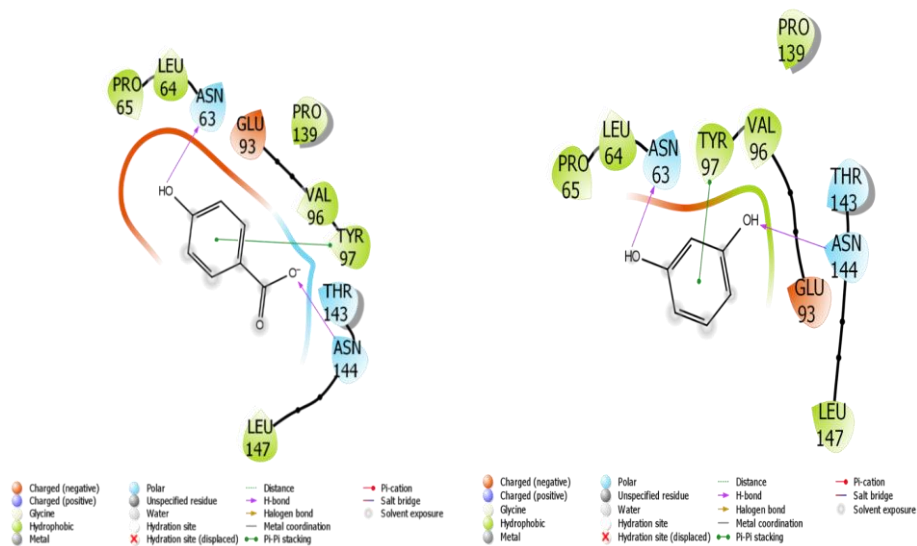


Figure 4.27: The binding pose of 4-hydroxybenzoic acid and Resorcinol within the binding pocket of IL-6, showing the interacting amino acids.

## CHAPTER FIVE

### 5.0: DISCUSSION AND CONCLUSION

#### 5.1 *T. tetraptera* is a Rich Source of Phytochemicals

One essential analytical method for the methodical identification and description of bioactive components in medicinal plants is phytochemical screening (Kemigisha *et al.*, 2018). This procedure is necessary for clarifying the molecular underpinnings of their pharmacological actions, which provides a strong scientific basis for their therapeutic uses and facilitates the creation of evidence-based phytotherapeutics (Erukainure *et al.*, 2017). It is thought that a large part of *T. tetraptera*'s medicinal qualities stem from its nutritional value and richness of antioxidant bioactive compounds. Several important secondary metabolites, such as alkaloids, steroids, phenols, flavonoids, and saponins, were identified in *T. tetraptera* during the phytochemical screening. This finding corresponds to a previous study done on an aqueous isolate of *T. tetraptera* pulp by Adusei *et al.*, (2019). Given their capacity to alter cellular signalling pathways and fend off neurotoxic insults, flavonoids are well known for their neuroprotective properties (Adusei *et al.*, 2019; Atta *et al.*, 2017). As an essential antioxidant, phenols aid in the inhibition of neuroinflammatory signalling pathways and the neutralisation of reactive oxygen species (ROS). They offer a molecular defence against metabolic and environmental stresses that impair brain health by activating genes linked to neuronal survival and resilience (Dzah, 2022; Anyamele *et al.*, 2023). Lipid peroxidation, which is linked to the development of neurodegenerative diseases, is decreased, and neuronal integrity is preserved by these activities (Kemigisha *et al.*, 2018). Even though tannins were not present in the extract, the presence of alkaloids, saponins, and steroids enhances *T. tetraptera*'s overall neuroprotective potential. Alkaloids help protect neurons from excitotoxicity by regulating neurotransmitter activity and also act as natural anti-inflammatory

agents (Anyamele *et al.*, 2023; Kuate *et al.*, 2015; Ali *et al.*, 2023). Through their interactions with several cellular receptors, saponins are thought to improve brain transmission and encourage tissue regeneration (Erukainure *et al.*, 2017).

### **5.2 *T. tetraptera* Attenuates Weight Loss in Pb-Exposed Rats**

Body and organ weight fluctuations are significant indicators of overall health and physiological state (Haouas *et al.*, 2014). Notable variations can be early indicators of underlying health issues and frequently indicate systemic imbalances (Haouas *et al.*, 2014). It has been demonstrated that exposure to specific drugs and harmful substances, like Pb, affects an animal's body weight (Collin *et al.*, 2022; Enogieru and Momodu, 2022). These weight changes, especially a decrease in body mass, can be useful markers of the negative consequences of these substances (Enogieru & Iyoha, 2024). Pb poisoning interferes with normal growth and developmental processes, sometimes resulting in developmental delays (Ortega *et al.*, 2021). In more severe circumstances, it can lead to stunted growth (Ortega *et al.*, 2021). The current study revealed a general reduction in body and brain weight in the Pb-only group, an observation that is in agreement with studies conducted by Enogieru & Iyoha (2024), Haouas *et al.*, (2014), and Allouche *et al.*, (2011). Those studies observed that Low food intake as a result of malabsorption of micronutrients in the digestive tract, which is an indirect symptom of Pb, is a possible cause of the reduction in weight gain (Haouas *et al.*, 2014; Enogieru & Iyoha, 2024). Notably, it has been documented that Pb consumption causes anorexia in experimental animals, a disorder characterised by a decrease in food intake (Allouche *et al.*, 2011). Furthermore, it has been demonstrated that Pb exposure reduces muscle mass and causes cachexia, a state marked by a persistent rise in baseline metabolic rate without a commensurate rise in protein or calorie intake (Allouche *et al.*, 2011; Haouas *et al.*, 2014; Collin *et al.*, 2022). The considerable weight loss seen in rats exposed to Pb may be caused by these

processes. Concurrently, an improvement in weight outcomes was observed in Pb-exposed groups, co-administered with *T. tetraptera*, an observation that could demonstrate *T. tetraptera*'s protective capacity against Pb-induced weight reduction, perhaps as a result of its antioxidant and appetite-stimulating alkaloids (Meziane *et al.*, 2025). The well-known nutritional and medicinal benefits of *T. tetraptera* may be the cause of this increase in body weight. Saponins and alkaloids, two bioactive substances found in *T. tetraptera*, have been shown to increase hunger and boost nutritional absorption (Ezea *et al.*, 2024). Furthermore, its antioxidant qualities might help guard against muscle deterioration and enhance metabolic efficiency, improving overall health (Ezea *et al.*, 2024).

### **5.3 *T. tetraptera* Inhibits Neurobehavioural Deficits in Pb-Exposed Rats**

In toxicology research, rodent models are commonly employed to get a mechanistic understanding of chronic disorders and exposure to heavy metals. Since behaviour can be viewed as the result of motor and learning processes occurring in the neural system and may potentially serve as sensitive endpoints of chemically induced neurotoxicity, neurobehavioral studies are essential for risk assessment. Furthermore, neurobehavioral studies reveal that exposure to neurotoxins, particularly Pb, impacts motor function, processing speed, working memory, visuospatial abilities, and motor learning (Ortega *et al.*, 2021).

The Open Field Test (OFT), a well-known behavioural tool, is employed in assessing cerebellar dysfunction by monitoring an animal's general locomotor activity, exploratory behaviour, and anxiety-like reactions. The OFT offers information on how well cerebellar circuits are functioning by tracking movement patterns, evaluating the locomotor activity and exploratory motor function of experimental rats that were allowed to move freely in an open field arena. Here, ambulation (which assesses motor function, exploration and anxiety), the number of central square entries and

line crossings (the distances covered by the four paws), and immobility (the duration of time the rat was completely motionless) were assessed. It is a useful technique for evaluating the effects of neurotoxins such as Pb on the cerebellum and for screening possible anxiolytic chemicals due to its sensitivity to changes in behavioural reactivity and motor performance. In an animal model of cerebellar dysfunction, Pb exposure impacts OFT behaviour, specifically by elevating anxiety, depression, and motor learning deficits, as well as by eliciting alterations in locomotory activity. Additionally, aberrant neurotransmitter release and other metabolic alterations associated with cerebellar disorders have been correlated to Pb poisoning (Hernández-Coro et al., 2021). According to Ortega et al. (2021), exposure to Pb causes cerebellar disorders by disrupting motor learning capacity, hindering movement, and impairing the ability to coordinate motions and respond adequately. Results from this study indicated a significant reduction in ambulation, central square crossing, and line crossing, as well as an increase in the immobility parameter of the open field tests in the Pb-only treated group. Pb neurotoxicity and subsequent cerebellar dysfunction are generally marked by a decrease in motor engagement, as evidenced by decreased exploratory desire and elevated anxiety levels. These results are consistent with earlier studies showing that Pb exposure significantly lowers the exploratory behaviours in Wistar rats, possibly due to altered neurotransmitter signalling, mitochondrial malfunction, and calcium dysregulation (Ortega *et al.*, 2021; Singh *et al.*, 2024; Tartaglione *et al.*, 2020). Lower ambulatory activity in an animal model of cerebellar disorder with compromised motor muscle function is frequently associated with reduced horizontal and vertical activity, total distance travelled, and movement time (Johnson *et al.*, 2018). The OFT displayed shorter central zone duration, line crossing, and significantly longer immobility duration, which indicates less spontaneous movement and exploratory behaviour, possibly as a sign of depression and anxiety-induced response to an unfamiliar environment

(Olajide *et al.*, 2017). Findings from the neurobehavioral activity also observed the Movement Initiation Test, Step test, and String Test, which are widely accepted behavioural assays used to evaluate voluntary movement control, postural stability, number of adjustment steps, as well as grip strength (Ijonome *et al.*, 2014; Fujiwara *et al.*, 2017). As a result, locomotory deficits are indicated by latency time defects. Results from this study indicated a significant decrease in latency to grip loss (string test), step test, and an increase in the duration for movement initiation in the Pb-only group. These values indicate a lack of exploratory behaviour, motor impairment, and increased anxiety, perhaps due to metabolic alterations as well as abnormal neurotransmitter release (Ortega *et al.*, 2021). This is further supported by studies from Enogieru and Egbon (2022) and Abdulmajeed *et al.* (2016), who observed that Pb can cause damage to neural networks, leading to impairment of neurotransmission and hence, motor function. According to Mansouri *et al.* (2013), these results probably suggest that exposure to Pb may affect the striatal and cerebellar neural circuits that regulate motor activity and motor coordination, leading to altered motor functions. Concurrently, these deficiencies were lessened by co-treatment with *T. tetraptera*, which improved stability, exploratory behaviour, and reduced anxiety-like responses, indicating potential neuroprotection (Ekong *et al.*, 2021).

#### **5.4 *T. tetraptera* Inhibits Oxidative Stress in Pb-Exposed Rats**

It is commonly acknowledged that one of the main ways that heavy metals harm the neurological system is through oxidative stress (Carocci *et al.*, 2016). By promoting the production of ROS, which are chemically unstable molecules that are capable of causing neuronal damage, metals like Pb aid in this process (Enogieru & Iyoha, 2024). Cerebellar dysfunction develops when the body's antioxidant systems and oxidative agents are not in balance; in other words, when the production of ROS exceeds the cell's capacity to neutralise them or repair the damage they cause (Zhang *et*

*al.*, 2024). Increased production of ROS, via compromised antioxidant-cofactor defences, and ionic mimicry may be the mechanism of this dysfunction (Carocci *et al.*, 2016; Talpur *et al.*, 2018). Due to the presence of their unpaired electrons, ROS interact destructively with proteins, lipids, and DNA, thereby altering their form to a functional relationship (Flora *et al.*, 2012). Pb can penetrate the blood-brain barrier and interfere with enzyme systems that are necessary for maintaining brain homeostasis (Collin *et al.*, 2022). Given its high oxygen demand and lipid-rich structure, the brain is particularly vulnerable to oxidative damage, making robust antioxidant defence essential for preserving cellular integrity (Collin *et al.*, 2022). The body uses antioxidants molecules that may safely donate electrons to ROS to fight oxidative stress. The tripeptide glutathione (GSH), catalase (CAT), and superoxide dismutase (SOD) are three of these defences' most important components; they all aid in preventing or repairing oxidative damage (Carocci *et al.*, 2016). Given that these enzymes rely on trace elements for structural and catalytic activity, they are particularly susceptible to Pb toxicity (Jomova *et al.*, 2025). Pb normally disrupts cerebellar neurotransmission by raising Malondialdehyde (MDA) and reactive oxygen species (ROS) levels, whereas glutathione (GSH), catalase (CAT), glutathione peroxidase (GPX), and superoxide dismutase (SOD) are usually reduced. By reducing cellular damage via the conversion of extremely reactive superoxide radicals into hydrogen peroxide and oxygen, SOD acts as the first line of defence (Carocci *et al.*, 2016). In the brain, where oxidative activity is high and ROS damage can impair neurological function, this function is essential (Enogieru & Iyoha, 2024). Subsequently, CAT breaks down hydrogen peroxide into water and oxygen, neutralising the molecule that, if unregulated, might worsen oxidative stress (Jomova, 2025). Additionally, CAT provides protection by maintaining SOD activity, which may be weakened by accumulating hydrogen peroxide (Jomova, 2025). High hydrogen peroxide levels can damage brain tissue,

particularly in regions like the cerebellum, if CAT function is impaired (Carocci *et al.*, 2016; Jomova, 2025). By directly attaching to and eliminating free radicals, GSH enhances these defences and acts as an essential cellular component defender (Averill-Bates, 2023)). Malondialdehyde (MDA), on the other hand, is a byproduct of lipid peroxidation that is frequently employed as an oxidative stress biomarker. MDA, which is produced when polyunsaturated fatty acids break down, is a measure of the degree of lipid membrane damage brought on by ROS (Enogieru & Iyoha, 2024). An accurate assessment of oxidative damage in tissues can be obtained by measuring MDA levels (Enogieru & Iyoha, 2024).

This study shows that Pb significantly increased cerebellar MDA level, while SOD, CAT, GPx, and GSH concentrations were all reduced in the Pb-only group. This agrees with previous studies, which showed that Pb deactivates antioxidants by binding to their thiol groups containing sulphhydryl and/or by replacing the calcium cofactor of the enzyme (Enogieru & Iyoha, 2024; Carocci *et al.*, 2016; Baird & Cann, 2012). The subsequent effect of this is the impairment of antioxidant capacity to scavenge free radicals, which disturbs the cerebellar redox balance, leading to an increase in reactive oxygen species. The resulting tissue oxidative stress plays a key role in toxicity, carcinogenesis, or apoptosis (Zhao *et al.*, 2023). *T. tetraptera* co-treatment reversed these effects, probably as a result of its flavonoid and phenol rich contents that offer strong antioxidant effects, thereby reducing oxidative stress (Anyamele *et al.*, 2023; Kuate *et al.*, 2015).

#### **5.5 *T. tetraptera* Mitigates Pb Accumulation and Histological Alterations in The Cerebellum of Pb-Exposed Rats**

By getting through the blood-brain barrier via the imitation of calcium, Pb can accumulate within the cerebellum, weaken its neurons' integrity, and obstruct neurotransmission pathways (Enogieru & Iyoha, 2024; Singh *et al.*, 2024). This severely impairs the transduction of nerve impulses,

resulting in fatigue, a lack of coordination, and muscular weakness (Roostaei *et al.*, 2014). Results from this study show that *T. tetraptera* pretreatment significantly lowered cerebellar Pb levels, indicating that it has metal-chelating, and neuroprotective properties (Mensah *et al.*, 2024; Lawal *et al.*, 2025). Given that Pb is slowly removed from brain tissue, *T. tetraptera* may have therapeutic use in reducing long-term neurotoxicity after exposure (Mensah *et al.*, 2024).

Due to the cerebellum being the primary hub for processes like motor coordination, equilibrium and motor learning, it is highly dependent on the structural and functional integrity of its neurons. The intricate neuronal structure of the cerebellum makes it susceptible to Pb toxicity (Nam *et al.*, 2019). According to a previous study, cortical neurons are particularly susceptible to Pb-induced degeneration, which can result in impairments in motor activities and skills (Gudadhe *et al.*, 2024). Pb damages cortical neurons, such as Purkinje and granule cells, by interfering with synaptic function and causing oxidative stress (Saleh & Meligy, 2018; Gudadhe *et al.*, 2024 ; Singh *et al.*, 2019). Pb neurotoxicity upsets cerebellar homeostasis and impairs motor function (Ortega *et al.*, 2021; Saleh & Meligy, 2018). The histoarchitectural analysis of the cerebellum showed a significantly altered cerebellum in the Pb-only group, with degenerating Purkinje cells bearing irregular, pyknotic nuclei as well as a vacuolated molecular layer. This aligns with previous studies done by Saleh & Meligy, (2018) and Gudadhe *et al.*, (2024), who observed that an elevated level of Pb in the cerebellum has a deleterious effect. However, an improvement in the histological structure was observed in the Pb-exposed rats co-treated with *T. tetraptera*, as well as in the *T. tetraptera*-only group, which maintained brain integrity, perhaps due to *T. tetraptera* antioxidant-rich flavonoids and phenolics (Ekong *et al.*, 2021, Meziane *et al.*, 2025).

### **5.6 *T. tetraptera* HPLC Analysis and Ligand–Receptor Interactions**

Polyphenols (phenolic compounds) are bioactive secondary metabolites that are ubiquitous in plant tissues, and have been documented to confer several health benefits, which include antioxidant, anti-inflammatory and antiapoptotic effects (Durazzo *et al.*, 2019). Results from the HPLC analysis of *T. tetraptera* show the presence of two key polyphenols, 4-Hydroxybenzoic Acid and Resorcinol. 4-hydroxybenzoic acid is a phenolic acid produced from benzoic acid during tyrosine metabolism (Durazzo *et al.*, 2019), while Resorcinol is one of the three isomeric benzenediols (1,3-isomer of benzenediol) (Reghuvaran and Ravindranath, 2012).

The antioxidant response is regulated by NRF2 (Nuclear Factor Erythroid 2-Related Factor 2), a transcription factor that regulates how genes related to cellular defence, redox balance, and detoxification are expressed (Ngo *et al.*, 2022; He *et al.*, 2020). In oxidative stress-related disorders such as Pb-induced neurotoxicity, ataxia and inflammatory disorders, NRF2 activation provides protection (He *et al.*, 2020). Results from the in-silico study indicate that 4-Hydroxybenzoic Acid exhibits the strongest predicted binding to NRF2 (-5.168 kcal/mol), while Resorcinol also exhibits notable binding power (-3.196 kcal/mol) when compared to the standards Riluzole (-3.161 kcal/mol) and Amantadine (0.235 kcal/mol). These findings suggest a highly stable interaction and possible activation or modulation, indicating that these secondary metabolites may effectively engage NRF2 and support antioxidant defence mechanisms. Due to their strong binding power, 4-hydroxybenzoic Acid and Resorcinol may increase the transcription of antioxidant enzymes such as glutathione peroxidase, superoxide dismutase, and heme oxygenase-1 (HO-1), which may reduce cellular damage and validate their well-known antioxidant properties (He *et al.*, 2020; Ngo *et al.*, 2022). As a result, this may indicate that the interactions between NRF2 and *T. tetraptera* secondary metabolites (Resorcinol, but most especially 4-

hydroxybenzoic acid) in the cerebellum of *T. tetraptera*-treated Wistar rats may have been engaged during Pb-induced oxidative stress, potentially lowering oxidative stress.

In the apoptotic cascade, caspase-3 is a key executioner enzyme that cleaves cellular substrates during programmed cell death. One characteristic of neuronal apoptosis in neurotoxicity models like cerebellar dysfunction, particularly those involving Pb exposure, is Caspase-3 activation (Asadi *et al.*, 2022; Panda *et al.*, 2021). Depending on the situation and binding dynamics, compounds that bind to Caspase-3 can either promote its activation (promoting apoptosis) or inhibit its activity (preventing cell death). The strongest anticipated binding to Caspase-3 was exhibited by Resorcinol (-3.983 kcal/mol). This points to a very stable association and possible apoptotic pathway modification. 4-hydroxybenzoic acid also showed notable binding power (-3.698 kcal/mol) when compared to the reference standards Riluzole (-3.967 kcal/mol) and Amantadine (0.18 kcal/mol), suggesting that it may also have a notable interaction with Caspase-3, thereby potentially affecting cell death or survival. According to their binding, they might have an impact on apoptotic signalling, thereby providing neuroprotective or regulatory benefits in models of neurodegeneration or heavy metal toxicity. Given that caspase-3 is one of the crucial proteins in the apoptotic process, its inhibition through a strong binding association with Resorcinol and 4-hydroxybenzoic acid ligands, as shown in the present study, may reduce and possibly reverse neuronal death in the early stages of Pb-induced cerebellar damage (Shahidi *et al.*, 2019; Xia, 2021).

Interleukin-6 (IL-6), Tissue necrosis factor-alpha (TNF- $\alpha$ ) and nuclear factor kappa B (Nf- $\kappa$ B) are key cytokines and transcription factors involved in inflammation, immune regulation, and neurodegeneration (Tanaka *et al.*, 2014). Multiple sclerosis, Alzheimer's disease, and Pb-induced neurotoxicity are among the conditions linked to elevated IL-6, TNF- $\alpha$ , and Nf- $\kappa$ B levels

(Gudadhe *et al.*, 2024). Effective IL-6, TNF- $\alpha$  and Nf- $\kappa$ B binding compounds may help control its activity, which could lessen inflammatory cascades and safeguard neuronal tissue (Atli, 2022). With a docking score of -4.424 kcal/mol, Resorcinol exhibits the highest predicted binding to IL-6, while 4-hydroxybenzoic acid, with (-3.595 kcal/mol), also showed notable binding power according to molecular docking results. For TNF- $\alpha$ , Resorcinol (-3.475 kcal/mol) followed by 4-hydroxybenzoic acid (-3.044 kcal/mol) exhibit the strongest binding scores, while for Nf- $\kappa$ B binding interactions, Resorcinol (-3.622 kcal/mol) and 4-hydroxybenzoic acid (-3.12 kcal/mol) showed the strongest docking scores, respectively. In comparison to the test compounds, the reference standards Riluzole and Amantadine exhibit generally lower binding scores to the three pro-inflammatory makers, indicating a less direct interaction with IL-6, TNF- $\alpha$  and Nf- $\kappa$ B. The strong interactions of Resorcinol and 4-hydroxybenzoic acid suggest a very stable complex that might obstruct IL-6, TNF- $\alpha$  and Nf- $\kappa$ B pro-inflammatory signalling, indicating possible anti-inflammatory potential in neurotoxicity models (Atli, 2022).

## 5.7 CONCLUSION

Bioactive compounds from *T. tetraptera* exhibit meaningful binding affinities to key neuroinflammatory, apoptotic, and oxidative markers, as demonstrated by the molecular docking analysis. Notably, significant interactions between the compounds Resorcinol and 4-hydroxybenzoic acid indicated their capacity to modulate apoptotic pathways, inhibit inflammatory signalling, and regulate oxidative stress. This finding corroborates the histological results demonstrating that rats treated with Pb alone exhibited significant cerebellar damage, characterised by vacuolations and pyknotic nuclei, particularly in the Purkinje cell and molecular layers. Behavioural results further corroborate the histology conclusions, showing that rats exposed to Pb exhibited notable impairments in locomotory and exploratory behaviour, which are

indicative of neurotoxicity. In contrast, rats co-treated with *T. tetraptera* extract exhibited a significant increase in performance across behavioural tests, as well as little or no neurodegenerative symptoms, indicating improved motor function and a decrease in anxiety-like behaviour, further suggesting a significant level of neuro-protection. Taken together, these results imply that *T. tetraptera* confers neuroprotection via a multi-target strategy that inhibits Caspase-3 capacity to boost apoptotic signalling, increases antioxidant activity by activating NRF2, and attenuates inflammation by inhibiting TNF- $\alpha$ , NF- $\kappa$ B and IL-6. This integrative evidence underscores *T. tetraptera's* therapeutic potential in reducing Pb-induced neurotoxicity, which further supports its continued exploration as a neuroprotective agent.

#### 5.8 RECOMMENDATIONS

Further investigations on *T. tetraptera* should focus on the isolation of bioactive compounds that confer *T. tetraptera* its neuroprotective properties against Pb-induced cerebellar dysfunction. Additional antioxidant, anti-inflammatory, and anti-apoptotic mechanisms should be investigated in other neurodegenerative models. Also, *T. tetraptera* should be considered for clinical trials in humans.

#### 5.9 CONTRIBUTION TO KNOWLEDGE

The study has contributed to knowledge in the following ways:

1. It revealed that aqueous *T. tetraptera* fruit extract attenuated Pb acetate-induced neurobehavioral deficits and inhibited elevated Pb levels in the cerebellum of experimental rats.
2. It showed that aqueous *T. tetraptera* fruit extract protected against Pb acetate-induced histological alterations in the cerebellum of experimental rats.

**Commented [h14]:** Note good in this form. Please list and number your recommendations. Your recommendations are only for further studies. Why?

**Commented [h15]:** Add 5

3. It demonstrated the presence of 4-hydroxybenzoic acid and resorcinol in the aqueous fruit extract of *T. tetraptera* and its high docking potential for antioxidant activation, pro-apoptotic inhibition, and pro-inflammatory deactivation.

## REFERENCES

- Abd El-Monem, D. D. (2012). The modulating effect of melatonin against the genotoxicity of lead acetate. *The Journal of Basic & Applied Zoology*, 65(4), 223-231.
- Abdulmajeed, W. I., Sulieman, H. B., Zubayr, M. O., Imam, A., Amin, A., Biliaminu, S. A., ... & Owoyele, B. V. (2016). Honey prevents neurobehavioural deficit and oxidative stress induced by lead acetate exposure in male wistar rats-a preliminary study. *Metabolic brain disease*, 31(1), 37-44.
- Abugri, D. A., & Pritchett, G. (2013). Determination of chlorophylls, carotenoids, and fatty acid profiles of Tetrapleura tetraptera seeds and their health implication. *Journal of herbs, spices & medicinal plants*, 19(4), 391-400.
- Abu-taweel, G. M. (2018). Curcumin attenuates lead (Pb)-induced neurobehavioral and neurobiochemical dysfunction: a review. *Int J Pharm Pharm Sci*, 10(8), 23-8.
- Acharya, S. (2024). Heavy Metal Contamination in Food: Sources, Impact, and Remedy. In *Food Safety and Quality in the Global South* (pp. 233-261). Singapore: Springer Nature Singapore.
- Adadi, P., & Kanwugu, O. N. (2020). Potential application of tetrapleura tetraptera and hibiscus sabdariffa (malvaceae) in designing highly flavoured and bioactive pito with functional properties. *Beverages*, 6(2), 22.
- Adesina, S. K., Iwalewa, E. O., & Johnny, I. I. (2016). Tetrapleura tetraptera Taub-ethnopharmacology, chemistry, medicinal and nutritional values-a review. *British Journal of Pharmaceutical Research*, 12(3), 1-22.

- Adusei, S., Otchere, J. K., Oteng, P., Mensah, R. Q., & Tei-Mensah, E. (2019). Phytochemical analysis, antioxidant and metal chelating capacity of *Tetrapleura tetraptera*. *Heliyon*, 5(11).
- Aikins, A. R., Birikorang, P. A., Chama, M., Dotse, E., Anning, A., & Appiah-Opong, R. (2021). Antiproliferative activities of methanolic extract and fractions of *tetrapleura tetraptera* fruit. *Evidence-Based Complementary and Alternative Medicine*, 2021(1), 4051555.
- Akinwumi, I. A., Adegoke, S. A., Oyelami, O. A., Akinwumi, A. E., & Adedeji, T. A. (2023). High blood lead levels of children in a gold mining community in Osun State, Nigeria: an urgent call for action. *Transactions of The Royal Society of Tropical Medicine and Hygiene*, 117(10), 714-726.
- Aktepe, N., Baran, M. F., & Baran, A. (2022). Effects of chronic exposure to Lead on some organs. *Assistant*, 18, 45.
- Ali, A. H. (2022). High-performance liquid chromatography (HPLC): A review. *Ann. Adv. Chem*, 6, 010-020.
- Alisha, V. P., & Gupta, P. (2018). A comprehensive review of environmental exposure of toxicity of lead. *J. Pharmacol. Phytochem*, 7, 1991-1995.
- Allouche, L., Hamadouche, M., Touabti, A., & Khennouf, S. (2011). Effect of long-term exposure to low or moderate lead concentrations on growth, lipid profile and liver function in albino rats. *Advances in biological research*, 5(6), 339-347.

- Anumudu, C. (2020). Biopreservative potential of the spices; piper guineense (uziza), xylopia aethiopica (uda) and tetrapleura tetraptera (oshorisho) in fresh fruit juices. *Journal of Food Technology & Nutrition Science*, 108(2).
- Anyamele, T., Onwuegbuchu, P. N., Ugbogu, E. A., & Ibe, C. (2023). Phytochemical composition, bioactive properties, and toxicological profile of Tetrapleura tetraptera. *Bioorganic Chemistry*, 131, 106288.
- Apps, R., & Garwicz, M. (2005). Anatomical and physiological foundations of cerebellar information processing. *Nature Reviews Neuroscience*, 6(4), 297-311.
- Asadi, M., Taghizadeh, S., Kaviani, E., Vakili, O., Taheri-Anganeh, M., Tahamtan, M., & Savardashtaki, A. (2022). Caspase-3: structure, function, and biotechnological aspects. *Biotechnology and Applied Biochemistry*, 69(4), 1633-1645.
- Assi, M. A., Hezme, M. N. M., Sabri, M. Y. M., & Rajion, M. A. (2016). The detrimental effects of lead on human and animal health. *Veterinary world*, 9(6), 660.
- Atli, N. (2022). *Investigating anti-inflammatory effects of common dietary phenolic acids and their structurally related synthetic analogues in immune cells* (Doctoral dissertation, University of East Anglia), 85696.
- Atta, E. M., Mohamed, N. H., & Abdelgawad, A. A. (2017). Antioxidants: An overview on the natural and synthetic types. *Eur. Chem. Bull*, 6(8), 365-375.
- Averill-Bates, D. A. (2023). The antioxidant glutathione. In *Vitamins and hormones* (Vol. 121, pp. 109-141). Academic Press.

- Ayoola, G. A., Adeleke, O., Johnson, O. O., & Adeyemi, D. K. (2018). Investigation of anti-inflammatory activity of fractions from the methanol extracts of the leaf of *tetrapleura tetraptera* (schumach & thonn) taub. *The Nigerian Journal of Pharmacy*, 52(1).
- Ayuba, Y., Ekanem, A. G. S. H., & Garba, S. H. (2017). Effect of oral administration of lead acetate exposure on the histology of the testis and testicular sperm concentration in Wistar albino rats. *Sch. J. Appl. Med. Sci*, 1, 2337-2344
- Bacanli, M., Dilsiz, S. A., Başaran, N., & Başaran, A. A. (2019). Effects of phytochemicals against diabetes. *Advances in food and nutrition research*, 89, 209-238.
- Baird, C., & Cann, M. (2012). The pollution and purification of water. *Environ Chem*, 601-660.
- Bancroft, J. D., & Layton, C. (2018). 10—The hematoxylin and eosin. *Bancroft's Theory and Practice of Histological Techniques, 8th ed.; Suvarna, SK, Layton, C., Bancroft, JD, Eds*, 126-138.
- Blume, S. R., Cass, D. K., & Tseng, K. Y. (2009). Stepping test in mice: a reliable approach in determining forelimb akinesia in MPTP-induced Parkinsonism. *Experimental neurology*, 219(1), 208-211.
- Bhushan, R., Ravichandiran, V., & Kumar, N. (2022). An overview of the anatomy and physiology of the brain. *Nanocarriers for Drug-Targeting Brain Tumors*, 3-29.
- Boldyrev, M. (2018). Lead: properties, history, and applications. *WikiJournal of Science*, 1(2), 1-23.
- Bonsou, I. N., Mbaveng, A. T., Nguenang, G. S., Chi, G. F., Kuete, V., & Efferth, T. (2022). Cytotoxicity, acute and sub-chronic toxicities of the fruit extract of *Tetrapleura tetraptera* (Schumm. & Thonn.) Taub. (Fabaceae). *BMC complementary medicine and therapies*, 22(1), 178.

- Boskabady, M., Ghorani, V., Beigoli, S., & Boskabady, M. H. (2022). The effects of environmental lead on teeth and bone status and the mechanisms of these effects, animal and human evidence, a review. *Toxin Reviews*, *41*(4), 1396-1415.
- Brodziak-Dopierała, B. (2020). Lead—factors affecting its content in bone tissue. *Pomeranian Journal of Life Sciences*, *66*(4).
- Brunner, H. (1984). Iterated collocation methods and their discretizations for Volterra integral equations. *SIAM journal on numerical analysis*, *21*(6), 1132-1145.
- Buckner, R. L. (2013). The cerebellum and cognitive function: 25 years of insight from anatomy and neuroimaging. *Neuron*, *80*(3), 807-815.
- Buege, J. A., & Aust, S. D. (1978). [30] Microsomal lipid peroxidation. In *Methods in enzymology* (Vol. 52, pp. 302-310). Academic press.
- Cabaraux, P., Gandini, J., Kakei, S., Manto, M., Mitoma, H., & Tanaka, H. (2020). Dysmetria and errors in predictions: the role of internal forward model. *International journal of molecular sciences*, *21*(18), 6900.
- Cabrero, F. R., & De Jesus, O. (2023). Dysdiadochokinesia. In *StatPearls [Internet]*. StatPearls Publishing, NBK559262.
- Carocci, A., Catalano, A., Lauria, G., Sinicropi, M. S., & Genchi, G. (2016). Lead toxicity, antioxidant defense and environment. *Reviews of environmental contamination and toxicology*, 45-67.
- Carstens, M. H., & Sarnat, H. B. (2023). The Neuromeric System: Segmentation of the Neural Tube. In *The Embryologic Basis of Craniofacial Structure: Developmental Anatomy*,

Evolutionary Design, and Clinical Applications (pp. 241-309). *Cham: Springer International Publishing*.

Christenhusz, M. J., & Byng, J. (2016). The number of known plants species in the world and its annual increase. *Phytotaxa*, 261(3), 201-217.

Cicalău, G. I. P., Babes, P. A., Calniceanu, H., Popa, A., Ciavoi, G., Iova, G. M., ... & Scrobotă, I. (2021). Anti-inflammatory and antioxidant properties of carvacrol and magnolol, in periodontal disease and diabetes mellitus. *Molecules*, 26(22), 6899.

Cohen, G., Dembiec, D., & Marcus, J. (1970). Measurement of catalase activity in tissue extracts. *Analytical biochemistry*, 34(1), 30-38.

Collin, M. S., Venkatraman, S. K., Vijayakumar, N., Kanimozhi, V., Arbaaz, S. M., Stacey, R. S., Anusha, J., Choudhary, R., Lvov, V., Tovar, G.I., Senatov, F., & Swamiappan, S. (2022). Bioaccumulation of Lead (Lead) and its effects on human: A review. *Journal of Hazardous Materials Advances*, 7, 100094.

da Silva, D. R. F., Bittencourt, L. O., Aragão, W. A. B., Nascimento, P. C., Leão, L. K. R., Oliveira, A. C. A., ... & Lima, R. R. (2020). Long-term exposure to lead reduces antioxidant capacity and triggers motor neurons degeneration and demyelination in spinal cord of adult rats. *Ecotoxicology and Environmental Safety*, 194, 110358.

Davidson, A., Ryman, J., Sutherland, C., Milner, E., Kerby, R., Teindl, H., Melin, A. & Bolt, H. (2014). *Ullmanns Encyclopedia of Industrial Chemistry—Lead*, 29.

- Davinelli, S., De Stefani, D., De Vivo, I., & Scapagnini, G. (2020). Polyphenols as caloric restriction mimetics regulating mitochondrial biogenesis and mitophagy. *Trends in Endocrinology & Metabolism*, 31(7), 536-550.
- de Carvalho, F. O., Silva, É. R., Gomes, I. A., Santana, H. S. R., do Nascimento Santos, D., de Oliveira Souza, G. P., ... & Nunes, P. S. (2020). Anti-inflammatory and antioxidant activity of carvacrol in the respiratory system: A systematic review and meta-analysis. *Phytotherapy research*, 34(9), 2214-2229.
- de Souza, I. D., de Andrade, A. S., & Dalmolin, R. J. S. (2018). Lead-interacting proteins and their implication in lead poisoning. *Critical reviews in toxicology*, 48(5), 375-386.
- Dongre, R. S. (2020). Lead: Toxicological Profile, Pollution Aspects and Remedial. *Lead chemistry*, 45.
- Durazzo, A., Lucarini, M., Souto, E. B., Cicala, C., Caiazzo, E., Izzo, A. A., ... & Santini, A. (2019). Polyphenols: A concise overview on the chemistry, occurrence, and human health. *Phytotherapy Research*, 33(9), 2221-2243.
- Dzah, C. S. (2022). Optimized ultrasound-assisted recovery, HPLC/LC-MS identification and biological activities of *Tetrapleura tetraptera* L. dry fruit polyphenols. *Food Chemistry Advances*, 1, 100093.
- Ebana, R., Edet, U., Ekanemesang, U., Ikon, G., Etok, C., & Edet, A. (2016). Antimicrobial activity, phytochemical screening and nutrient analysis of *Tetrapleura tetraptera* and *Piper guineense*. *Asian Journal of medicine and Health*, 1(3), 1-8.

Edeoga, H. O., Okwu, D. E., & Mbaebie, B. O. (2005). Phytochemical constituents of some Nigerian medicinal plants. *African Journal of Biotechnology*, 4(7), 685-688.

**Commented [h16]:** Capital letters J and B are needed.

Eggers, S. D. (2019). Approach to the Examination and Classification of Nystagmus. *Journal of Neurologic Physical Therapy*, 43, S20-S26.

Ekong, M. B., Iniodu, C. F., Essien, I. G., & Edem, S. J. (2021). Tetrapleura tetraptera (Schumach.) Taub. fruit extract improves cognitive behaviour and some brain areas of pentylenetetrazol-kindling rats. *J. Neurosci*, 12(1), 29-39.

**Commented [h17]:** Use full names for all journals.

Elekofehinti, O. O., Onunkun, A. T., & Olaleye, T. M. (2020). Cymbopogon citratus (DC.) Stapf mitigates ER-stress induced by streptozotocin in rats via down-regulation of GRP78 and up-regulation of Nrf2 signaling. *Journal of ethnopharmacology*, 262, 113130.

Ellman, G. L. (1959). Tissue sulfhydryl groups. *Archives of biochemistry and biophysics*, 82(1), 70-77.

Emsley, J. (2011). *Nature's building blocks: an AZ guide to the elements*. Oxford University Press, 9780199605637.

Enabulele, S. A., & Ugha, O. (2019). Antimicrobial, Phytochemical and Nutritional Properties of Tetrapleura tetraptera Seed and Fruit Extracts: doi. org/10.26538/tjnpr/v3i6. 2. *Tropical Journal of Natural Product Research (TJNPR)*, 3(6), 190-194.

Enogieru, A.B., & Egbon, F.O. (2022). Neurobehavioural and Histological Alterations in Lead Acetate-Exposed Rats Pretreated with Aqueous Leaf Extract of Vernonia amygdalina. *African Journal of Biomedical Research*, 25(2).

- Enogieru, A. B., & Iyoha, E. N. (2024). Role of nitric oxide, TNF- $\alpha$  and Caspase-3 in lead acetate-exposed rats pretreated with Aqueous Rosmarinus officinalis Leaf Extract. *Biological Trace Element Research*, 202(9), 4021-4031.
- Enogieru, A. B., and Momodu, O. (2022). Neuroprotective effects of *Zingiber officinale* against lead-induced toxicity in Wistar rats. *Nutrire*, 48(1), 2.
- Erukainure, O. L., Onifade, O. F., Odjobo, B. O., Olasehinde, T. A., Adesioye, T. A., Tugbobo-Amisu, A. O., ... & Okonrokwo, G. I. (2017). Ethanol extract of Tetrapleura tetraptera fruit peels: Chemical characterization, and antioxidant potentials against free radicals and lipid peroxidation in hepatic tissues. *Journal of Taibah University for Science*, 11(6), 861-867.
- Ezea, J., Ezike, J. C., Nathaniel, J., Ewa, E. U., & Isaac, U. C. (2024). Growth Performance and Blood Profile of Pre-pubertal Boars Fed Aidan (*Tetrapleura tetraptera*) Pod Meal. *Nigerian Journal of Biotechnology*, 41(1), 1-6.
- Famobuwa, O., Lajide, L., Owolabi, B., Osho, I., & Amuho, U. (2016). Antioxidant activity of the fruit and stem bark of *Tetrapleura tetraptera* Taub (Mimosaceae). *British Journal of Pharmaceutical Research*, 9(3), 1-4.
- Flora, G., Gupta, D., & Tiwari, A. (2012). Toxicity of Lead: a review with recent updates. *Interdisciplinary toxicology*, 5(2), 47.
- Fujiwara, M., Iwata, M., Inoue, T., Aizawa, Y., Yoshito, N., Hayashi, K., & Suzuki, S. (2017). Decreased grip strength, muscle pain, and atrophy occur in rats following long-term exposure to excessive repetitive motion. *FEBS open bio*, 7(11), 1737-1749.

- Ghasemi, A., Ataei Nakhaei, A., Alizadeh Ghamsari, A., Salehi, M., & Kalani-Moghaddam, F. (2017). Anemia, iron deficiency anemia and lead poisoning in children with opioid toxicity: a study in North East of Iran. *Iranian Journal of Pediatric Hematology and Oncology*, 7(2), 90-97.
- Goodlett, C. R., & Mittleman, G. (2017). The cerebellum. In *Conn's Translational Neuroscience* (pp. 191-212). Academic Press.
- Gudadhe, S., Singh, S. K., & Ahsan, J. (2024). Cellular and neurological effects of Lead (Lead) toxicity. In *Lead toxicity mitigation: Sustainable nexus approaches* (pp. 125-145). Cham: Springer Nature Switzerland.
- Gudlavalleti, A., & Tenny, S. (2022). Cerebellar neurological signs. In *StatPearls [Internet]*. StatPearls Publishing, NBK556080.
- Han, Q., Zhang, W., Guo, J., Zhu, Q., Chen, H., Xia, Y., & Zhu, G. (2021). Mitochondrion: a sensitive target for lead exposure. *The Journal of toxicological sciences*, 46(8), 345-358.
- Haouas, Z., Sallem, A., Zidi, I., Hichri, H., Mzali, I., & Mehdi, M. (2014). Hepatotoxic effects of lead acetate in rats: histopathological and cytotoxic studies. *Journal of Cytology & Histology*, 5(5), 1.
- Harborne, J. B. (1973). Phenolic compounds. In *Phytochemical methods: A guide to modern techniques of plant analysis* (pp. 33-88). Dordrecht: Springer Netherlands.
- He, F., Ru, X., & Wen, T. (2020). NRF2, a transcription factor for stress response and beyond. *International journal of molecular sciences*, 21(13), 4777.

- Heidelberg, D., Ronsin, S., Bonneville, F., Hannoun, S., Tilikete, C., & Cotton, F. (2018). Main inherited neurodegenerative cerebellar ataxias, how to recognize them using magnetic resonance imaging?. *Journal of Neuroradiology*, *45*(5), 265-275.
- Hernández-Coro, A., Sánchez-Hernández, B. E., Montes, S., Martínez-Lazcano, J. C., González-Guevara, E., & Pérez-Severiano, F. (2021). Alterations in gene expression due to chronic lead exposure induce behavioral changes. *Neuroscience & Biobehavioral Reviews*, *126*, 361-367.
- Hoxha, E., Tempia, F., Lippiello, P., & Miniaci, M. C. (2016). Modulation, plasticity and pathophysiology of the parallel fiber-purkinje cell synapse. *Frontiers in synaptic neuroscience*, *8*, 35.
- Hsu, C. C., Cheng, C. H., Hsu, C. L., Lee, W. J., Huang, S. C., & Huang, Y. C. (2015). Role of vitamin B6 status on antioxidant defenses, glutathione, and related enzyme activities in mice with homocysteine-induced oxidative stress. *Food & nutrition research*, *59*(1), 25702.
- Ijomone, O. M., Olaibi, O. K., Biose, I. J., Mba, C., Umoren, K. E., & Nwoha, P. U. (2014). Performance of motor associated behavioural tests following chronic nicotine administration. *Annals of Neurosciences*, *21*(2), 42.
- Iwaloye, O., Elekofehinti, O. O., Oluwarotimi, E. A., Kikiowo, B. I., & Fadipe, T. M. (2020). Insight into glycogen synthase kinase-3 $\beta$  inhibitory activity of phyto-constituents from *Melissa officinalis*: in silico studies. *In silico pharmacology*, *8*(1), 2.

- Johnson Jr, J., Pajarillo, E. A. B., Taka, E., Reams, R., Son, D. S., Aschner, M., & Lee, E. (2018). Valproate and sodium butyrate attenuate manganese-decreased locomotor activity and astrocytic glutamate transporters expression in mice. *Neurotoxicology*, *64*, 230-239.
- Jomova, K., Alomar, S. Y., Nepovimova, E., Kuca, K., & Valko, M. (2025). Heavy metals: toxicity and human health effects. *Archives of toxicology*, *99*(1), 153-209.
- Kemigisha, E., Owusu, E. O., Elusiyan, C. A., Omujal, F., Tweheyo, M., & Bosu, P. P. (2018). Tetrapleura tetraptera in Ghana, Nigeria and Uganda: households uses and local market. *Forests, Trees and Livelihoods*, *27*(4), 243-256.
- Kim, H. C., Jang, T. W., Chae, H. J., Choi, W. J., Ha, M. N., Ye, B. J., ... & Hong, Y. S. (2015). Evaluation and management of Lead exposure. *Annals of occupational and environmental medicine*, *27*, 1-9.
- Knierim, J. (2020). Overview: Functions of the Cerebellum. *Neuroscience Online*, *October*, *20*, 2020, 3, 5.
- Koma, O. S., Olawumi, O. O., Godwin, E. U., & Theophilus, O. A. (2016). Phytochemical screening, in-vitro antimicrobial activity and antioxidant characteristics of Tetrapleura tetraptera extracts. *Eur J Med Plants*, *17*(2), 1-10.
- Kuate, D., Kengne, A. P. N., Biapa, C. P. N., Azantsa, B. G. K., & Wan Muda, W. A. M. B. (2015). Tetrapleura tetraptera spice attenuates high-carbohydrate, high-fat diet-induced obese and type 2 diabetic rats with metabolic syndrome features. *Lipids in Health and Disease*, *14*, 1-13.

- Kuo, S. H., Lin, C. C., & Ashizawa, T. (2021). Cerebellar ataxia. In *Bradley and Daroff's Neurology in Clinical Practice* (pp. 288-309). Elsevier.
- Kuraeiad, S., & Kotepui, M. (2021). Blood lead level and renal impairment among adults: A meta-analysis. *International journal of environmental research and public health*, 18(8), 4174.
- Langmuir, C. H., & Broecker, W. (2012). *How to build a habitable planet: the story of earth from the big bang to humankind-revised and expanded edition*. Princeton University Press, 9781400841974
- Lara-Aparicio, S. Y., Laureani-Fierro, A. J., Morgado-Valle, C., Beltrán-Parrazal, L., Rojas-Durán, F., García, L. I., ... & Pérez, C. A. (2022). Latest research on the anatomy and physiology of the cerebellum. *Neurology perspectives*, 2(1), 34-46.
- Larbie, C., Mills-Robertson, F. C., Quaicoe, E. B., Opoku, R., Kabiri, N. C., & Abrokwah, R. O. (2020). Tetrapleura tetraptera of Ghanaian origin: phytochemistry, antioxidant and antimicrobial activity of extracts of plant parts. Antioxidant and Antimicrobial Activity of Extracts of Plant Parts. *Journal of Pharmaceutical Research International*, 32(35): 78-96
- Lawal, A. O., Agboola, O. O., Akinjiyan, M. O., Ijatuyi, T. T., Dahunsi, D. T., Okeowo, O. M., ... & Elekofehinti, O. O. (2025). The antioxidative, Anti-inflammatory and Anti-apoptotic effects of Tetrapleura tetraptera (Aidan) ethanol leaf extract in the brain of Wistar rats exposed to aspartame. *Molecular Neurobiology*, 1-19.
- Lawal, K. K., Ekeleme, I. K., Onuigbo, C. M., Ikpeazu, V. O., & Obiekezie, S. O. (2021). A review on the public health implications of heavy metals. *World Journal of Advanced Research and Reviews*, 10(3), 255-265.

- León, O. L. L., & Pacheco, J. M. S. (2020). Effects of Lead on Reproductive. *Lead chemistry*, 3.
- Lin, L., Agyemang, K., Abdel-Samie, M. A. S., & Cui, H. (2019). Antibacterial mechanism of Tetrapleura tetraptera extract against Escherichia coli and Staphylococcus aureus and its application in pork. *Journal of Food Safety*, 39(6), e12693.
- Llinás, R. R., Walton, K. D., & Lang, E. J. (2004). Ch. 7 cerebellum. *The synaptic Organization of the Brain*. Oxford University Press, New York, 271-309.
- Lochner, J. (2003). *What is Your Cosmic Connection to the Elements?* (No. NASA/EG-2003-7-023-GSFC).
- Lorke, D. (1983). A new approach to practical acute toxicity testing. *Archives of toxicology*, 54(4), 275-287.
- Lyu, W., Wu, Y., Huynh, K. M., Ahmad, S., & Yap, P. T. (2024). A multimodal submillimeter MRI atlas of the human cerebellum. *Scientific reports*, 14(1), 5622.
- Mandal, G. C., Mandal, A., & Chakraborty, A. (2022). The toxic effect of lead on human health: A review. *Human biology and public health*, 3, 45.
- Mani, M. S., Kabekkodu, S. P., Joshi, M. B., & Dsouza, H. S. (2019). Ecogenetics of lead toxicity and its influence on risk assessment. *Human & Experimental Toxicology*, 38(9), 1031-1059.
- Manoj Kumar, V., Henley, A. K., Nelson, C. J., Indumati, O., Prabhakara Rao, Y., Rajanna, S., & Rajanna, B. (2017). Protective effect of Allium sativum (garlic) aqueous extract against

lead-induced oxidative stress in the rat brain, liver, and kidney. *Environmental Science and Pollution Research*, 24(2), 1544-1552.

Mansouri, M. T., Naghizadeh, B., López-Larrubia, P., & Cauli, O. (2013). Behavioral deficits induced by lead exposure are accompanied by serotonergic and cholinergic alterations in the prefrontal cortex. *Neurochemistry International*, 62(3), 232–239.

Manto, M., Bower, J. M., Conforto, A. B., Delgado-García, J. M., Da Guarda, S. N. F., Gerwig, M., ... & Timmann, D. (2012). Consensus paper: roles of the cerebellum in motor control—the diversity of ideas on cerebellar involvement in movement. *The Cerebellum*, 11, 457-487.

Mary, C. P. V., Vijayakumar, S., & Shankar, R. (2018). Metal chelating ability and antioxidant properties of Curcumin-metal complexes—A DFT approach. *Journal of Molecular Graphics and Modelling*, 79, 1-14.

Mason, L. H., Harp, J. P., & Han, D. Y. (2014). Lead neurotoxicity: neuropsychological effects of Lead toxicity. *BioMed Research International*, 2014(1), 840547.

Mbaveng, A. T., Chi, G. F., Bonsou, I. N., Ombito, J. O., Yeboah, S. O., Kuete, V., & Efferth, T. (2021). Cytotoxic phytochemicals from the crude extract of *Tetrapleura tetraptera* fruits towards multi-factorial drug resistant cancer cells. *Journal of ethnopharmacology*, 267, 113632.

McNeill, J., Barrie, F. R., Buck, W. R., Demoulin, V., Greuter, W., Hawksworth, D. L., ... & Turland, N. J. (2012). International Code of Nomenclature for algae, fungi and plants. *Regnum vegetabile*, 154.

- Mehta, S. K., & Gowder, S. J. T. (2015). Members of antioxidant machinery and their functions. *Basic principles and clinical significance of oxidative stress*, 11, 59-85.
- Mensah, R. Q., Adusei, S., Azupio, S., & Kwakye, R. (2024). Nutritive value, biological properties, health benefits and applications of *Tetrapleura tetraptera*: An updated comprehensive review. *Heliyon*, 10(6).
- Meziane, H., Zraibi, L., Albusayr, R., Bitari, A., Oussaid, A., Hammouti, B., & Touzani, R. (2025). *Tetrapleura tetraptera* Linn.: Unveiling its multifaceted nature in nutrition, diverse applications, and advanced extraction methods. *Journal of Umm Al-Qura University for Applied Sciences*, 11, 9–37.
- Misra, H. P., & Fridovich, I. (1972). The role of superoxide anion in the autoxidation of epinephrine and a simple assay for superoxide dismutase. *Journal of Biological chemistry*, 247(10), 3170-3175.
- Mitoma, H., Manto, M., & Gandini, J. (2019). Recent advances in the treatment of cerebellar disorders. *Brain Sciences*, 10(1), 11.
- Molavi Vasei, F., Zamanian, M. Y., Golmohammadi, M., Mahmoodi, M., Khademalhosseini, M., Tavakoli, T., Esmaeili, O.S., Zarei, S., Mirzaei, M.R., & Hajizadeh, M. R. (2024). The Impact of Vitamin E Supplementation on Oxidative Stress, Cognitive Functions, and Aging-Related Gene Expression in Aged Mice. *Food Science & Nutrition*, 12(11), 9834-9845.
- Nam, S. M., Seo, J. S., Go, T. H., Nahm, S. S., & Chang, B. J. (2019). Ascorbic acid supplementation prevents the detrimental effects of prenatal and postnatal lead exposure on the Purkinje cell

and related proteins in the cerebellum of developing rats. *Biological Trace Element Research*, 190(2), 446-456.

National Research Council (2011). *Guide to the Care and Use of laboratory animals*, 8th Edition.

The National Academics Press: Washington, DC, 246.

Ngo, V., Karunatileke, N. C., Brickenden, A., Choy, W. Y., & Duennwald, M. L. (2022). Oxidative stress-induced misfolding and inclusion formation of Nrf2 and Keap1. *Antioxidants*, 11(2), 243.

Ogunwande, I. A., Olawore, N. O., Setzer, W. N., & Olaleye, O. N. (2014). 2014 shelf-life extension of tomato (lycopersicum. *J. Agric. Sci. Technol.*, 4, 806-810.

Olajide, O. J., Yawson, E. O., Gbadamosi, I. T., Arogundade, T. T., Lambe, E., Obasi, K., Lawal, I. T., Ibrahim, A., & Ogunrinola, K. Y. (2017). Ascorbic acid ameliorates behavioural deficits and neuropathological alterations in rat model of Alzheimer's disease. *Environmental Toxicology and Pharmacology*, 50, 200–211.

Omonkhua, A., Adebayo, E., Saliu, J., Adeyelu, T., Ogunwa, T., & Omonkhua, A. A. (2014). Effect of aqueous root bark extract of *Tetrapleura tetraptera* (Taub) on blood glucose and lipid profile of streptozotocin diabetic rats. *Nig QJ Hosp Med*, 24(4), 279-283.

Omotuyi, O.I., Nash, O., Inyang, O.K., Ogidigo, J., Enejoh, O., Okpalefe, O., and Hamada, T. (2018). Flavonoid-rich extract of *Chromolaena odorata* modulate circulating GLP-1 in Wistar rats: computational evaluation of TGR5 involvement. *Biotechnology*. 8, 1–8.

Onda, E. E., Sonibare, M. A., Ajayi, A. M., & Umukoro, S. (2017). Anti-inflammatory and antioxidant effects of *Tetrapleura Tetraptera* (Schumach & Thonn.) taub. fruit extract in

- Carrageenan/Kaolin-induced acute monoarthritis in rats. *Nigerian Journal of Pharmaceutical Research*, 13(2), 157-166.
- Onitsha, E. N., & Okutu, J. B. (2021). Influence of vitamin E and selenium on reproductive hormones and lipid peroxidation levels in lead-induced toxicity in female Wistar rats. *IOSR Journal of Environmental Science, Toxicology and Food Technology (IOSR-JESTFT)*, 15(2), 01-9.
- Ortega, D. R., Esquivel, D. F. G., Ayala, T. B., Pineda, B., Manzo, S. G., Quino, J. M., ... & de la Cruz, V. P. (2021). Cognitive impairment induced by lead exposure during lifespan: Mechanisms of Lead neurotoxicity. *Toxics*, 9(2), 23.
- Ozaslan, M., Karagoz, I. D., Lawal, R. A., Kilic, I. H., Cakir, A., Odesanmi, O. S., Guler, I., & Ebuehi, O. A. T. (2016). Cytotoxic and anti-proliferative activities of the *Tetrapleura tetraptera* fruit extract on ehrlich ascites tumor cells. *International Journal of Pharmacology*, 12: 655-662.
- Panda, S., Behera, S., Alam, M. F., & Syed, G. H. (2021). Endoplasmic reticulum & mitochondrial calcium homeostasis: The interplay with viruses. *Mitochondrion*, 58, 227-242.
- Pande, M., & Flora, S. J. S. (2002). Lead induced oxidative damage and its response to combined administration of  $\alpha$ -lipoic acid and succimers in rats. *Toxicology*, 177(2-3), 187-196.
- Parcheta, M., Świsłocka, R., Orzechowska, S., Akimowicz, M., Choińska, R., & Lewandowski, W. (2021). Recent developments in effective antioxidants: The structure and antioxidant properties. *Materials*, 14(8), 1984.

- Patestas, M. A., Meyer, A. J., & Gartner, L. P. (2025). *A textbook of neuroanatomy*. John Wiley & Sons. Pp 285-309.
- Paul, M. S., & Limaiem, F. (2019). Histology, purkinje cells. 31424738.
- Pedroso, J. L., Vale, T. C., Braga-Neto, P., Dutra, L. A., França Jr, M. C., Teive, H. A., & Barsottini, O. G. (2019). Acute cerebellar ataxia: differential diagnosis and clinical approach. *Arquivos de neuro-psiquiatria*, 77(03), 184-193.
- Perals, D., Griffin, A. S., Bartomeus, I., & Sol, D. (2017). Revisiting the open-field test: what does it really tell us about animal personality? *Animal Behaviour*, 123, 69-79.
- Pisotta, I., & Molinari, M. (2014). Cerebellar contribution to feedforward control of locomotion. *Frontiers in human neuroscience*, 8, 47
- Rahman, S., Iqbal, M., & Husen, A. (2023). Medicinal plants and abiotic stress: an overview. *medicinal plants: their response to abiotic stress*, 1-34.
- Raphaël, K. J., Hervé, M. K., Ruben, N. T., Ronald, K., Antoine, Y., Francklin, T., & Alexis, T. (2017). Growth performances and serum biochemical response of broiler chickens fed on diet supplemented with Tetrapleura tetraptera fruit powder as substitute to antibiotic growth promoters. *International Journal of Innovation and Applied Studies*, 21(1), 68.
- Reghuvaran, A., & Ravindranath, A. D. (2012). Biochemical aspects and formation of phenolic compounds by coir pith degraded by Pleurotus sajor caju. *Journal of Toxicology and Environmental Health Sciences*, 4(1), 29-36.
- Release, S. (2018): QikProp. New York, NY: Schrödinger, LLC.

- Reuben, A. (2018). Childhood Lead exposure and adult neurodegenerative disease. *Journal of Alzheimer's disease*, 64(1), 17-42.
- Rieuwerts, J. (2017). *The elements of environmental pollution*. Routledge. 13, 9780203798690
- Ristanovic, D., Milosevic, N. T., Stefanovic, B. D., Maric, D. L., & Rajkovic, K. (2010). Morphology and classification of large neurons in the adult human dentate nucleus: A qualitative and quantitative analysis of 2D images. [Article]. *Neuroscience Research*, 67(1), 1-7.
- Roederer, I. U., Kratz, K. L., Frebel, A., Christlieb, N., Pfeiffer, B., Cowan, J. J., & Sneden, C. (2009). The end of nucleosynthesis: production of lead and thorium in the early galaxy. *The Astrophysical Journal*, 698(2), 1963.
- Roostaei, T., Nazeri, A., Sahraian, M. A., & Minagar, A. (2014). The human cerebellum: a review of physiologic neuroanatomy. *Neurologic clinics*, 32(4), 859-869.
- Saleh, S., & Meligy, F. (2018). Study on Toxic Effects of Lead Acetate on Cerebellar Cortical Tissue of Adult Albino Rats and the Role of Vitamin E as a Protective Agent. *Ain Shams Journal of Forensic Medicine and Clinical Toxicology*, 31(2), 110-118.
- Schmahmann, J. D. (2019). The cerebellum and cognition. *Neuroscience letters*, 688, 62-75.
- Schumach & Thonn. (1891). *Tetrapleura tetraptera* (Schumach. & Thonn.) Taub. *Botanisches Centralblatt*. 47: 395
- Shahidi, F., Ramakrishnan, V. V., & Oh, W. Y. (2019). Bioavailability and metabolism of food bioactives and their health effects: A review. *Journal of Food Bioactives*, 8.

- Shanaida, M., Lysiuk, R., Mykhailenko, O., Hudz, N., Abdulsalam, A., Gontova, T., ... & Bjørklund, G. (2025). Alpha-lipoic acid: An antioxidant with anti-aging properties for disease therapy. *Current Medicinal Chemistry*, 32(1), 23-54.
- Siddiqui, S. (2025). Global patterns and drivers of species and genera richness of Fabaceae. *Frontiers in Plant Science*, 16, 1581814.
- Singh, C., Singh, R., & Shekhar, A. (2024). Effects of Lead: Neurological and Cellular Perspective. In *Lead Toxicity Mitigation: Sustainable Nexus Approaches* (pp. 17-33). Cham: Springer Nature Switzerland.
- Singh, N., Kumar, A., Gupta, V. K., & Sharma, B. (2018). Biochemical and molecular bases of Lead-induced toxicity in mammalian systems and possible mitigations. *Chemical research in toxicology*, 31(10), 1009-1021.
- Singh, P. K., Singh, M. K., Yadav, R. S., Nath, R., Mehrotra, A., Rawat, A., & Dixit, R. K. (2019). Omega-3 fatty acid attenuates oxidative stress in cerebral cortex, cerebellum, and hippocampus tissue and improves neurobehavioral activity in chronic Lead-induced neurotoxicity. *Nutritional Neuroscience*, 22(2), 83-97.
- Smykal, P., Coyne, C. J., Ambrose, M. J., Maxted, N., Schaefer, H., Blair, M. W., ... & Varshney, R. K. (2015). Legume crops phylogeny and genetic diversity for science and breeding. *Critical Reviews in Plant Sciences*, 34(1-3), 43-104.
- Stoodley, C. J. (2016). The cerebellum and neurodevelopmental disorders. *The Cerebellum*, 15(1), 34-37.

- Sukhum, K. V., Shen, J., & Carlson, B. A. (2018). Extreme enlargement of the cerebellum in a clade of teleost fishes that evolved a novel active sensory system. *Current Biology*, 28(23), 3857-3863.
- Tada, M., Nishizawa, M., & Onodera, O. (2015). Redefining cerebellar ataxia in degenerative ataxias: lessons from recent research on cerebellar systems. *Journal of Neurology, Neurosurgery & Psychiatry*, 86(8), 922-928.
- Talpur, S., Afridi, H. I., Kazi, T. G., & Talpur, F. N. (2018). Interaction of lead with calcium, iron, and zinc in the biological samples of malnourished children. *Biological Trace Element Research*, 183(2), 209-217.
- Tarrago, O., & Brown, M. J. (2017). Case studies in environmental medicine (CSEM) Lead toxicity. *Agency for toxic substances and disease registry*, WB2832.
- Tartaglione, A. M., Serafini, M. M., Raggi, A., Iacoponi, F., Zianni, E., Scalfari, A., Minghetti, L., Ricceri, L., Cubadda, F., Calamandrei, G., & Viviani, B. (2020). Sex-dependent effects of developmental lead exposure in Wistar rats: Evidence from behavioral and molecular correlates. *International Journal of Molecular Sciences*, 21(8), 2664
- Tchounwou, P. B., Yedjou, C. G., Patlolla, A. K., & Sutton, D. J. (2012). Heavy metal toxicity and the environment. *Molecular, clinical and environmental toxicology: volume 3: environmental toxicology*, 133-164.
- Tesfaye, A. (2021). Revealing the therapeutic uses of garlic (*Allium sativum*) and its potential for drug discovery. *The Scientific World Journal*, 2021(1), 8817288.

- Tirima, S., Bartrem, C., von Lindern, I., von Braun, M., Lind, D., Anka, S. M., & Abdullahi, A. (2018). Food contamination as a pathway for Lead exposure in children during the 2010–2013 lead poisoning epidemic in Zamfara, Nigeria. *Journal of Environmental Sciences*, *67*, 260-272.
- Udaipurwala, A., Pimple, P., & Sawarkar, S. (2025). Exploring the Pharmacotherapeutic Potential of Natural Compound Alpha Lipoic Acid. *The Natural Products Journal*, *15*(8), e22103155309474.
- US Food and Drug Administration. (2015). Q3D elemental impurities guidance for industry. *US Department of Health and Human Services: Washington, DC, USA*, 41.
- Uyoh, E. A., Ita, E. E., & Nwofia, G. E. (2013). Evaluation of the chemical composition of *Tetrapleura tetraptera* (Schum and Thonn.) Taub. accessions from Cross River State, Nigeria. *International Journal of Medicinal and Aromatic Plants* *3*(3), 386-394.
- Wright, M., Skaggs, W., & Nielsen, F. A. (2016). The cerebellum. *WikiJournal of Medicine*, *3*(1), 1-15.
- Xia, H. (2021). Extensive metabolism of flavonoids relevant to their potential efficacy on Alzheimer's disease. *Drug Metabolism Reviews*, *53*(4), 563-591.
- Zesiewicz, T. A., Wilmot, G., Kuo, S. H., Perlman, S., Greenstein, P. E., Ying, S. H., ... & Sullivan, K. L. (2018). Comprehensive systematic review summary: Treatment of cerebellar motor dysfunction and ataxia: Report of the Guideline Development, Dissemination, and Implementation Subcommittee of the American Academy of Neurology. *Neurology*, *90*(10), 464.

Zhang, Y., Pei, X., Jing, L., Zhang, Q., & Zhao, H. (2024). Lead induced cerebellar toxicology of developmental Japanese quail (*Coturnix japonica*) via oxidative stress-based Nrf2/Keap1 pathway inhibition and glutathione-mediated apoptosis signaling activation. *Environmental Pollution*, 352, 124114.

Zhao, Y., Ye, X., Xiong, Z., Ihsan, A., Ares, I., Martínez, M., ... & Martínez, M. A. (2023). Cancer metabolism: the role of ROS in DNA damage and induction of apoptosis in cancer cells. *Metabolites*, 13(7), 796.

Please stick to APA 7<sup>th</sup> edition referencing style.

**Commented [h18]:** See this.